EVALUATION OF PUSHOVER ANALYSIS PROCEDURES FOR FRAME STRUCTURES

A THESIS SUBMITTED TO
THE GRADUATE SCHOOL OF NATURAL AND APPLIED SCIENCES
OF
MIDDLE EAST TECHNICAL UNIVERSITY

BY

SERMİN OĞUZ

IN PARTIAL FULFILLMENT OF THE REQUIREMENTS
FOR
THE DEGREE OF MASTER OF SCIENCE
IN
CIVIL ENGINEERING

APRIL 2005

Approval of the Graduate School of Natural and Applied Sciences

Prof. Dr. Canan Özgen
Director

I certify that this thesis satisfies all the requirements as a thesis for the degree of Master of Science.

Prof. Dr. Erdal Çokça
Head of Department

This is to certify that we have read this thesis and that in our opinion it is fully adequte, in scope and quality, as a thesis for the degree of Master of Science.

Asst. Prof. Dr. Ahmet Yakut
Supervisor

Examining Committee Members

Prof. Dr. Polat Gülkan	(METU, CE)	
Asst. Prof. Dr. Ahmet Yakut	(METU, CE)	
Prof. Dr. Haluk Sucuoğlu	(METU, CE)	
Asst. Prof. Dr. Sinan Akkar	(METU, CE)	
Asst. Prof. Dr. Burcu Güneş	(ATILIM UNIVERSITY)	

I hereby declare that all information in this document has been obtained and presented in accordance with academic rules and ethical conduct. I also declare that, as required by these rules and conduct, I have fully cited and referenced all material and results that are not original to this work.

Name, Last name : Sermin OĞUZ

Signature :

ABSTRACT

EVALUATION OF PUSHOVER ANALYSIS PROCEDURES FOR FRAME STRUCTURES

Oğuz, Sermin
M.S., Department of Civil Engineering
Supervisor : Asst. Prof. Dr. Ahmet Yakut

April 2005, 156 pages

Pushover analysis involves certain approximations and simplifications that some amount of variation is always expected to exist in seismic demand prediction of pushover analysis. In literature, some improved pushover procedures have been proposed to overcome the certain limitations of traditional pushover procedures.

The effects and the accuracy of invariant lateral load patterns utilised in pushover analysis to predict the behavior imposed on the structure due to randomly selected individual ground motions causing elastic and various levels of nonlinear response were evaluated in this study. For this purpose, pushover analyses using various invariant lateral load patterns and Modal Pushover Analysis were performed on reinforced concrete and steel moment resisting frames covering a broad range of fundamental periods. Certain response parameters predicted by each pushover procedure were compared with the 'exact' results obtained from nonlinear dynamic analysis. The primary observations from the study showed that the accuracy of the pushover results depends strongly on the load path, properties of the structure and the characteristics of the ground motion.

Pushover analyses were performed by both DRAIN-2DX and SAP2000. Similar pushover results were obtained from the two different softwares employed in the study

provided that similar approach is used in modeling the nonlinear properties of members as well as their structural features.

The accuracy of approximate procedures utilised to estimate target displacement was also studied on frame structures. The accuracy of the predictions was observed to depend on the approximations involved in the theory of the procedures, structural properties and ground motion characteristics.

Keywords: Pushover analysis, seismic performance evaluation, nonlinear response, Modal Pushover Analysis, approximate procedures

ÖZ

ÇERÇEVE YAPILARDA İTME ANALİZİ YÖNTEMLERİNİN DEĞERLENDİRİLMESİ

Oğuz, Sermin
Yüksek Lisans, İnşaat Mühendisliği Bölümü
Tez Yöneticisi : Y. Doç. Dr. Ahmet Yakut

Nisan 2005, 156 sayfa

Elastik ötesi itme analizinin bazı basitleştirilmiş yaklaşımlar içermesi, elastik ötesi itme analizi sismik davranış tahminlerinin gerçek davranıştan her zaman bir miktar farklı olmasına neden olmaktadır. Geleneksel elastik ötesi itme analizinin içerdiği bazı kısıtlamaları gidermek için literatürde gelişmiş elastik ötesi itme analizi yöntemleri önerilmiştir.

Bu çalışmada, elastik ötesi itme analizinde kullanılan sabit yatay yük dağılımlarının, rastgele seçilen yer hareketleri nedeniyle elastik ve farklı seviyede elastik ötesi davranışa maruz kalan yapıların sözkonusu deformasyon seviyelerindeki davranışını tahmin etmedeki etkileri ve doğruluğu değerlendirilmiştir. Bu amaçla, farklı sabit yatay yük dağılımları kullanılarak elastik ötesi itme analizleri ve Modal Elastik Ötesi İtme Analizi geniş bir birinci mod periyodu aralığını kapsayan betonarme ve çelik çerçevelerde uygulanmıştır. Herbir analiz yöntemi tarafından tahmin edilen bazı davranış parametreleri elastik ötesi dinamik analizden elde edilen gerçek sonuçlarla karşılaştırılmıştır. Yapılan

çalışma üzerindeki temel gözlemler elastik ötesi itme analizi sonuçlarının yük dağılımı, yapı ve yer hareketi özelliklerine son derece bağlı olduğunu göstermiştir.

Elastik ötesi itme analizleri DRAIN-2DX ve SAP2000 programları ile yapılmıştır. Her iki programın da elastik ötesi eleman özellikleri ve yapısal özellikleri modellemede benzer yaklaşımlar kullanması nedeniyle programlardan benzer elastik ötesi itme analizi sonuçları elde edilmiştir.

Maksimum global deplasman tahmin edilmesinde kullanılan yaklaşık yöntemlerin doğruluk derecesi de çerçeve yapılar üzerinde değerlendirilmiştir. Tahminlerin doğruluk seviyesinin yöntemlerin teorisinde yer alan basitleştirilmiş yaklaşımlar, yapısal özellikler ve yer hareketi özelliklerine bağlı olduğu gözlemlenmiştir.

Anahtar Kelimeler : Elastik ötesi itme analizi, sismik performans değerlendirmesi, elastik ötesi davranış, Modal Elastik Ötesi İtme Analizi, yaklaşık yöntemler

ACKNOWLEDGMENTS

This study was conducted under the supervision of Asst. Prof. Dr. Ahmet Yakut. I would like to express my sincere appreciation for the support, guidance and insights that he has provided me throughout the study.

I am thankful to Serhat Bayılı and Ufuk Yazgan for their helps in this study.

Nazan Yılmaz Öztürk is highly acknowledged for her supports and close friendship throughout my graduate life.

I would like to thank my friends at Structural Mechanics Laboratory; Emre Akın, Seval Pınarbaşı, Sezgin Küçükçoban, Beyhan Bayhan, Dilek Okuyucu, Gökhan Özdemir, Emrah Erduran, Hakan Erdoğan, Okan Özcan, Tuğba Eroğlu and Barış Erdil for their friendship during my assistantship at METU.

My dear friend Emre Kara deserves thanks for his invaluable friendship.

I would like to express my deepest appreciation to my parents -the most precious people in my life- for their confidence in me and for the support, love and understanding that they have provided me throughout my life.

TABLE OF CONTENTS

PAGE

PAGE

PAGE

CHAPTER 1

INTRODUCTION

1.1 BACKGROUND

Nonlinear static analysis, or pushover analysis, has been developed over the past twenty years and has become the preferred analysis procedure for design and seismic performance evaluation purposes as the procedure is relatively simple and considers post-elastic behavior. However, the procedure involves certain approximations and simplifications that some amount of variation is always expected to exist in seismic demand prediction of pushover analysis.

Although, in literature, pushover analysis has been shown to capture essential structural response characteristics under seismic action, the accuracy and the reliability of pushover analysis in predicting global and local seismic demands for all structures have been a subject of discussion and improved pushover procedures have been proposed to overcome the certain limitations of traditional pushover procedures. However, the improved procedures are mostly computationally demanding and conceptually complex that use of such procedures are impractical in engineering profession and codes.

As traditional pushover analysis is widely used for design and seismic performance evaluation purposes, its limitations, weaknesses and the accuracy of its predictions in routine application should be identified by studying the factors affecting the pushover predictions. In other words, the applicability of pushover analysis in predicting seismic demands should be investigated for low, mid and high-rise structures by identifying certain issues such as modeling nonlinear member behavior, computational scheme of the procedure, variations in the predictions of various lateral load patterns utilized in traditional pushover analysis, efficiency of invariant lateral load patterns in

representing higher mode effects and accurate estimation of target displacement at which seismic demand prediction of pushover procedure is performed.

1.2 METHODS OF ANALYSIS

For seismic performance evaluation, a structural analysis of the mathematical model of the structure is required to determine force and displacement demands in various components of the structure. Several analysis methods, both elastic and inelastic, are available to predict the seismic performance of the structures.

1.2.1 Elastic Methods of Analysis

The force demand on each component of the structure is obtained and compared with available capacities by performing an elastic analysis. Elastic analysis methods include code static lateral force procedure, code dynamic procedure and elastic procedure using demand-capacity ratios. These methods are also known as force-based procedures which assume that structures respond elastically to earthquakes.

In code static lateral force procedure, a static analysis is performed by subjecting the structure to lateral forces obtained by scaling down the smoothened soil-dependent elastic response spectrum by a structural system dependent force reduction factor, "R". In this approach, it is assumed that the actual strength of structure is higher than the design strength and the structure is able to dissipate energy through yielding.

In code dynamic procedure, force demands on various components are determined by an elastic dynamic analysis. The dynamic analysis may be either a response spectrum analysis or an elastic time history analysis. Sufficient number of modes must be considered to have a mass participation of at least 90% for response spectrum analysis. Any effect of higher modes are automatically included in time history analysis.

In demand/capacity ratio (DCR) procedure, the force actions are compared to corresponding capacities as demand/capacity ratios. Demands for DCR calculations must include gravity effects. While code static lateral force and code dynamic procedures reduce the full earthquake demand by an R-factor, the DCR approach takes the full earthquake demand without reduction and adds it to the gravity demands. DCRs approaching 1.0 (or higher) may indicate potential deficiencies.

Although force-based procedures are well known by engineering profession and easy to apply, they have certain drawbacks. Structural components are evaluated for serviceability in the elastic range of strength and deformation. Post-elastic behavior of

structures could not be identified by an elastic analysis. However, post-elastic behavior should be considered as almost all structures are expected to deform in inelastic range during a strong earthquake. The seismic force reduction factor "R" is utilized to account for inelastic behavior indirectly by reducing elastic forces to inelastic. Force reduction factor, "R", is assigned considering only the type of lateral system in most codes, but it has been shown that this factor is a function of the period and ductility ratio of the structure as well [38].

Elastic methods can predict elastic capacity of structure and indicate where the first yielding will occur, however they don't predict failure mechanisms and account for the redistribution of forces that will take place as the yielding progresses. Real deficiencies present in the structure could be missed. Moreover, force-based methods primarily provide life safety but they can't provide damage limitation and easy repair.

The drawbacks of force-based procedures and the dependence of damage on deformation have led the researches to develop displacement-based procedures for seismic performance evaluation. Displacement-based procedures are mainly based on inelastic deformations rather than elastic forces and use nonlinear analysis procedures considering seismic demands and available capacities explicitly [22].

1.2.2 Inelastic Methods of Analysis

Structures suffer significant inelastic deformation under a strong earthquake and dynamic characteristics of the structure change with time so investigating the performance of a structure requires inelastic analytical procedures accounting for these features. Inelastic analytical procedures help to understand the actual behavior of structures by identifying failure modes and the potential for progressive collapse. Inelastic analysis procedures basically include inelastic time history analysis and inelastic static analysis which is also known as pushover analysis.

The inelastic time history analysis is the most accurate method to predict the force and deformation demands at various components of the structure. However, the use of inelastic time history analysis is limited because dynamic response is very sensitive to modeling and ground motion characteristics. It requires proper modeling of cyclic load-deformation characteristics considering deterioration properties of all important components. Also, it requires availability of a set of representative ground motion records that accounts for uncertainties and differences in severity, frequency and duration characteristics. Moreover, computation time, time required for input preparation and

interpreting voluminous output make the use of inelastic time history analysis impractical for seismic performance evaluation.

Inelastic static analysis, or pushover analysis, has been the preferred method for seismic performance evaluation due to its simplicity. It is a static analysis that directly incorparates nonlinear material characteristics. Inelastic static analysis procedures include Capacity Spectrum Method [3], Displacement Coefficient Method [20] and the Secant Method [10].

The theoretical background, reliability and the accuracy of inelastic static analysis procedure is discussed in detail in the following sections.

1.2.3 Summary

The uncertainties involved in accurate determination of material properties, element and structure capacities, the limited prediction of ground motions that the structure is going to experience and the limitations in accurate modeling of structural behavior make the seismic performance evaluation of structures a complex and difficult process.

Displacement-based procedures provide a more rational approach to these issues compared to force-based procedures by considering inelastic deformations rather than elastic forces. The analytical tool for evaluation process should also be relatively simple which can capture critical response parameters that significantly effect the evaluation process.

1.3 DESCRIPTION OF PUSHOVER ANALYSIS

Pushover analysis is an approximate analysis method in which the structure is subjected to monotonically increasing lateral forces with an invariant height-wise distribution until a target displacement is reached.

Pushover analysis consists of a series of sequential elastic analyses, superimposed to approximate a force-displacement curve of the overall structure. A two or three dimensional model which includes bilinear or trilinear load-deformation diagrams of all lateral force resisting elements is first created and gravity loads are applied initially. A predefined lateral load pattern which is distributed along the building height is then applied. The lateral forces are increased until some members yield. The structural model is modified to account for the reduced stiffness of yielded members and lateral forces are again increased until additional members yield. The process is continued until a control

displacement at the top of building reaches a certain level of deformation or structure becomes unstable. The roof diplacement is plotted with base shear to get the global capacity curve (Figure 1.1).

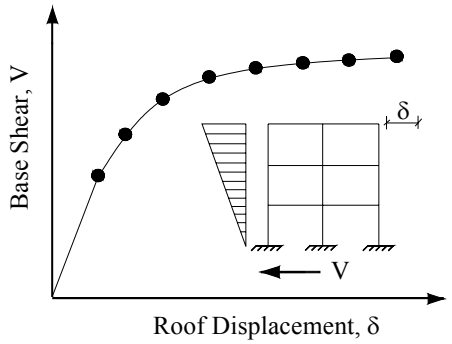

Figure 1.1: Global Capacity (Pushover) Curve of a Structure

Pushover analysis can be performed as force-controlled or displacement-controlled. In force-controlled pushover procedure, full load combination is applied as specified, i.e, force-controlled procedure should be used when the load is known (such as gravity loading). Also, in force-controlled pushover procedure some numerical problems that affect the accuracy of results occur since target displacement may be associated with a very small positive or even a negative lateral stiffness because of the development of mechanisms and P-delta effects.

Generally, pushover analysis is performed as displacement-controlled proposed by Allahabadi [1] to overcome these problems. In displacement-controlled procedure, specified drifts are sought (as in seismic loading) where the magnitude of applied load is not known in advance. The magnitude of load combination is increased or decreased as necessary until the control displacement reaches a specified value. Generally, roof displacement at the center of mass of structure is chosen as the control displacement.

The internal forces and deformations computed at the target displacement are used as estimates of inelastic strength and deformation demands that have to be compared with available capacities for a performance check.

1.3.1 Use of Pushover Results

Pushover analysis has been the preferred method for seismic performance evaluation of structures by the major rehabilitation guidelines and codes because it is

conceptually and computationally simple. Pushover analysis allows tracing the sequence of yielding and failure on member and structural level as well as the progress of overall capacity curve of the structure.

The expectation from pushover analysis is to estimate critical response parameters imposed on structural system and its components as close as possible to those predicted by nonlinear dynamic analysis. Pushover analysis provide information on many response characteristics that can not be obtained from an elastic static or elastic dynamic analysis. These are [30];

- estimates of interstory drifts and its distribution along the height
- determination of force demands on brittle members, such as axial force demands on columns, moment demands on beam-column connections
- determination of deformation demands for ductile members
- identification of location of weak points in the structure (or potential failure modes)
- consequences of strength deterioration of individual members on the behavior of structural system
- identification of strength discontinuties in plan or elevation that will lead to changes in dynamic characteristics in the inelastic range
- verification of the completeness and adequacy of load path

Pushover analysis also expose design weaknesses that may remain hidden in an elastic analysis. These are story mechanisms, excessive deformation demands, strength irregularities and overloads on potentially brittle members.

1.3.2 Limitations of Pushover Analysis

Although pushover analysis has advantages over elastic analysis procedures, underlying assumptions, the accuracy of pushover predictions and limitations of current pushover procedures must be identified. The estimate of target displacement, selection of lateral load patterns and identification of failure mechanisms due to higher modes of vibration are important issues that affect the accuracy of pushover results.

Target displacement is the global displacement expected in a design earthquake. The roof displacement at mass center of the structure is used as target displacement. The accurate estimation of target displacement associated with specific performance objective affect the accuracy of seismic demand predictions of pushover analysis.

In pushover analysis, the target displacement for a multi degree of freedom (MDOF) system is usually estimated as the displacement demand for the corresponding equivalent single degree of freedom (SDOF) system. The basic properties of an equivalent SDOF system are obtained by using a shape vector which represents the deflected shape of the MDOF system. The theoretical background for the determination of basic properties of equivalent SDOF system is given in Chapter 5. Most of the researchers recommend the use of normalized displacement profile at the target displacement level as a shape vector but an iteration is needed since this displacement is not known a priori. Thus, a fixed shape vector, elastic first mode, is used for simplicity without regards to higher modes by most of the approaches.

Moreover, hysteretic characteristics of MDOF should be incorporated into the equivalent SDOF model, if displacement demand is affected from stiffness degradation or pinching, strength deterioration, P-Δ effects. Foundation uplift, torsional effects and semi-rigid diaphragms are also expected to affect the target displacement [30].

Lateral loads represent the likely distribution of inertia forces imposed on structure during an earthquake. The distribution of inertia forces vary with the severity of earthquake and with time during earthquake since

$$F_{k,i} = \frac{W_k}{g} \ddot{u}_i \tag{1.1}$$

$F_{k,i}$: inertia force at k-th story at time i

W_k : weight of k-th story

$\ddot{u}_i$: instantaneous story acceleration

However, in pushover analysis, generally an invariant lateral load pattern is used that the distribution of inertia forces is assumed to be constant during earthquake and the deformed configuration of structure under the action of invariant lateral load pattern is expected to be similar to that experienced in design earthquake. As the response of structure, thus the capacity curve is very sensitive to the choice of lateral load distribution [31], selection of lateral load pattern is more critical than the accurate estimation of target displacement.

The lateral load patterns used in pushover analysis are proportional to product of story mass and displacement associated with a shape vector at the story under consideration. Commonly used lateral force patterns are uniform, elastic first mode, "code" distributions and a single concentrated horizontal force at the top of structure. Multi-modal load pattern derived from Square Root of Sum of Squares (SRSS) story

shears is also used to consider at least elastic higher mode effects for long period structures. These loading patterns usually favor certain deformation modes that are triggered by the load pattern and miss others that are initiated and propagated by the ground motion and inelastic dynamic response characteristics of the structure [30]. Moreover, invariant lateral load patterns could not predict potential failure modes due to middle or upper story mechanisms caused by higher mode effects. Invariant load patterns can provide adequate predictions if the structural response is not severely affected by higher modes and the stucture has only a single load yielding mechanism that can be captured by an invariant load pattern.

FEMA-273 [18] recommends utilising at least two fixed load patterns that form upper and lower bounds for inertia force distributions to predict likely variations on overall structural behavior and local demands. The first pattern should be uniform load distribution and the other should be "code" profile or multi-modal load pattern. The 'Code' lateral load pattern is allowed if more than 75% of the total mass participates in the fundamental load.

The invariant load patterns can not account for the redistribution of inertia forces due to progressive yielding and resulting changes in dynamic properties of the structure. Also, fixed load patterns have limited capability to predict higher mode effects in post-elastic range. These limitations have led many researchers to propose adaptive load patterns which consider the changes in inertia forces with the level of inelasticity. The underlying approach of this technique is to redistribute the lateral load shape with the extent of inelastic deformations. Altough some improved predictions have been obtained from adaptive load patterns [37], they make pushover analysis computationally demanding and conceptually complicated. The scale of improvement has been a subject of discussion that simple invariant load patterns are widely preferred at the expense of accuracy.

Whether lateral loading is invariant or adaptive, it is applied to the structure statically that a static loading can not represent inelastic dynamic response with a large degree of accuracy.

The above discussion on target displacement and lateral load pattern reveals that pushover analysis assumes that response of structure can be related to that of an equivalent SDOF system. In other words, the response is controlled by fundamental mode which remains constant throughout the response history without considering progressive yielding. Although this assumption is incorrect, some researchers obtained satisfactory

local and global pushover predictions on low to mid-rise structures in which response is dominated by fundamental mode and inelasticity is distributed throughout the height of the structure [30].

1.3.3 Summary

Pushover analysis yields insight into elastic and inelastic response of structures under earthquakes provided that adequate modeling of structure, careful selection of lateral load pattern and careful interpretation of results are performed. However, pushover analysis is more appropriate for low to mid-rise buildings with dominant fundamental mode response. For special and high-rise buildings, pushover analysis should be complemented with other evaluation procedures since higher modes could certainly affect the response.

1.4 OBJECTIVE AND SCOPE

The various aspects of pushover analysis and the accuracy of pushover analysis in predicting seismic demands were investigated by several researchers. However, most of these researches made use of specifically designed structures in the context of the study or specific forms of pushover procedure was implemented. In this study, some important issues that affect the accuracy of traditional nonlinear static analysis, or pushover analysis, were studied on 2, 5, 8 and 12-story reinforced concrete and 2, 5 and 13-story steel moment resisting frames covering a broad range of fundamental periods and the applicability of pushover analysis in predicting seismic demands was investigated for low, mid and high-rise frame structures.

Firstly, the superiority of pushover analysis over elastic procedures in evaluating the seismic performance of a structure was discussed by identifying the advantages and limitations of the procedure. Then, pushover analyses were performed on case study frames using both SAP2000 [14] and DRAIN-2DX [44] to illustrate the similarities and/or the differences in the computational scheme of each software in performing pushover analysis. Modeling of nonlinear member behavior and the assumptions and the limitations involved were discussed for each software.

Also, the effects and the accuracy of various invariant lateral load patterns ('Uniform', 'Elastic First Mode', 'Code', 'FEMA-273' and 'Multi-Modal (or SRSS)') utilized in traditional pushover analysis to predict the behavior imposed on the structure due to randomly selected individual ground motions causing elastic and various levels of

nonlinear response were evaluated. For this purpose, six deformation levels represented as peak roof displacements on the capacity curve of the frames were firstly predetermined and the response parameters such as story displacements, inter-story drift ratios, story shears and plastic hinge locations were then estimated from the results of pushover analyses for any lateral load pattern at the considered deformation level. Story displacements, inter-story drift ratios and plastic hinge locations were also estimated by performing an improved pushover procedure named Modal Pushover Analysis (MPA) on case study frames. Pushover predictions were compared with the 'exact' values of response parameters obtained from the nonlinear time history analyses to assess the accuracy of pushover predictions.

Moreover, maximum inelastic displacement demands referred as target displacements of reinforced concrete (R/C) frames were estimated at elastic and various levels of nonlinear deformation levels using Nonlinear Dynamic Analysis of Equivalent SDOF System, Capacity Spectrum Method (ATC-40 Procedure A) [3], Displacement Coefficient Method (FEMA-356) [20] and Constant Ductility Procedure (Chopra&Goel) [8]. The assumptions and the accuracy of approximate procedures in predicting target displacement were identified.

This thesis is composed of six main chapters and an appendix. Chapter 1 includes a discussion of analysis methods used for seismic performance evaluation and a brief information about pushover analysis and its limitations. Chapter 2 reviews the previous research on simplified nonlinear analysis procedures and on pushover analysis. In Chapter 3, the computational scheme, the assumptions involved in modeling nonlinear member behavior and underlying principles of SAP2000 [14] and DRAIN-2DX [44] utilized to perform pushover analysis are explained in detail. The accuracy of various invariant lateral load patterns and Modal Pushover Analysis (MPA) [9] in predicting the seismic demands for frame structures experiencing individual ground motion excitations that cause elastic and certain levels of nonlinear deformation are identified in Chapter 4. Maximum inelastic displacement demands of R/C case study frames using four commonly known approximate procedures are estimated and the assumptions and the accuracy of approximate procedures in predicting target displacement are identified in Chapter 5. Chapter 6 contains the summary, conclusions and future recommendations to on the study. Appendix A contains description of case study frames and figures that represent the estimates of certain response parameters.

CHAPTER 2

REVIEW OF PREVIOUS RESEARCH

2.1 GENERAL

Structures are expected to deform inelastically when subjected to severe earthquakes, so seismic performance evaluation of structures should be conducted considering post-elastic behavior. Therefore, a nonlinear analysis procedure must be used for evaluation purpose as post-elastic behavior can not be determined directly by an elastic analysis. Moreover, maximum inelastic displacement demand of structures should be determined to adequately estimate the seismically induced demands on structures that exhibit inelastic behaviour.

Various simplified nonlinear analysis procedures and approximate methods to estimate maximum inelastic displacement demand of structures are proposed in literature. The widely used simplified nonlinear analysis procedure, pushover analysis, has also been an attractive subject of study.

2.2 PAST STUDIES ON SIMPLIFIED NONLINEAR ANALYSIS PROCEDURES

The accuracy and reliability of nonlinear time history analysis in simulating the actual behavior of structure under seismic action has been widely accepted since 1960s. However, the time required for proper modeling, input preparation, computation time, computer costs and the effort for the interpretation of voluminous output make use of such analyses impractical. This led researchers to propose simplified nonlinear analysis procedures and structural models to estimate inelastic seismic demands. The proposed simplified nonlinear analysis procedures and structural models are usually based on the reduction of MDOF model of structures to an equivalent SDOF system.

Rosenblueth and Herrera [46] proposed a procedure in which the maximum deformation of inelastic SDOF system is estimated as the maximum deformation of a linear elastic SDOF system with lower lateral stiffness (higher period of vibration, T_{eq}) and higher damping coefficient (ζ_{eq}) than those of inelastic system. In this procedure, a sequence of equivalent linear systems with successively updated values of T_{eq} and ζ_{eq} provide a basis to estimate the deformation of the inelastic system. Rosenblueth and Herrera [46] used the secant stiffness at maximum deformation to represent period shift and equivalent damping ratio is calculated by equating the energy dissipated per cycle in nonlinear and equivalent linear SDOF system subjected to harmonic loading.

Gülkan and Sözen [23] noted that most of the time the displacement would be significantly smaller than the maximum response under earthquake loading. Thus the equivalent damping proposed by Rosenblueth and Herrera [46] would result in an overestimation of equivalent viscous damping that the response would be underestimated. Gülkan and Sözen [23] developed an empirical equation for equivalent damping ratio using secant stiffness Takeda hysteretic model [52] and the results obtained from experiments made on single story, single bay frames supported the proposed procedure.

The empirical procedure proposed by Gülkan and Sözen [23] was later extended to MDOF in the well known substitute structure procedure by Shibata and Sözen [51]. Inelastic seismic design force requirements of a R/C structure can be determined by analysing a substitute structure having the stiffness and damping properties derived from the original frame under an elastic response spectrum. In the procedure, the displacement ductility ratio was replaced with a damage ratio in the equivalent viscous damping ratio equation proposed by Gülkan and Sözen [23]. Only 2D models of stuctures which are regular in plan and elevation can be analysed by the procedure.

Iwan [25] and Kowalsky [29] developed empirical equations to define the period shift and equivalent viscous damping ratio to estimate maximum displacement demand of inelastic SDOF system from its linear representation.

In 1981, Q-model which is a ‘low-cost’ analytical model for the calculation of displacement histories of multistory reinforced concrete structures subjected to ground motions was proposed by Saiidi and Sözen [48]. Q-model is a SDOF system consisting of an equivalent mass, a viscous damper, a massless rigid bar and a rotational spring. The hysteretic response of the spring was based on force-displacement curve of actual structure under monotonically increasing lateral force with a triangular height-wise distribution. The measured displacement histories of eight 10-story small scale R/C

structures with frame and frame-wall structural systems were used to test the Q-model. For structures without abrupt changes in stiffness and mass along their heights, the overall performance of Q-model in simulating earthquake response was satisfactory.

Later, Fajfar and Fischinger [16] proposed the N2 method as a simple nonlinear procedure for seismic damage analysis of reinforced concrete buildings. The method uses response spectrum approach and nonlinear static analysis. The method was applied to three 7-story buildings [17]. The capacity curve of a MDOF system was converted to that of a SDOF and a global demand was obtained. A damage model which includes cumulative damage was determined at global demand. The method yields reasonably accurate results provided that the structure vibrates predominantly in the first mode.

Capacity Spectrum Method [3] is one of the most popular methods utilized for a quick estimate to evaluate the seismic performance of structures. The method is recommended by ATC-40 [3] as a displacement-based design and assessment tool for structures. The method was developed by Freeman [21] and it has gone through several modifications since then. The most recent three versions (Procedures A, B and C) of Capacity Spectrum Method [3] are presented in detail in ATC-40 [3]. The method requires construction of a structural capacity curve and its comparison with the estimated demand response spectrum, both of which are expressed in Acceleration-Displacement Response Spectrum (ADRS) format. Mahaney et al. [32] introduced the ADRS format that the spectral accelerations are plotted against spectral displacements with radial lines representing the period, T. The demand (inelastic) response spectrum accounting for hysteretic nonlinear behaviour of structure is obtained by reducing elastic response spectrum with spectral reduction factors which depend on effective damping. A performance point that lies on both the capacity spectrum and the demand spectrum (reduced for nonlinear effects) is obtained for performance evaluation of the structure. The dependence of spectral reduction factors on structural behaviour type (hysteretic properties) and ground motion duration and the approximations involved in determination of these characteristics are the main weaknesses of the method.

Newmark and Hall [39] and Miranda [33] proposed procedures based on displacement modification factors in which the maximum inelastic displacement demand of MDOF system is estimated by applying certain displacement modification factors to maximum deformation of equivalent elastic SDOF system having the same lateral stiffness and damping coefficient as that of MDOF system.

Similarly, Displacement Coefficient Method described in FEMA-356 [20] is a non-iterative approximate procedure based on displacement modification factors. The expected maximum inelastic displacement of nonlinear MDOF system is obtained by modifying the elastic spectral displacement of an equivalent SDOF system with a series of coefficients.

The procedure proposed by Newmark and Hall [39] is based on the estimation of inelastic response spectra from elastic response spectra while displacement modification factor varies depending on the spectral region.

Miranda [33] conducted a statistical analysis of ratios of maximum inelastic to maximum elastic displacements computed from ground motions recorded on firm soils and proposed a simplified expression which depends on ductility and initial vibration period.

Miranda and Ruiz-García [34] conducted a study to evaluate the accuracy of approximate procedures proposed by Rosenblueth and Herrera [46], Gülkan and Sözen [23], Iwan [25], Kowalsky [29], Newmark and Hall [39] and Miranda [33]. SDOF systems with elasto-plastic, modified Clough stiffness degrading model [11] and Takeda hysteretic model [52] and periods between 0.05 and 3.0 s undergoing six different levels of maximum displacement ductility demands when subjected to 264 ground motions recorded on firm sites from 12 California were used. For each procedure, mean ratios of approximate to exact displacement and dispersion of relative errors were computed as a function of vibration period and displacement ductility ratio. Despite having relatively small mean errors, dispersion of results, particularly for large levels of inelastic behaviour, is substantial. It is concluded that approximate procedures can lead to significant errors in estimation of maximum displacement demand when applied to individual ground motion records.

Moreover, Chopra and Goel [8] have proposed an improved capacity-demand diagram method that uses constant ductility demand spectrum to estimate seismic deformation of inelastic SDOF systems.

More recently, Bracci, Kunnath and Reinhorn [5], Munshi and Goash [36], Kappos and Manafpour [28] proposed seismic performance evaluation procedures that utilize the basic principles of aforementioned simplified nonlinear analysis procedures.

2.3 PAST STUDIES ON PUSHOVER ANALYSIS

Most of the simplified nonlinear analysis procedures utilized for seismic performance evaluation make use of pushover analysis and/or equivalent SDOF representation of actual structure. However, pushover analysis involves certain approximations that the reliability and the accuracy of the procedure should be identified. For this purpose, researchers investigated various aspects of pushover analysis to identify the limitations and weaknesses of the procedure and proposed improved pushover procedures that consider the effects of lateral load patterns, higher modes, failure mechanisms, etc.

Krawinkler and Seneviratna [30] conducted a detailed study that discusses the advantages, disadvantages and the applicability of pushover analysis by considering various aspects of the procedure. The basic concepts and main assumptions on which the pushover analysis is based, target displacement estimation of MDOF structure through equivalent SDOF domain and the applied modification factors, importance of lateral load pattern on pushover predictions, the conditions under which pushover predictions are adequate or not and the information obtained from pushover analysis were identified. The accuracy of pushover predictions were evaluated on a 4-story steel perimeter frame damaged in 1994 Northridge earthquake. The frame was subjected to nine ground motion records. Local and global seismic demands were calculated from pushover analysis results at the target displacement associated with the individual records. The comparison of pushover and nonlinear dynamic analysis results showed that pushover analysis provides good predictions of seismic demands for low-rise structures having uniform distribution of inelastic behaviour over the height. It was also recommended to implement pushover analysis with caution and judgement considering its many limitations since the method is approximate in nature and it contains many unresolved issues that need to be investigated.

Mwafy and Elnashai [37] performed a series of pushover analyses and incremental dynamic collapse analyses to investigate the validity and the applicability of pushover analysis. Twelve reinforced concrete buildings with different structural systems (four 8-story irregular frame, four 12-story regular frame and four 8-story dual frame-wall), with different design accelerations (0.15g and 0.30g) and with different design ductility levels (low, medium and high) were utilized for the study. Nonlinear dynamic analysis using four natural and four artificial earthquake records scaled to peak ground accelerations of 0.15g and 0.30g were performed on detailed 2D models of the structures considering predefined local and global collapse limits. Then, complete pushover-like load-

displacement curves in the form of upper and lower response envelopes as well as the best fit (ideal envelope) were obtained for each structure by performing regression analyses using the results of nonlinear dynamic analyses. Also, pushover analyses using uniform, triangular and multimodal load patterns were conducted and pushover curves were obtained. The results showed that the triangular load pattern outcomes were in good correlation with dynamic analysis results and a conservative prediction of capacity and a reasonable estimation of deformation were obtained using triangular load pattern. It was also noted that pushover analysis is more appropriate for low-rise and short period structures and triangular loading is adequate to predict the response of such structures. Further developments on accounting the inelasticity of lateral load patterns which would enable more accurate analysis of high-rise and highly irregular structures were recommended.

The inability of invariant lateral load patterns to account for the redistribution of inertia forces and to predict higher mode effects in post-elastic range have led many researchers to propose adaptive load patterns. Fajfar and Fischinger [16] suggested using story forces proportional to the deflected shape of the structure, Eberhard and Sozen [15] proposed using load patterns based on mode shapes derived from secant stiffness at each load step and Bracci et. al [5] proposed the use of stiffness-dependent lateral force distributions in which story forces are proportional to story shear resistances at the previous step.

İnel, Tjhin and Aschheim [26] conducted a study to evaluate the accuracy of various lateral load patterns used in current pushover analysis procedures. First mode, inverted triangular, rectangular, "code", adaptive lateral load patterns and multimode pushover analysis were studied. Pushover analyses using the indicated lateral load patterns were performed on four buildings consisting of 3- and 9-story regular steel moment resisting frames designed as a part of SAC joint venture (FEMA-355C) [19] and modified versions of these buildings with a weak first story. Peak values of story displacement, interstory drift, story shear and overturning moment obtained from pushover analyses at different values of peak roof drifts representing elastic and various degrees of nonlinear response were compared to those obtained from nonlinear dynamic analysis. Nonlinear dynamic analyses were performed using 11 ground motion records selected from Pacific Earthquake Research Center (PEER) strong motion database. Approximate upper bounds of error for each lateral load pattern with respect to mean dynamic response were reported to illustrate the trends in the accuracy of load patterns. Simplified inelastic procedures

were found to provide very good estimates of peak displacement response for both regular and weak-story buildings. However, the estimates of interstory drift, story shear and overturning moment were generally improved when multiple modes were considered. The results also indicated that simplifications in the first mode lateral load pattern can be made without an appreciable loss of accuracy

Sasaki, Freeman and Paret [49] proposed Multi-Mode Pushover (MMP) procedure to identify failure mechanisms due to higher modes. The procedure uses independent load patterns based on higher modes besides the one based on fundamental mode. A pushover analysis is performed and a capacity curve is obtained for each load pattern considering the modes of interest. Structure's capacity for each mode is compared with earthquake demand by using Capacity Spectrum Method [3]. Capacity curves and response spectrum are plotted in ADRS format on the same graph and the intersections of capacity spectra with the response spectrum represent the seismic demand on the structure. A 17-story steel frame damaged by 1994 Northridge earthquake and a 12-story steel frame damaged by 1989 Loma Prieta earthquake were evaluated using MMP. For both frames, pushover analysis based only on first mode load pattern was inadequate to identify the actual damage. However, pushover results of higher modes and/or combined effect of 1st mode and higher modes matched more closely the actual damage distribution. It was concluded that MMP can be useful in identifying failure mechanisms due to higher modes for structures with significant higher-order modal response.

Although MMP is very useful to identify the effects of higher modes qualitatively, it can not provide an estimation of seismic responses and their distribution in the structure. Moghadam [35] proposed a procedure to quantify the effects of higher mode responses in tall buildings. A series of pushover analysis is performed on the buildings using elastic mode shapes as load pattern. Maximum seismic responses are estimated by combining the responses from the individual pushover analyses. The proposed combination rule is that response for each mode is multiplied by mass participating factor for the mode considered and contribution of each mode is summed. The procedure was applied to a 20-story steel moment resisting frame to assess the accuracy of the procedure. The frame was subjected to six earthquake ground motions and mean of maximum displacements and inter-story drift ratios of each story of the frame in six analyses were calculated. Also, pushover analyses for first three modes were performed on the frame and the responses for each mode were combined to estimate the final response. Comparison of estimated

displacements and inter-story drifts with the mean of maximum responses resulted from six nonlinear dynamic analysis indicated a good correlation.

Gupta [22] analysed the recorded responses of eight real buildings that experienced ground accelerations in the excess of 0.25g in 1994 Northridge earthquake to understand the behaviour of real structures and to evaluate the acceptability of pushover analysis. The selected buildings were 5, 7, 10, 13, 14, 17, 19- and 20-story structures having moment resisting and shear wall lateral force resisting sytems and were instrumented at the time of the earthquake. The recorded story displacement, inter-story drift, story inertia force and story shear profiles at various instants of time were evaluated. It was observed that the response of buildings were significantly affected by higher modes with the exception of low-rise structures and these effects were better understood by analysing the inertia force and story drift profiles rather than displacements. These observations indicated that the pushover analysis is inadequate and unconservative. Hence, Gupta [22] proposed Adaptive Modal Pushover Procedure which accounts for the effects of higher modes and limitations of traditional pushover analysis. The proposed method is, at any step, identical to response spectrum analysis. An incremental static analysis of the structure for story forces corresponding to each mode is performed independently. Any response quantity is calculated by an SRSS combination of respective modal quantities. Whenever some member(s) yield, a new structure is created by changing the stiffness of yielded member(s) and the procedure is repeated. The process is repeated until a specified global drift limit is reached. Any number of mode can be considered by the proposed procedure. The applicability and the accuracy of the procedure were evaluated by applying it to 4, 8, 12, 16- and 20-story frames with a variety of lateral force resisting systems (moment resisting frames, frames with soft first story, frames with weak stories and flexure-controlled isolated shear wall). The results of the proposed adaptive procedure were compared with the ones obtained from nonlinear dynamic analyses and pushover analyses with uniform and "code" lateral load patterns. Fifteen earthquake data from the SAC ground motion records [47] for Los Angeles area were used. PGAs of all ground motions used for nonlinear dynamic analyses of a given structure were scaled to have identical elastic 5 percent damped spectral acceleration at the fundamental period to reduce the variability of nonlinear response and to study the effects of higher modes. Global structure behaviour, inter-story drift distributions and plastic hinge locations were studied in detail. The results of the proposed adaptive procedure were in very good correlation with dynamic analyses while pushover analyses failed to capture the effects of

higher modes. The procedure was also validated using an existing multistory building for which instrumented data was available. The procedure can use site-specific spectra but it is unable to account for the effects of hysteretic degradation.

Chopra and Goel [9] developed an improved pushover analysis procedure named as Modal Pushover Analysis (MPA) which is based on structural dynamics theory. Firstly, the procedure was applied to linearly elastic buildings and it was shown that the procedure is equivalent to the well known response spectrum analysis. Then, the procedure was extended to estimate the seismic demands of inelastic systems by describing the assumptions and approximations involved. Earthquake induced demands for a 9-story SAC building were determined by MPA, nonlinear dynamic analysis and pushover analysis using uniform, "code" and multi-modal load patterns. The comparison of results indicated that pushover analysis for all load patterns greatly underestimates the story drift demands and lead to large errors in plastic hinge rotations. The MPA was more accurate than all pushover analyses in estimating floor displacements, story drifts, plastic hinge rotations and plastic hinge locations. MPA results were also shown to be weakly dependent on ground motion intensity based on the results obtained from El Centro ground motion scaled by factors varying from 0.25 to 3.0. It was concluded that by including the contributions of a sufficient number of modes (two or three), the height-wise distribution of responses estimated by MPA is generally similar to the 'exact' results from nonlinear dynamic analysis.

Chintanapakdee and Chopra [6] evaluated the accuracy of MPA procedure for a wide range of buildings and ground motions. Generic one-bay frames of 3, 6, 9, 12, 15- and 18-stories with five strength levels corresponding to SDOF-system ductility factors of 1, 1.5, 2, 4 and 6 were utilized. Each frame was analysed by a set of 20 large-magnitude-small-distance records obtained from California earthquakes. Median values of story drift demands from MPA and nonlinear dynamic analyses were calculated and compared. It was shown that with two or three modes included, MPA predictions were in good correlation with nonlinear dynamic analyses and MPA predicted the changing height-wise variation of demand with building height and SDOF-system ductlity factor accurately. The bias and dispersion in MPA estimates of seismic demands were found to increase for longer-period frames and larger SDOF-system ductility factor although no perfect trends were observed. It was also illustrated that the bias and dispersion in MPA estimates of seismic demand for inelastic frames were larger than those for elastic systems due to additional approximations involved in MPA procedure. Finally, the MPA procedure was

extended to estimate seismic demand of inelastic systems with seismic demand being defined by an elastic design spectrum.

Jan, Liu and Kao [27] proposed an upper bound pushover analysis procedure to estimate seismic demands of high-rise buildings by considering higher mode effects. In this procedure, the elastic displacement-response contribution ratios of higher modes with respect to fundamental mode is first obtained for a set of earthquake records and number of modes that dominate the displacement response is determined from the envelope curves of contribution ratios. Then, a pushover analysis using the newly formulated lateral load pattern and target displacement considering the contributions of higher modes as well as fundamental mode is performed to estimate seismic demands. The procedure was applied to 2, 5, 10, 20- and 30-story moment resisting frames of strong column-weak beam systems designed according to seismic code of Taiwan. The elastic displacement-response contribution ratios of higher modes were obtained by subjecting the frames to 13 earthquake records chosen from Chi Chi earhtquake. The envelope curves of contribution ratios showed that first two mode contributions were dominant that other higher modes were ignored. The proposed pushover analysis method was performed considering first two modes to estimate floor displacements, story drift ratios and plastic hinge rotations. The accuracy of the procedure was evaluated by comparing the results obtained from pushover analysis with triangular loading, modal pushover analysis and nonlinear dynamic analysis. Seismic predictions of pushover analysis with triangular loading and modal pushover analysis were in good correlation with nonlinear dynamic analysis for frames not taller than 10 stories while only the proposed procedure could predict the seismic demands of 20- and 30-story buildings.

CHAPTER 3

PUSHOVER ANALYSIS WITH DRAIN-2DX vs SAP2000

3.1 GENERAL

Nonlinear static analysis, or pushover analysis, could be performed directly by a computer program which can model nonlinear behavior of lateral load resisting members of a structure. However, the computational scheme and the assumptions involved in modeling nonlinear member behavior could be different that there may be variations in the pushover results obtained from different softwares. Therefore, the underlying principles of any software utilized for pushover analysis should be well understood to interprete the results of pushover analysis.

In this study, pushover analyses were performed on steel and reinforced concrete moment resisting frames by DRAIN-2DX [44] and SAP2000 [14] using various lateral load patterns to identify the basic principles of each software utilized in the implementation of pushover analysis. The approach of each software to model nonlinear force-displacement relationships was investigated. The pushover analysis results obtained from each software were compared to evaluate the ability of these softwares to perform pushover analysis on frame structures.

3.2 PUSHOVER ANALYSIS PROCEDURE

Pushover analysis can be performed as either force-controlled or displacement-controlled depending on the physical nature of the load and the behavior expected from the structure. Force-controlled option is useful when the load is known (such as gravity loading) and the structure is expected to be able to support the load. Displacement-controlled procedure should be used when specified drifts are sought (such as in seismic

loading), where the magnitude of the applied load is not known in advance, or when the structure can be expected to lose strength or become unstable.

Some computer programs (e.g. DRAIN-2DX [44], Nonlinear version of SAP2000 [14], ANSYS [2]) can model nonlinear behavior and perform pushover analysis directly to obtain capacity curve for two and/or three dimensional models of the structure. When such programs are not available or the available computer programs could not perform pushover analysis directly (e.g. ETABS [13], RISA [45], SAP90 [12]), a series of sequential elastic analyses are performed and superimposed to determine a force-displacement curve of the overall structure. A displacement-controlled pushover analysis is basically composed of the following steps:

1. A two or three dimensional model that represents the overall structural behavior is created.
2. Bilinear or trilinear load-deformation diagrams of all important members that affect lateral response are defined.
3. Gravity loads composed of dead loads and a specified portion of live loads are applied to the structural model initially.
4. A predefined lateral load pattern which is distributed along the building height is then applied.
5. Lateral loads are increased until some member(s) yield under the combined effects of gravity and lateral loads.
6. Base shear and roof displacement are recorded at first yielding.
7. The structural model is modified to account for the reduced stiffness of yielded member(s).
8. Gravity loads are removed and a new lateral load increment is applied to the modified structural model such that additional member(s) yield. Note that a separate analysis with zero initial conditions is performed on modified structural model under each incremental lateral load. Thus, member forces at the end of an incremental lateral load analysis are obtained by adding the forces from the current analysis to the sum of the those from the previous increments. In other words, the results of each incremental lateral load analysis are superimposed.
9. Similarly, the lateral load increment and the roof displacement increment are added to the corresponding previous total values to obtain the accumulated values of the base shear and the roof displacement.

10. Steps 7, 8 and 9 are repeated until the roof displacement reaches a certain level of deformation or the structure becomes unstable.
11. The roof diplacement is plotted with the base shear to get the global capacity (pushover) curve of the structure (Figure 3.1).

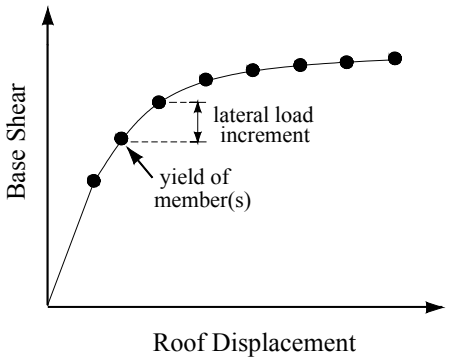

Figure 3.1 : Global Capacity (Pushover) Curve of Structure

3.3 PUSHOVER ANALYSIS WITH DRAIN-2DX

DRAIN-2DX is a general purpose computer program for static and dynamic analysis of inelastic plane structures. It performs nonlinear static and dynamic analyses, and for dynamic analysis considers ground accelerations (all supports moving in phase), ground displacements (supports may move out of phase), imposed dynamic loads and specified initial velocities. Mode shapes and periods can be calculated for any stressed state of structure. Linear response spectrum analyses can also be performed for the unstressed state.

3.3.1 Implementation of Pushover Analysis by DRAIN-2DX

A two dimensional structural model that represents the overall structural behavior is prepared through an input file that contains geometry, mass distribution, strength, stiffness and loading data of the structure.

Pushover analysis can consist of any number of pushover cases and each pushover case can have a different distribution of lateral load on the structure. A pushover case may start from zero initial conditions, or it may start from the end of a previous pushover case.

Pushover analysis is carried out by performing the "Gravity" analysis segment initially if the effects of gravity loads need to be considered. In "Gravity" analysis, only gravity loads are applied to the structure. The behavior under gravity loads must be linear

that the analysis terminates and does not continue for subsequent pushover analyses if plastic hinges occur during "Gravity" analysis.

The loading (load or displacement increment) for pushover analysis segment is applied in a specified number of steps and an event-to-event solution strategy is used within each step by dividing each step into substeps at each event. In other words, the program further selects a load substep size within any step by determining when the next stiffness change (event) occurs and ending the substep at that event [44].

In force-controlled pushover analysis of DRAIN-2DX, a constant load factor increment for each step is specified and load is applied incrementally until specified full load is reached. In displacement-controlled procedure, a constant displacement increment for each step is specified that the force increment is adjusted to achieve the specified displacement increment at each step. The analysis ends when the specified control displacement at the specified control node is reached.

The number of steps, maximum number of events in any step and number of successive direction changes (under displacement control only) are specified in pushover analysis input file that the analysis quits if these specified values are exceeded. Event overshoot tolerances are defined to determine the actual yield point of elements and a different value of event overshoot tolerance can be assigned for each element. The program also calculates the unbalanced loads at the end of each step and applies them as corrections in the next step without iterating on the unbalance. If unbalanced loads are significant, either the analysis is repeated with more steps to make unbalanced correction more often or a dummy static analysis with zero load is added so that an iteration on unbalanced load is performed.

Geometric nonlinearity can be considered through P-delta effects by adding a geometric stiffness matrix to the stiffness matrix of each element. The geometric stiffness matrix is changed at each event in a pushover analysis. However, none of the currently available elements of DRAIN-2DX accounts for true large displacement effects.

3.3.2 Element Description of DRAIN-2DX

DRAIN-2DX describes six types of frame element models. The description of element models is as follows:

Type 01 : Inelastic Truss Bar Element to model truss bars, simple columns and nonlinear support springs (Elastic buckling can be modeled)

Type 02 : Plastic Hinge Beam-Column Element to model beams and beam-columns of

steel and reinforced concrete type.

Type 04: Simple Inelastic Connection Element to model structural connections with rotational and/or translational flexibility

Type 06 : Elastic Panel Element to model only elastic behavior of rectangular panels with extensional, bending and/or shear stiffness.

Type 09 : Compression/Tension Link Element to model inelastic bar element with initial gap or axial force.

Type 15 : Fiber Beam-Column Element to model inelastic steel, reinforced concrete and composite steel-concrete members.

In DRAIN-2DX, the behavior in shear is assumed to be elastic and it is not possible to consider nonlinear shear effects.

In this study, pushover analyses were performed on steel and R/C moment resisting frames and frame elements were modeled as inelastic beam-column elements indicated as "Type 02" in the program element description guide [43]. "Type 02" element consists of a member with two rigid plastic hinges at member ends and optional rigid end zones. The nonlinear behavior of beam members are defined by specifying moment-curvature relationships for both positive and negative bending and interaction diagrams are specified for columns to represent nonlinear behavior.

However, "Type 02" element has serious limitations that have to be considered during modeling. The inelastic behavior is concentrated in zero-length plastic hinges that could only be defined at member ends and yielding takes place only in the plastic hinges. Besides, the plastic hinges are assumed to yield only in bending that inelastic axial deformations are neglected although the effect of axial forces on bending strength is considered by specifying interaction diagrams for columns. Moreover, "Type 02" element is assumed to be composed of elastic and inelastic components in parallel to model strain hardening in bending as shown in Figure 3.2. Plastic hinges that yield at constant moment form in the inelastic component and the moments in the elastic component continue to increase to simulate strain hardening [43].

Plastic hinges can exhibit only bilinear moment-curvature relationships and the interaction diagram of columns is composed of a series of straigth line segments which are idealized form of smooth interaction diagrams as shown in Figure 3.3.

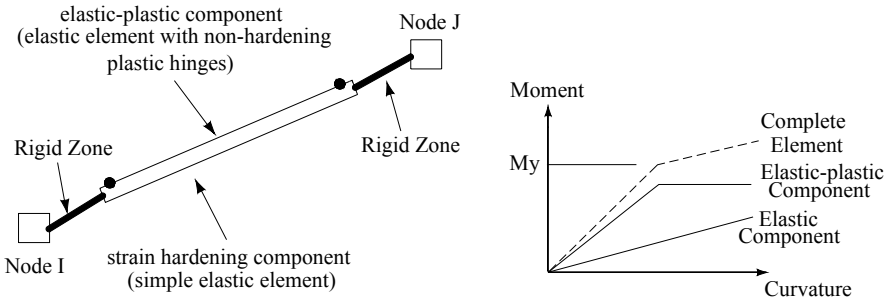

Figure 3.2 : Geometry and Moment-Curvature Relationship of "Type 02" Element

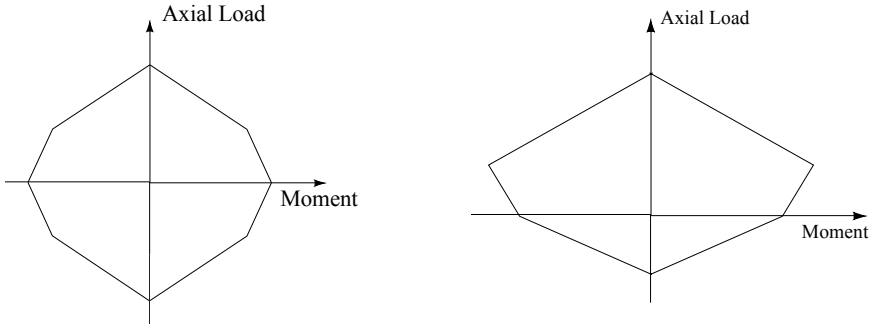

a) Steel Column b) Reinforced Concrete Column

Figure 3.3 : General Shape of Interaction Diagrams of Columns for "Type 02" Element

3.4 PUSHOVER ANALYSIS WITH SAP2000

Nonlinear static pushover analysis is a very powerful feature offered in the Nonlinear version of SAP2000. Pushover analysis can be performed on both two and three dimensional structural models.

Similar to DRAIN-2DX, pushover analysis can consist of any number of pushover cases and each pushover case can have a different distribution of lateral load on the structure. A pushover case may start from zero initial conditions, or it may start from the end of a previous pushover case. However, SAP2000 allows plastic hinging during "Gravity" pushover analysis.

SAP2000 can also perform pushover analysis as either force-contolled or displacement-controlled. The "Push To Load Level Defined By Pattern" option button is used to perform a force-controlled analysis (Figure 3.4). The pushover typically proceeds to the full load value defined by the sum of all loads included in the "Load Pattern" box (unless it fails to converge at a lower force value). "The Push To Displacement Magnitude" option button is used to perform a displacement-controlled analysis. The

pushover typically proceeds to the specified displacement in the specified control direction at the specified control joint (unless it fails to converge at a lower displacement value) [14].

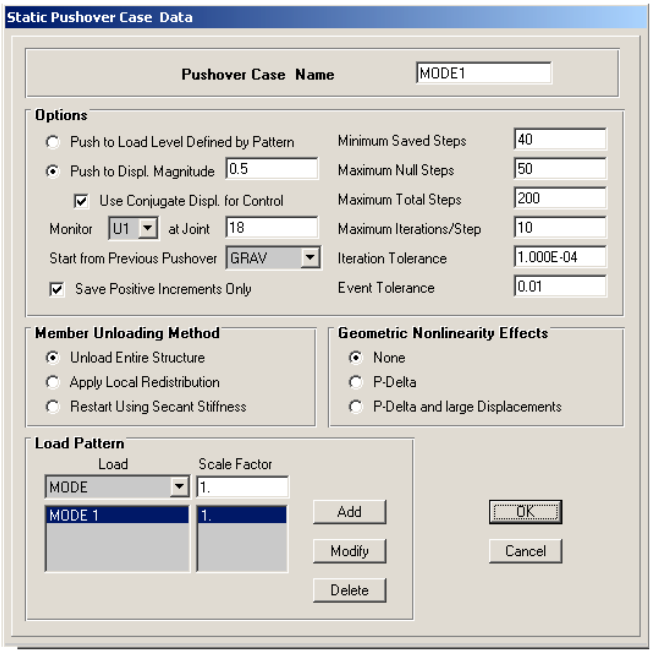

Figure 3.4 : Static Pushover Case Data Dialog Box (SAP2000)

An event-to-event solution strategy is utilized by SAP2000 pushover analysis and the parameters in the right-hand side of the "Options" area (Figure 3.4) control the pushover analysis. The "Minimum Saved Steps" and "Maximum Total Steps" provide control over the number of points actually saved in the pushover analysis. Only steps resulting in significant changes in the shape of the pushover curve are saved for output. "The Maximum Null Steps" is a cumulative counter through the entire analysis to account for the non-convergence in a step due to numerical sensitivity in the solution or a catastrophic failure in the structure. "Iteration Tolerance" and "Maximum Iteration/Step" are control parameters to check static equilibrium at the end of each step in a pushover analysis. If the ratio of the unbalanced-load to the applied-load exceeds the "Iteration Tolerance", the unbalanced load is applied to the structure in a second iteration for that step. These iterations continue until the unbalanced load satisfies the "Iteration Tolerance" or the "Maximum Iterations/Step" is reached [14]. A constant "Event Tolerance" for all elements is used to determine when an event actually occurs for a hinge.

Geometric nonlinearity can be considered through P-delta effects or P-delta effects plus large displacements (Figure 3.4).

Modal and uniform lateral load patterns can be directly defined by SAP2000 in addition to any user-defined static lateral load case. Modal load pattern is defined for any Eigen or Ritz mode while uniform load pattern is defined by uniform acceleration acting in any of the three global directions (acc dir X, acc dir Y and acc dir Z).

Nonlinear behavior of a frame element is represented by specified hinges in SAP2000 and a capacity drop occurs for a hinge when the hinge reaches a negative-sloped portion of its force-displacement curve during pushover analysis (Figure 3.5).

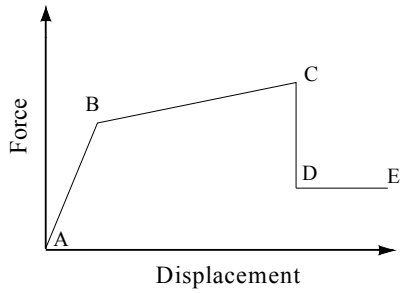

Figure 3.5 : Generalized Force-Displacement Characteristic of a Non-Degrading Frame Element of SAP2000

Such unloading along a negative slope is unstable in a static analysis and SAP2000 provides three different member unloading methods to remove the load that the hinge was carrying and redistribute it to the rest of the structure (Figure 3.4). In the "Unload Entire Structure" option, when the hinge reaches point C on its force-displacement curve (Figure 3.5) the program continues to try to increase the base shear. If this results in increased lateral deformation the analysis proceeds. If not, base shear is reduced by reversing the lateral load on the whole structure until the force in that hinge is consistent with the value at point D on its force-displacement curve (Figure 3.5). All elements unload and lateral displacement is reduced since the base shear is reduced. After the hinge is fully unloaded, base shear is again increased, lateral displacement begins to increase and other elements of the structure pick up the load that was removed from the unloaded hinge. If hinge unloading requires large reductions in the applied lateral load and two hinges compete to unload, i.e., where one hinge requires the applied load to increase while the other requires the load to decrease, the method fails.

In the "Apply Local Redistribution" option, only the element containing the hinge is unloaded instead of unloading the entire structure. If the program proceeds by reducing the base shear when a hinge reaches point C, the hinge unloading is performed by

applying a temporary, localized, self-equilibrating, internal load that unloads the element [14]. Once the hinge is unloaded, the temporary load is reversed, transferring the removed load to neighboring elements. This method will fail if two hinges in the same element compete to unload, i.e., where one hinge requires the temporary load to increase while the other requires the load to decrease.

In the "Restart Using Secant Stiffness" option, whenever any hinge reaches point C on force-displacement curve, all hinges that have become nonlinear are reformed using secant stiffness properties, and the analysis is restarted. This method may fail when the stress in a hinge under gravity load is large enough that the secant stiffness is negative. On the other hand, this method may also give solutions where the other two methods fail due to hinges with small (nearly horizontal) negative slopes [14].

If "Save Positive Increments Only" option box (Figure 3.4) is not checked in a pushover analysis, steps in which hinge unloading occur are also saved to represent the characteristics of member unloading method on pushover curve. However, pushover curve will become an envelope curve of all saved points if "Save Positive Increments Only" option box is checked.

The effects of "Member Unloading Method" and "Save Positive Increments Only" on pushover curve are illustrated in Figures 3.6-3.8.

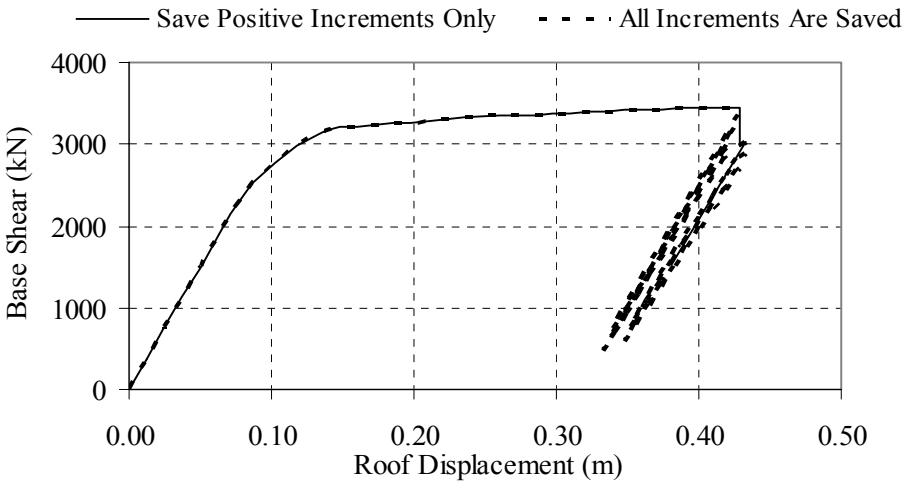

Figure 3.6 : Member Unloading Method-"Unload Entire Structure"

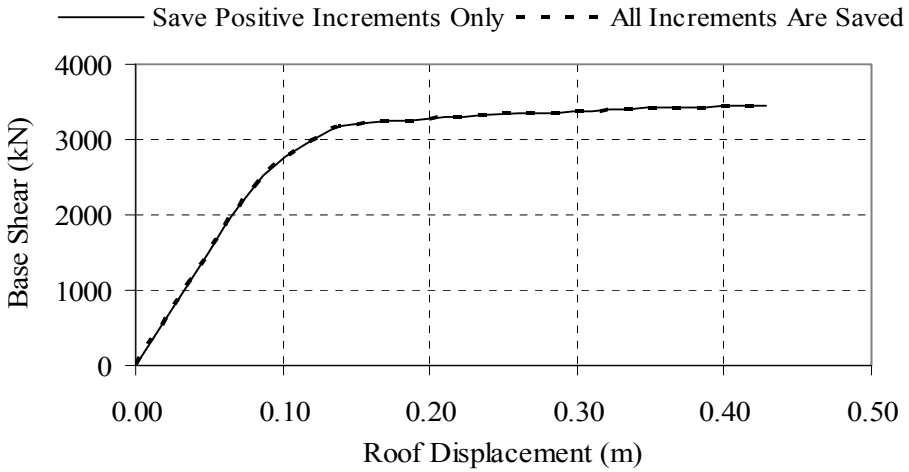

Figure 3.7 : Member Unloading Method-"Apply Local Redistribution"

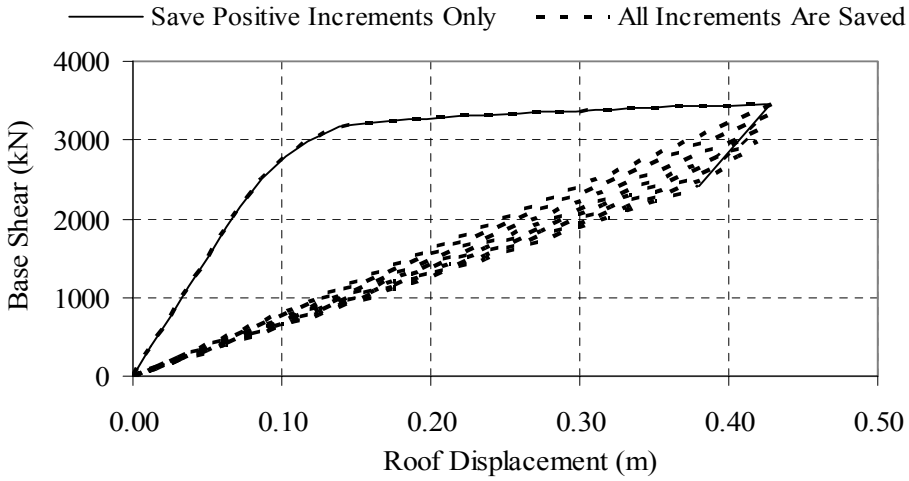

Figure 3.8 : Member Unloading Method-"Restart Loading Using Secant Stiffness"

Although pushover curves obtained from each method have same base shear capacity and maximum lateral displacement, pushover analysis is generally performed by using "Unload Entire Structure" unloading method with "Save Positive Increments Only" option because "Unload Entire Structure" is the most efficient method and uses a moderate number of total and null steps. However, "Apply Local Redistribution" requires a lot of very small steps and null steps that the unloading branch of pushover curve could not be observed usually. "Restart Loading Using Secant Stiffness" is the least efficient method with the number of steps required increasing as the square of the target displacement. It is also the most robust (least likely to fail) provided that the gravity load is not too large [14].

3.4.1 Element Description of SAP2000

In SAP2000, a frame element is modeled as a line element having linearly elastic properties and nonlinear force-displacement characteristics of individual frame elements are modeled as hinges represented by a series of straight line segments. A generalized force-displacement characteristic of a non-degrading frame element (or hinge properties) in SAP2000 is shown in Figure 3.5.

Point A corresponds to unloaded condition and point B represents yielding of the element. The ordinate at C corresponds to nominal strength and abscissa at C corresponds to the deformation at which significant strength degradation begins. The drop from C to D represents the initial failure of the element and resistance to lateral loads beyond point C is usually unreliable. The residual resistance from D to E allows the frame elements to sustain gravity loads. Beyond point E, the maximum deformation capacity, gravity load can no longer be sustained.

Hinges can be assigned at any number of locations (potential yielding points) along the span of the frame element as well as element ends. Uncoupled moment (M2 and M3), torsion (T), axial force (P) and shear (V2 and V3) force-displacement relations can be defined. As the column axial load changes under lateral loading, there is also a coupled P-M2-M3 (PMM) hinge which yields based on the interaction of axial force and bending moments at the hinge location. Also, more than one type of hinge can be assigned at the same location of a frame element.

There are three types of hinge properties in SAP2000. They are default hinge properties, user-defined hinge properties and generated hinge properties. Only default hinge properties and user-defined hinge properties can be assigned to frame elements. When these hinge properties (default and user-defined) are assigned to a frame element, the program automatically creates a new generated hinge property for each and every hinge.

Default hinge properties could not be modified and they are section dependent. When default hinge properties are used, the program combines its built-in default criteria with the defined section properties for each element to generate the final hinge properties. The built-in default hinge properties for steel and concrete members are based on ATC-40 [3] and FEMA-273 [18] criteria.

User-defined hinge properties can be based on default properties or they can be fully user-defined. When user-defined properties are not based on default properties, then

the properties can be viewed and modified. The generated hinge properties are used in the analysis. They could be viewed, but they could not be modified.

3.4.2 Force-Displacement Relationships

In SAP2000, the nonlinear behavior of beams and columns is represented by assigning concentrated plastic hinges at member ends where flexural yielding is assumed to occur. Flexural characteristics of beams are defined by moment-rotation relationships assigned as moment hinges at beam ends. A three dimensional interaction surface with five equally spaced axial force-bending moment interaction diagrams and a moment-rotation relationship are defined to represent the flexural characteristics of plastic hinges at column ends.

Both default and user-defined force-displacement characteristics of plastic hinges were utilized to perform pushover analyses. Moment-curvature relationships of beams and columns and interaction diagrams of columns were calculated based on the section and material properties given in Appendix A to define the user-defined force-displacement characteristics of the members. For this purpose, the axial forces in beams were assumed to be zero. The column axial forces were assumed to be constant during an earthquake and the axial forces due to dead load and 25% live load were used to calculate the moment-curvature relationships of columns. Response 2000 [4] was utilized to determine cross-sectional properties of R/C members.

For user-defined hinge properties, the procedure used by Saidii and Sozen [48] and Park and Paulay [41] was utilized to determine moment-rotation relationships of members from the moment-curvature relationships. In this procedure, the moment is assumed to vary linearly along the beams and columns with a contraflexure point at the middle of the members. Based on this assumption, the relationship between curvature and rotation at yield is obtained as follows;

$$\theta_y = \frac{L \cdot \varphi_y}{6} \tag{3.1}$$

where L : Member length

φ_y : Curvature at yield

θ_y : Rotation at yield

Plastic hinge rotation capacity of members is estimated using the following equation proposed by ATC-40 [3] and rotation value at ultimate moment is obtained by adding plastic rotation to the yield rotation.

$$\theta_p = (\varphi_{ult} - \varphi_y)\, l_p \tag{3.2}$$

where l_p : Plastic hinge length

φ_{ult} : Ultimate curvature

θ_p : Plastic rotation

ATC-40 [3] suggests that plastic hinge length equals to half of the section depth in the direction of loading is an acceptable value which generally gives conservative results. This suggestion was adapted to calculate plastic hinge length in this study.

In addition to moment-rotation relationships, a three dimensional interaction surface with five equally spaced axial force-bending moment interaction diagrams has to be defined for columns. Although the program could not update the moment-rotation relationships due to the variations in axial load levels during pushover analysis, the yield and ultimate moment values are updated by using the three dimensional interaction surface. Axial force-bending moment interaction diagrams about two major axes of each column section are utilized to determine the other three axial force-bending moment interaction diagrams required to define the three dimensional interaction surface according to the following equation proposed by Parme et al. [42].

$$\left(\frac{M_{ux}}{M_{uxo}}\right)^{\log 0.5 / \log \beta} + \left(\frac{M_{uy}}{M_{uyo}}\right)^{\log 0.5 / \log \beta} = 1 \tag{3.3}$$

where M_{uxo} : Uniaxial flexural strength about x-axis

M_{uyo} : Uniaxial flexural strength about y-axis

M_{ux} : Component of biaxial flexural strength on the x-axis at required inclination

M_{uy} : Component of biaxial flexural strength on the y-axis at required inclination

β : Parameter dictating the shape of interaction surface

However, the program is very sensitive to the shape of the interaction surfaces that user-defined interaction surfaces could cause an error warning which terminates the analysis.

The comparison of default and user-defined hinge properties for steel and concrete sections and the effect of hinge properties on pushover analysis, hence the capacity (pushover) curve, are discussed in the following sections.

3.4.2.1 Default vs User-Defined Hinge Properties for Steel Sections

The built-in default hinge characteristics of steel sections are based on ATC-40 [3] and FEMA-273 [18] criteria. FEMA-273 [18] proposes the following equations to calculate the yield moment and yield rotation of steel beams and columns;

$$M_y = F_y Z \tag{3.4}$$

$$\theta_y = F_y ZL/6EI \tag{3.5}$$

where F_y : Yield strength of steel

Z : Plastic section modulus

L : Member length

E : Modulus of elasticity

I : Moment of inertia with respect to the bending axis

Slope between points B and C is taken as 3% strain hardening and the points C, D and E are based on FEMA-273 [18] for built-in default steel hinges (Figure 3.5). It should be mentioned that Equation 3.5 proposed by FEMA-273 [18] exactly equals to the Equation 3.1 since $\varphi_y = M_y / EI$. Also, the program makes use of ultimate strength-interaction equations to define axial force-bending moment interaction diagrams of steel columns.

The yield moment, yield rotation and axial force-bending moment interaction diagrams about two major axes can be calculated numerically using section and material properties for user-defined steel moment and PMM hinges and the equations used for those calculations are exactly same with the ones that FEMA-273 [18] proposes for default hinges. However, plastic rotation capacities and strain hardening of hinges should be determined from the moment-curvature relationships. The moment-curvature relationships of steel sections depend on both axial load level and slenderness ratio that determination of moment-curvature relationships of each steel section becomes a complex

task. In other words, default and user-defined steel moment and PMM hinges have same characteristics except plastic rotation capacities and strain hardening ratios.

For this reason, although user-defined moment-rotation relationships would yield different plastic rotation capacities and strain hardening ratios, default steel moment and PMM hinges were used to perform pushover analyses for steel frames for the sake of simplicity in this study.

The effects of plastic rotation capacities and strain hardening ratios of hinges on pushover analysis are studied in detail for concrete sections for which the conclusions are also applicable for steel sections.

3.4.2.2 Default vs User-Defined Hinge Properties for Concrete Sections

The built-in default hinge characteristics of concrete sections are based on ATC-40 [3] and FEMA-273 [18] criteria which consider basic parameters controlling the behavior. Based on these parameters, in this study, default moment hinges assigned to all beams have same plastic rotation capacities and default PMM hinges assigned to all columns have same plastic rotation capacities regardless of the section dimensions. Slope between points B and C is taken as 10% total strain hardening for steel and yield rotation is taken as zero for default concrete moment and PMM hinges.

On the other hand, user-defined moment-rotation relationships and interaction surfaces were obtained using the procedure described in Section 3.4.2.

The default and user-defined moment-rotation relationships and interaction diagrams for 5-story R/C frame are presented in Tables 3.1-3.2 and Figure 3.9, respectively. Scale factors (SF) for rotations are taken as unity while scale factors (SF) for moment capacities of beams are presented in Table 3.3. Only the interaction diagram with respect to the bending axis is considered for comparison since a two dimensional structure is studied.

Table 3.1: Moment-Rotation Relationships of Default Concrete Moment and PMM Hinges

		BEAMS	COLUMNS
Point	**Moment/SF**	**Rotation/SF**	**Rotation/SF**
E-	-0.2	-0.035	-0.025
D-	-0.2	-0.02	-0.015
C-	-1.1	-0.02	-0.015
B-	-1	0	0
A	0	0	0
B	1	0	0
C	1.1	0.02	0.015
D	0.2	0.02	0.015
E	0.2	0.035	0.025

Table 3.2: Moment-Rotation Relationships of User-Defined Moment and PMM Hinges for 5-Story R/C Frame

		BEAM1	BEAM2	COLUMNS
Point	**Moment/SF**	**Rotation/SF**	**Rotation/SF**	**Rotation/SF**
E-	-0.2	-0.040	-0.040	-0.030
D-	-0.2	-0.028	-0.029	-0.027
C-	-1.1	-0.028	-0.029	-0.027
B-	-1	-0.008	-0.011	-0.004
A	0	0	0	0
B	1	0.007	0.009	0.004
C	1	0.035	0.037	0.027
D	0.2	0.035	0.037	0.027
E	0.2	0.040	0.040	0.030

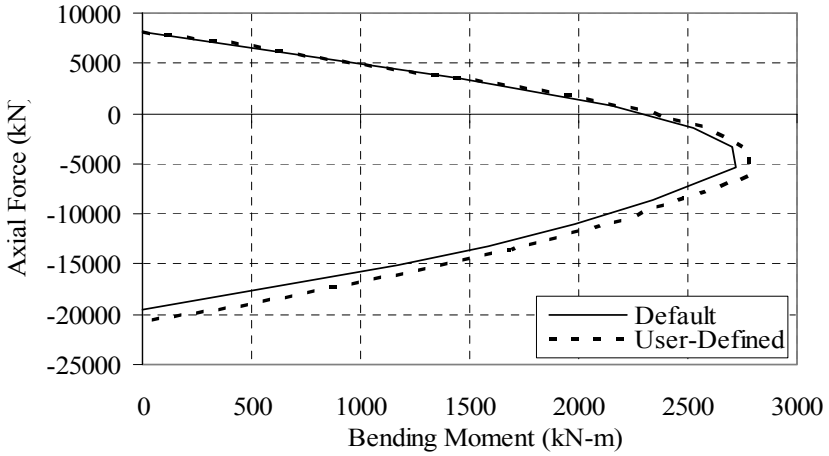

Figure 3.9 : Default and User-Defined Interaction Diagrams About Bending Axis for 5-Story R/C Frame

Table 3.3: Moment Capacity Scale Factors for Default and User-Defined Moment Hinges for 5-Story R/C Frame

	DEFAULT		USER-DEFINED	
	$+M_{SF}$ (kN)	$-M_{SF}$ (kN)	$+M_{SF}$ (kN)	$-M_{SF}$ (kN)
BEAM1	763.8	1101.5	782	1226
BEAM2	467.1	614.7	474	699

The comparison of default and user-defined moment-rotation relationships of hinges shows that default and user-defined concrete moment and PMM hinges could have totally different characteristics. User-defined hinges have higher plastic rotation capacities than default hinges for both moment and PMM hinges and user-defined hinges have a yield rotation value at yield point though yield rotation is not used in analysis. Moment capacities of user-defined moment hinges are higher than those of default moment hinges but user-defined hinges are elasto-plastic while default hinges have 10% total strain hardening for steel. Also, the default and user-defined interaction diagrams are almost same for tensile and low level of compressive axial loads but the discrepancy is substantial for high levels of compressive axial loads.

Pushover analyses were performed using both default and user-defined hinge properties and the effect of hinge properties were illustrated on pushover curves as shown in Figures 3.10-3.11.

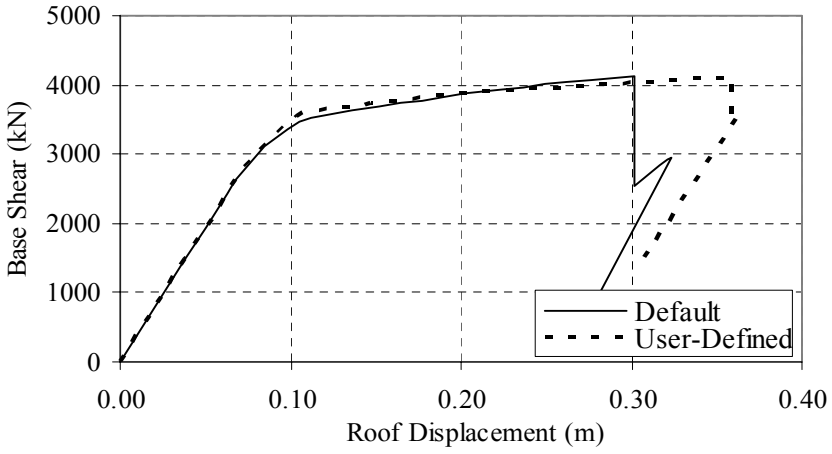

Figure 3.10 : Pushover Curves Obtained Using Default and User-Defined Hinge Properties for 5-Story R/C Frame Under 'Uniform' Lateral Load Pattern

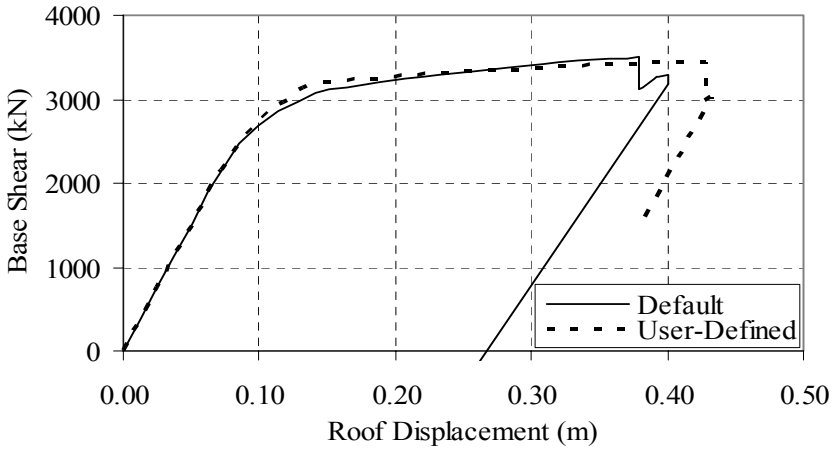

Figure 3.11 : Pushover Curves Obtained Using Default and User-Defined Hinge Properties for 5-Story R/C Frame Under 'Elastic First Mode' Lateral Load Pattern

The comparison of pushover curves obtained using default and user-defined hinge properties shows that the higher plastic rotation capacities, or rotation ductilities, of user-defined hinges yield to a higher maximum lateral displacement of the structure. Base shear capacity of the structure may be expected to be lower when default hinge properties are used because default hinges have lower moment capacities for beams and the interaction diagrams of default hinges remain inside the interaction diagrams of user-defined hinges. However, pushover analyses using default and user-defined hinges yielded almost the same base shear capacity since during pushover analyses the axial load levels of columns reached to very low values for which the difference between interaction diagrams were negligible and the strain hardening associated with default hinges accounted for the difference in moment capacities of beams in the inelastic range. On the other hand, the negligible difference in the interaction diagrams between default and user-defined hinges would be amplified and could cause variations in the base shear capacity of a structure if plastic hinging at columns are widely observed. Also, the difference in the interaction diagrams of default and user-defined hinges could cause more important variations in the pushover analysis of a three dimensional structure because not only interaction diagram about major axis but also interaction diagrams about other axes will be utilized as biaxial bending will occur in a three dimensional structure

Pushover analyses with default and user-defined hinge properties yield differences in sequence of plastic hinging and hinge pattern. The rotation value at the yield point of

hinges is not needed for pushover analyses performed by SAP2000 because the program uses cross-sectional dimensions in the elastic range.

Default hinge properties based on ATC-40 [3] and FEMA-273 [18] criteria are generally peferred to perform pushover analysis by SAP2000 because determination of cross-sectional characteristics of all members of a structure, especially for a three dimensional structure, and inputting these sectional properties into the program make the pushover analysis impractical. Thus, the results of a pushover analysis with default hinge properties should be interpreted with caution since default hinges could not simulate the exact nonlinear behavior of the structure.

Although the effects of default and user-defined hinges on pushover analysis are studied for 5-story R/C frame in this section, pushover analyses with default and user-defined hinges were also performed for 2, 5, 8- and 12-story R/C frames using various lateral load patterns and same conclusions were also derived from all cases considered.

3.5 COMPARISON OF PUSHOVER ANALYSIS WITH DRAIN-2DX vs SAP2000

Pushover anlayses using various lateral load patterns ('Uniform', 'Elastic First Mode', 'Code', 'FEMA-273', 'Multi-Modal (SRSS)' and 'Mode 2') were performed on steel and reinforced concrete frames by DRAIN-2DX and SAP2000 to understand the underlying principles of each software utilized for pushover analyses and to compare the pushover results obtained from each software.

Pushover analyses for steel frames were performed using default hinge properties by SAP2000. Positive and negative bending moment capacities of beams and interaction diagrams of columns which are exactly same with default hinge properties of SAP2000 were determined as described in Section 3.4.2.1 and were input to DRAIN-2DX to represent the nonlinear behavior. Also, to be consistent, same strain hardening ratio with default hinges were specified in DRAIN-2DX since exact moment-curvatures of steel sections were not determined. For steel frames, all specified cross-sectional properties that represent nonlinear behavior are exactly same in both softwares. The pushover curves obtained from both softwares for 2, 5- and 13-story steel frames with various lateral load patterns are presented in Figures 3.13-3.15.

Pushover analyses using user-defined hinge properties were performed by SAP2000 to make comparison with the results of DRAIN-2DX for concrete frames. User-defined moment-rotation relationships and interaction surfaces were obtained using the procedure described in Section 3.4.2. Positive and negative bending moment capacities of

beams, strain hardening ratios of members obtained from moment-curvature relationships and idealized form of smooth interaction diagrams of columns as shown in Figure 3.3 were input to DRAIN-2DX to represent the nonlinear behavior. For concrete frames, all specified cross-sectional properties that represent nonlinear behavior are exactly same in both softwares except the interaction diagrams of columns (Figure 3.12). The pushover curves obtained from both softwares for 2, 5, 8- and 12-story reinforced concrete frames with various lateral load patterns are presented in Figures 3.16-3.19.

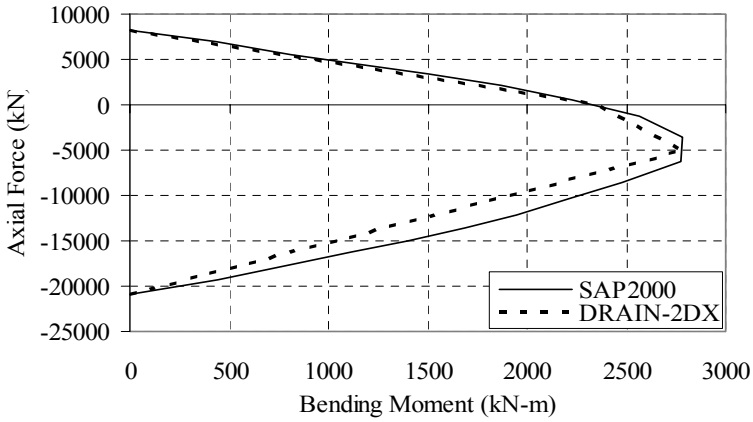

Figure 3.12 : Interaction Diagrams of Columns for SAP2000 and DRAIN-2DX

The computational approach of DRAIN-2DX and SAP2000 on pushover analysis is similar that both programs use an event-to-event solution strategy and utilize some parameters that control the pushover analysis such as number of steps, maximum number of events, event tolerance, etc. although there are some variations in these parameters as discussed in this study. SAP2000 proposes three types of member unloading methods whose effects on the pushover analysis procedure could be reflected on the pushover curve. Based on the general shape of pushover curves, DRAIN-2DX probably performs pushover analysis by "Unload Entire Structure" option although no information is presented in the user guide.

However, the results of a pushover analysis mainly depend on the modeling of nonlinear behavior of lateral load resisting members and there are variations in modeling the nonlinear member behavior for both softwares. Both softwares utilize concentrated plastic hinges to represent the nonlinear behavior of members but plastic hinges can only be defined at member ends in DRAIN-2DX while plastic hinges can be defined at any point along the span of member as well as member ends in SAP2000. In DRAIN-2DX,

plastic hinges are assumed to yield only in bending and nonlinear behavior of columns are simulated by idealized interaction diagrams which neglect inelastic axial deformations that actual column behavior could not be defined. The use of fiber models would be more appropriate to simulate column behavior although input preparation for fiber models is more complex.

The comparison of pushover curves obtained from both softwares shows that both softwares produced almost the same pushover curves for both steel and R/C frames for the lateral load patterns considered. However, the approach utilized by DRAIN-2DX to model strain hardening in bendig causes a difference in the capacity curves of steel frames and DRAIN-2DX yielded negligibly smaller base shear capacity for steel frames. Also, pushover curves obtained from DRAIN-2DX for 8- and 12-story R/C frames have base shear capacities of about 5% lower than those of SAP2000 because these frames have plastic hinging at columns at initial stages of yielding and the discrepancy in the interaction diagrams of both softwares caused the difference in the base shear capacity. The effectiveness of the idealized interaction diagrams to represent inelastic column behavior affects the accuracy of pushover predictions of DRAIN-2DX, especially plastic hinging at columns are widely observed.

An oddly-shaped pushover curve was obtained from pushover analysis performed by SAP2000 for 2-story R/C frame under second mode lateral load pattern. The load pattern caused the roof displacement to first increase in one direction and then the reverse direction. However, DRAIN-2DX could not catch this behavior and quits the analysis when reversal starts to occur.

The comparison of pushover curves also reveals an important feature of DRAIN-2DX. DRAIN-2DX could only model bilinear moment-curvature relationships of members to represent nonlinear behavior during pushover analysis and the program could not set a limit for maximum deformation capacities of the members. Therefore, pushover curves obtained from DRAIN-2DX yield unlimited lateral deformation capacities for structures that DRAIN-2DX could not specify a reliable permitted maximum lateral response of the structures for seismic performance evaluation purposes. On the other hand, SAP2000 could model initial failure (strength degradation) and maximum deformation capacities of members under lateral loading that the structures have a definite maximum lateral displacement capacity.

Also, both softwares yielded almost same sequence of plastic hinging and plastic hinge patterns for the pushover analyses with the lateral load patterns considered here.

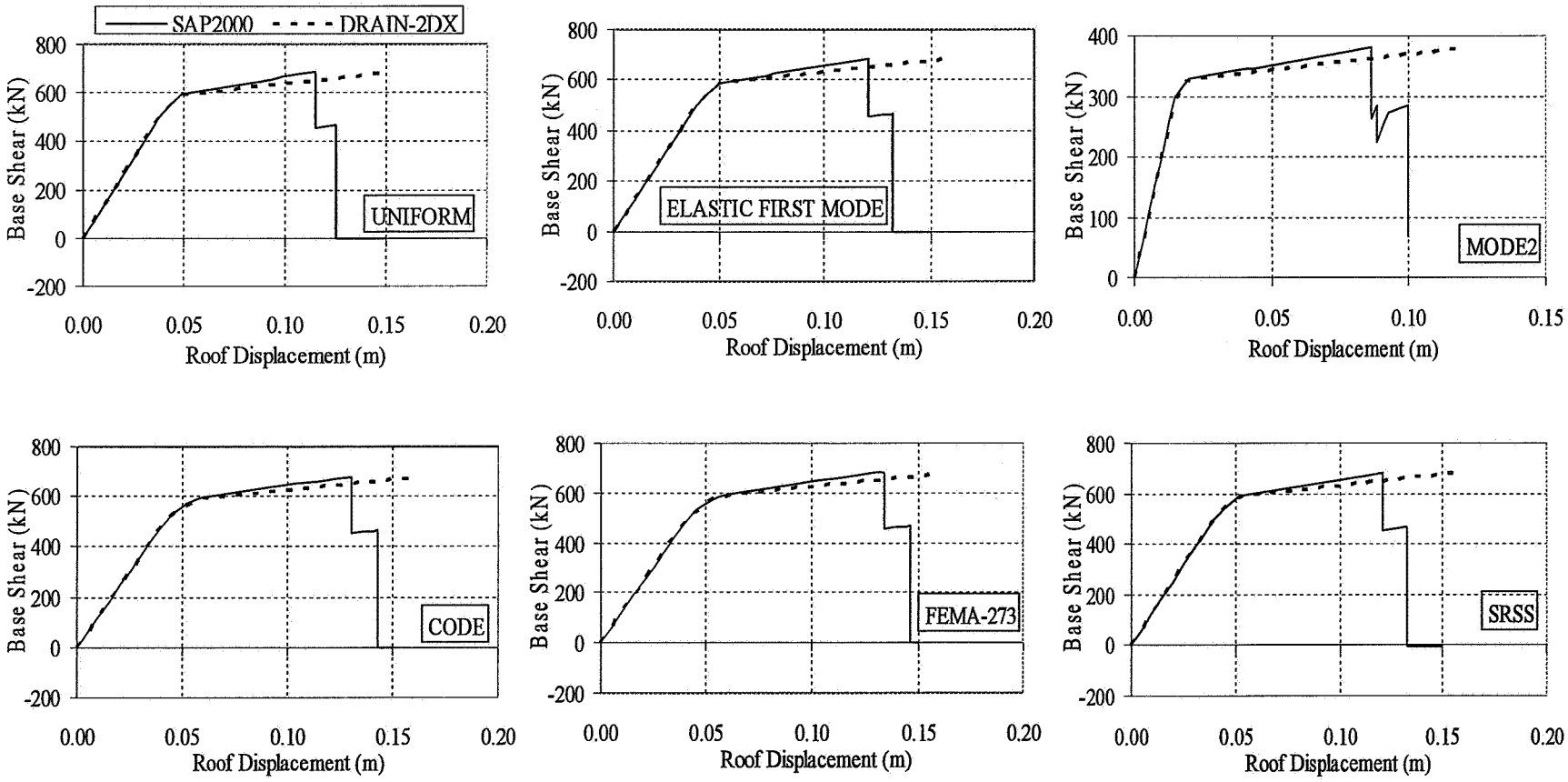

Figure 3.13 : Pushover (Capacity) Curves for 2-Story Steel Frame

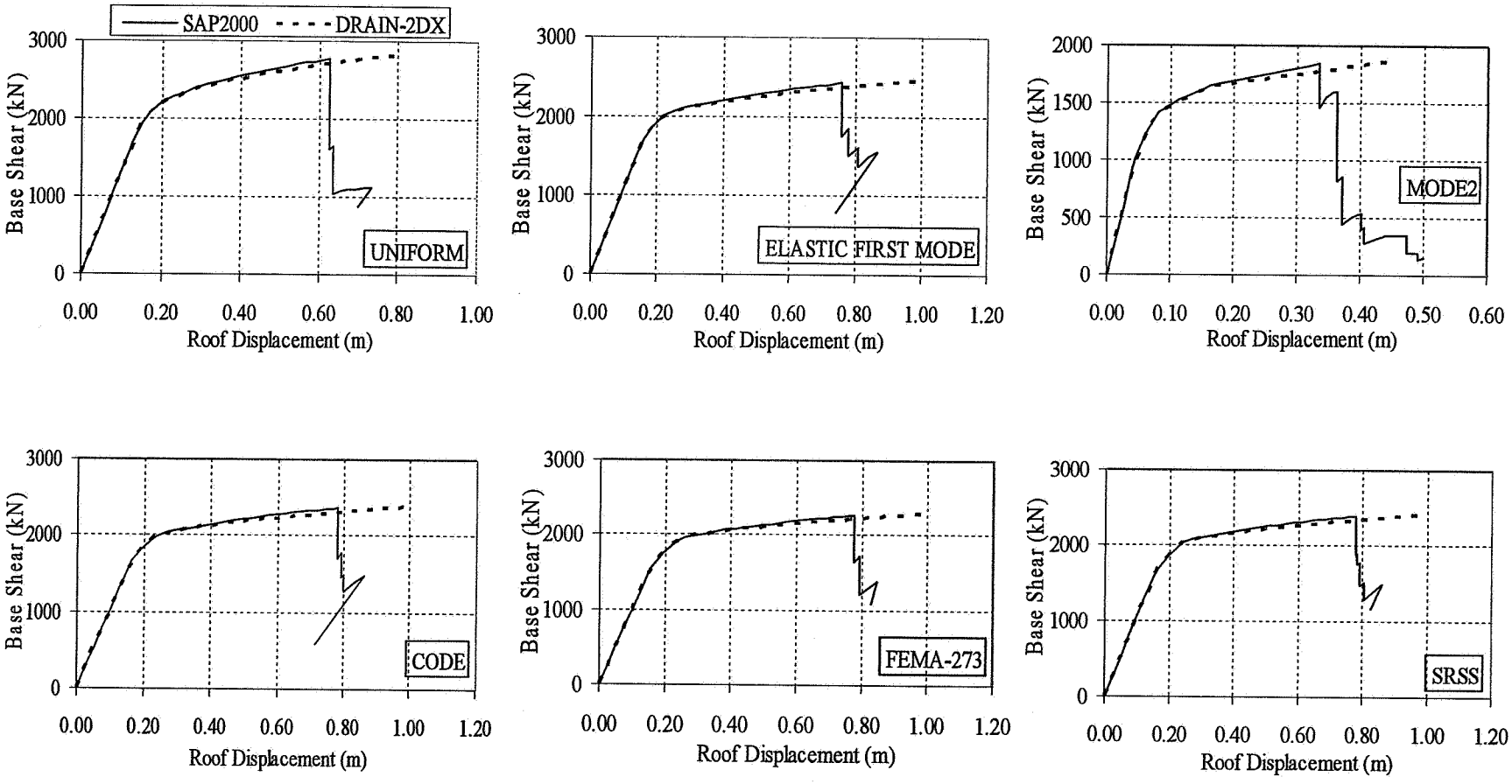

Figure 3.14 : Pushover (Capacity) Curves for 5-Story Steel Frame

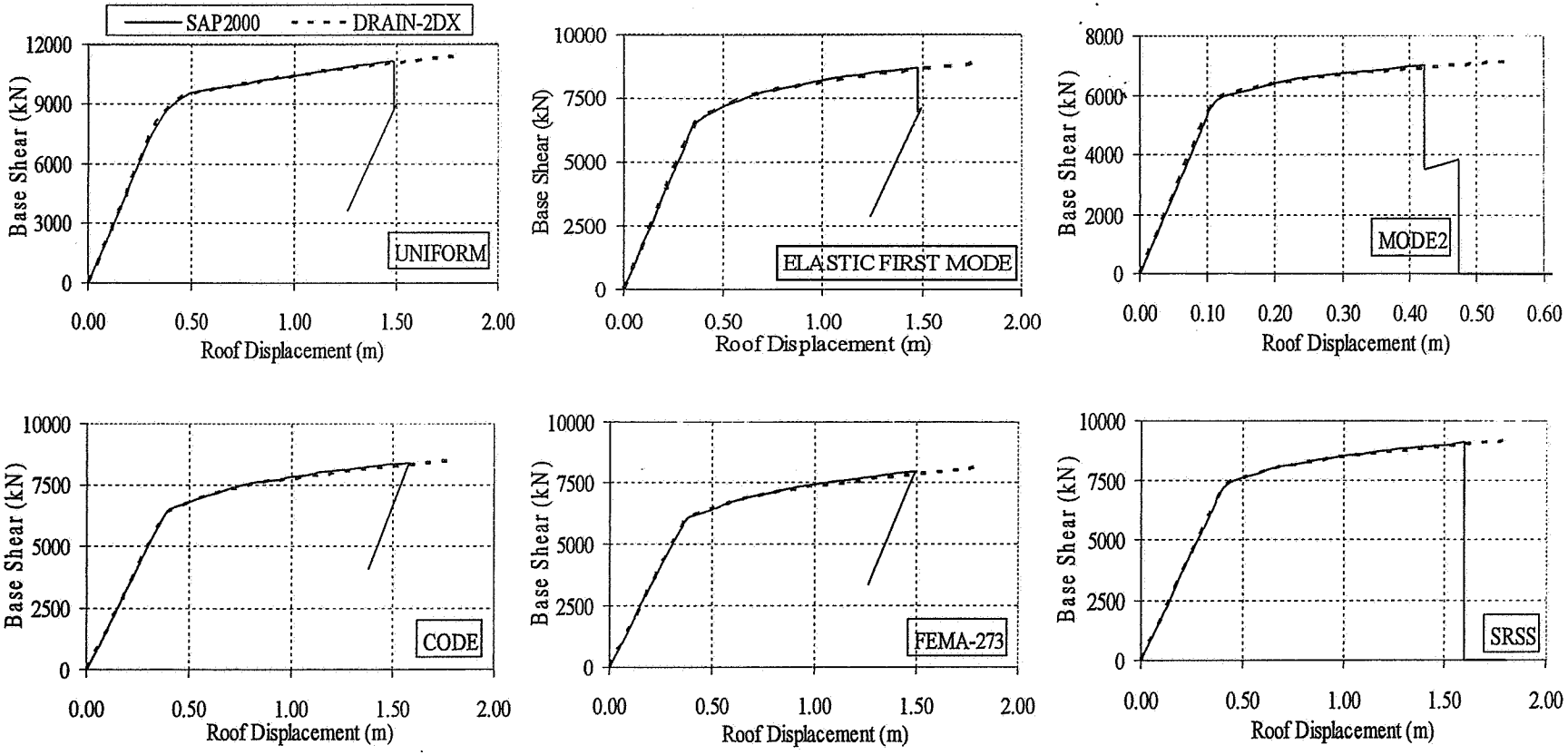

Figure 3.15 : Pushover (Capacity) Curves for 13-Story Steel Frame

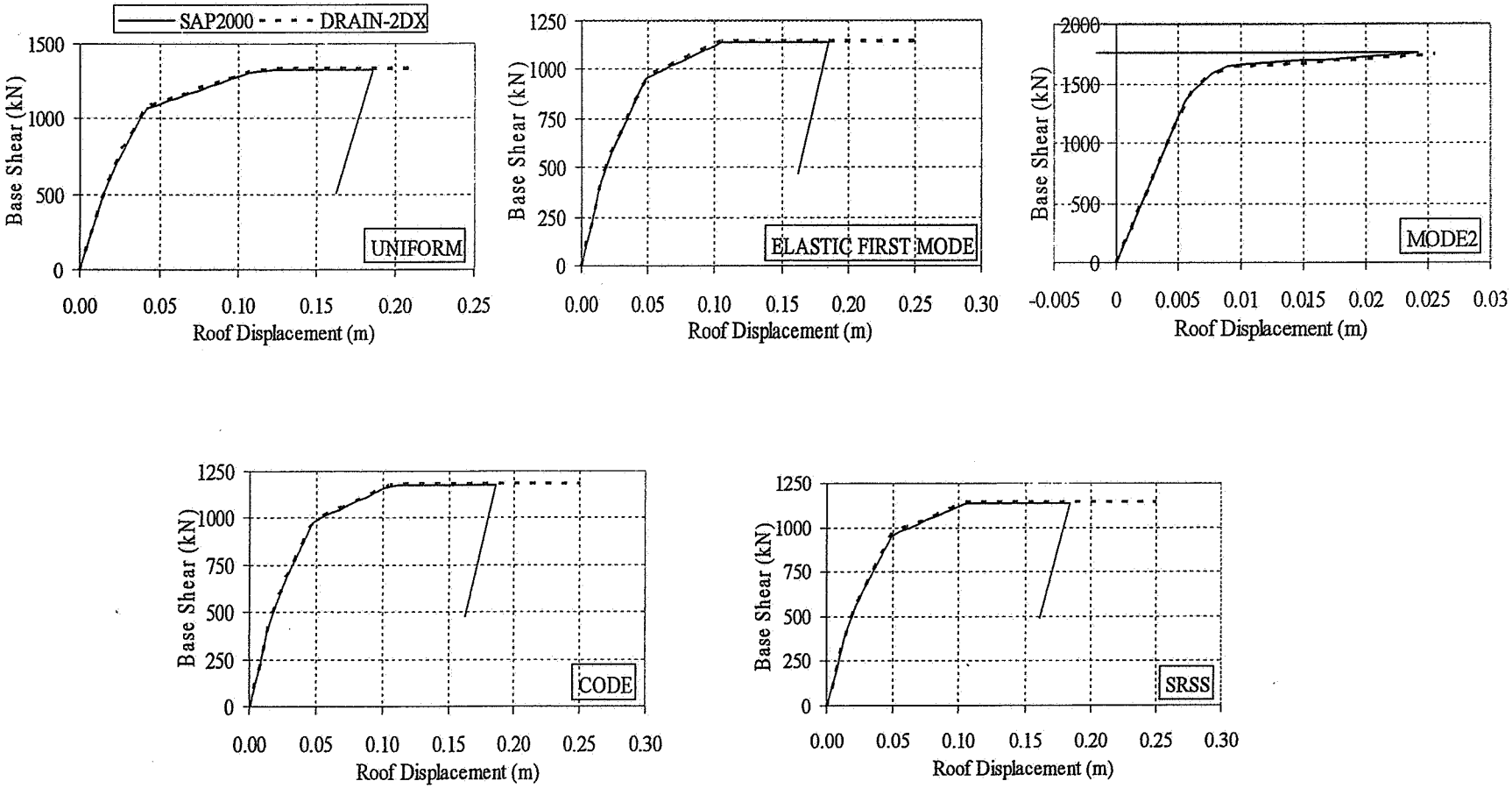

Figure 3.16 : Pushover (Capacity) Curves for 2-Story R/C Frame

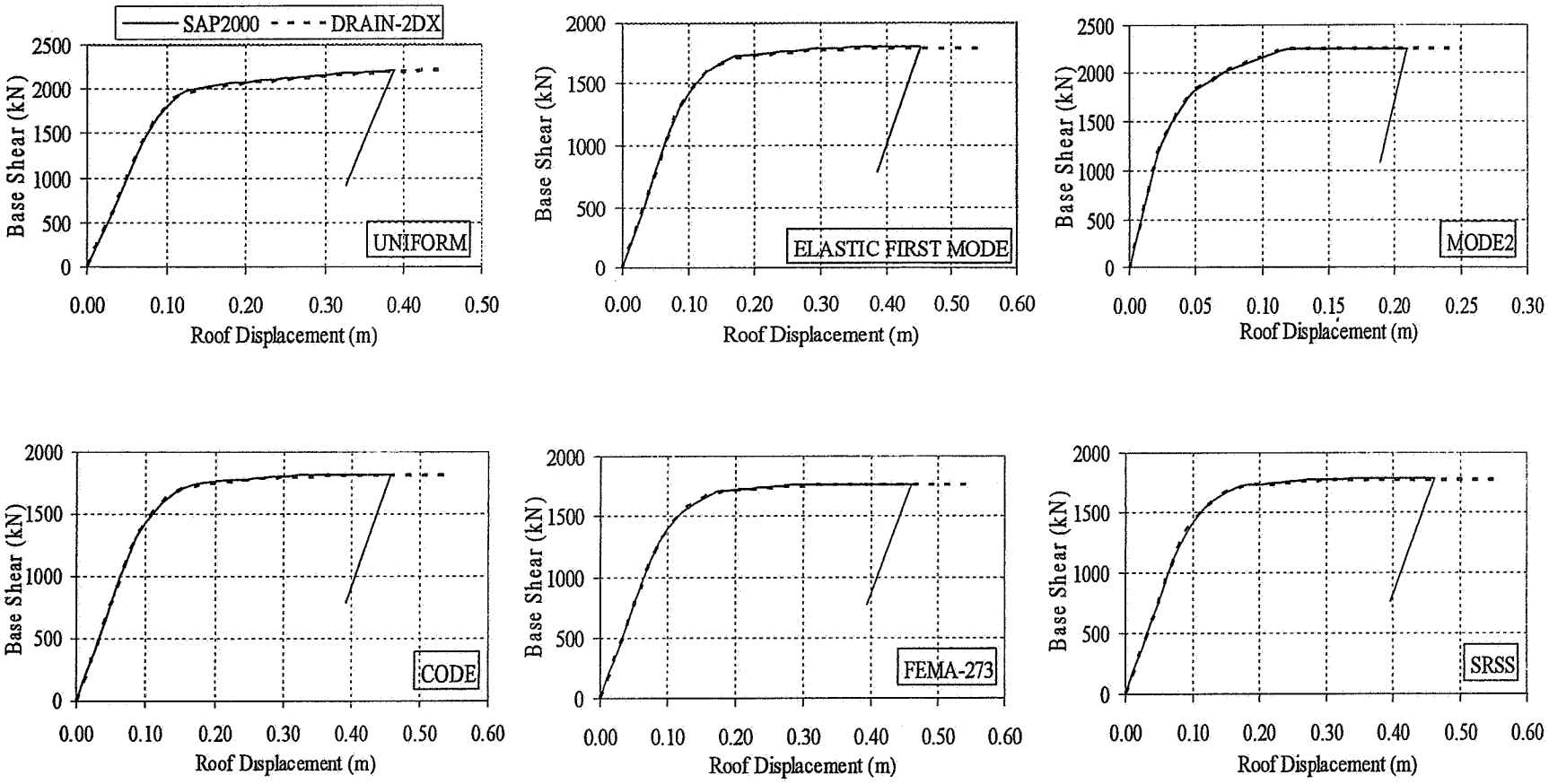

Figure 3.17 : Pushover (Capacity) Curves for 5-Story R/C Frame

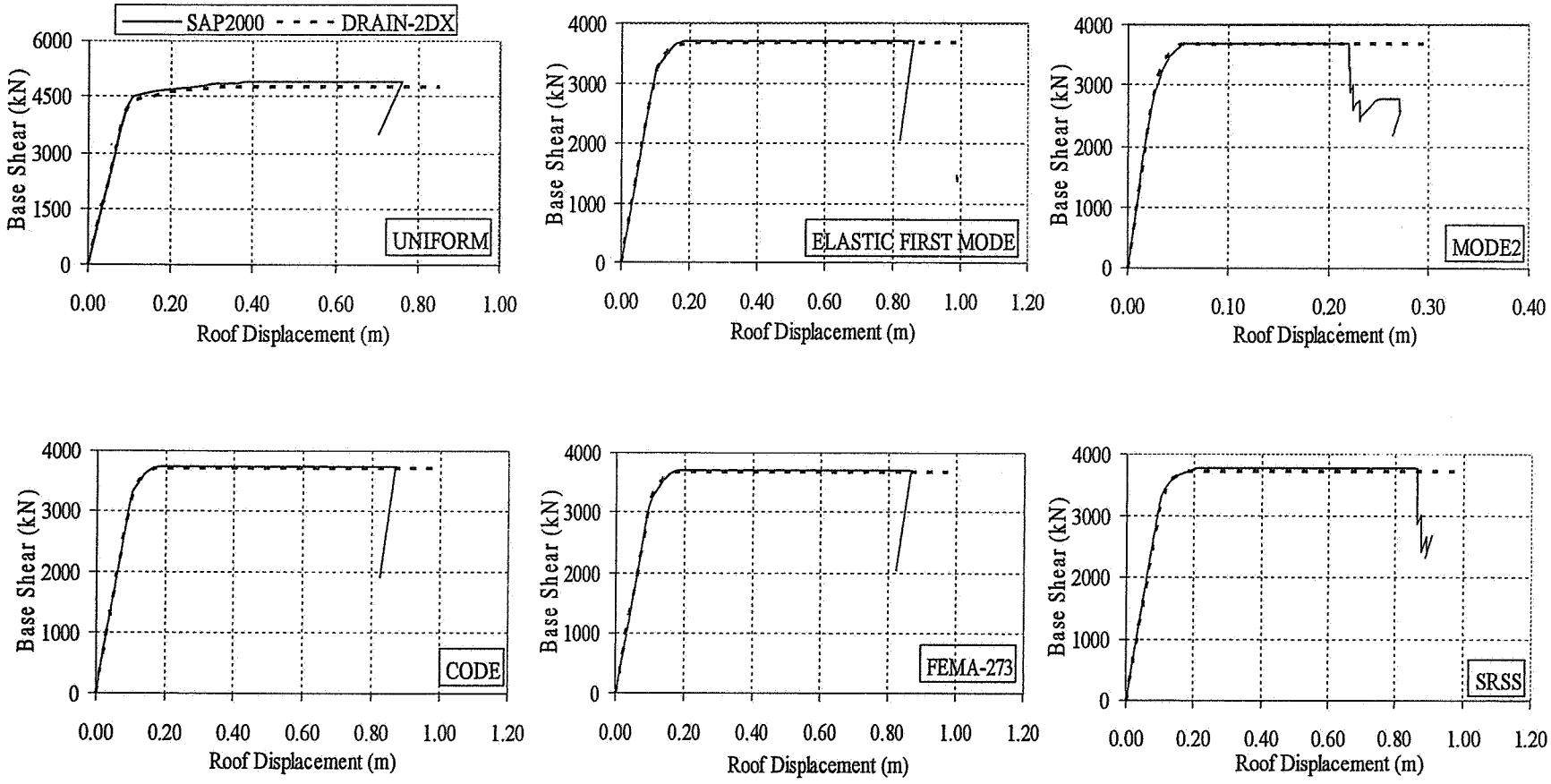

Figure 3.18 : Pushover (Capacity) Curves for 8-Story R/C Frame

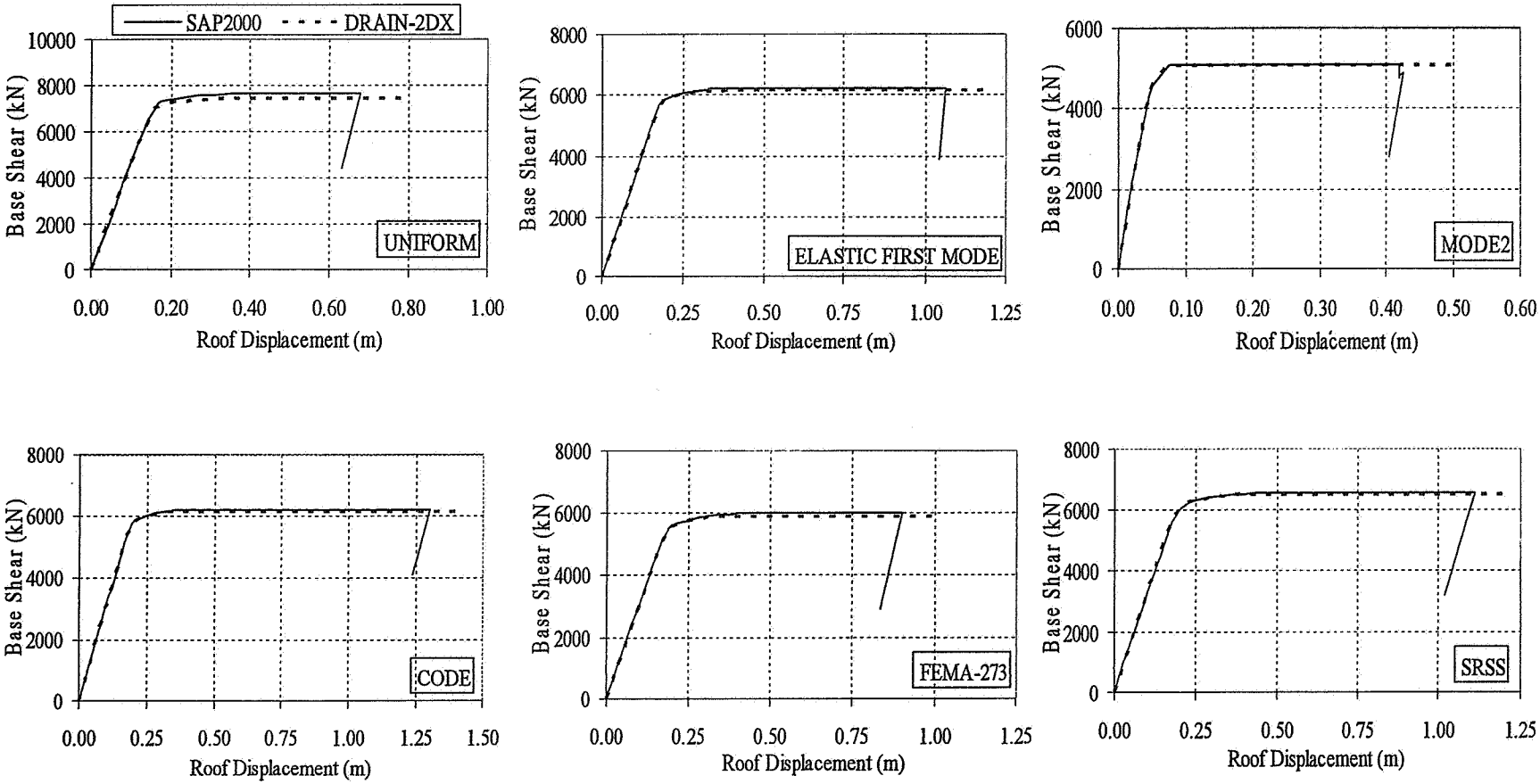

Figure 3.19 : Pushover (Capacity) Curves for 12-Story R/C Frame

CHAPTER 4

SEISMIC DEMAND PREDICTION BY PUSHOVER ANALYSIS FOR FRAME STRUCTURES

4.1 INTRODUCTION

Although, in literature, pushover analysis has been shown to capture essential structural response characteristics under seismic action, the accuracy and the reliability of pushover analysis in predicting global and local seismic demands have been the subject of discussion. The limitations of pushover analysis and the issues affecting the accuracy of pushover predictions were discussed in detail in Section 1.3.2 and it was presented that accurate estimation of target displacement, selection of lateral load pattern and identification of failure mechanisms due to higher modes of vibration are among the important issues that affect the accuracy of pushover predictions.

In this study, pushover analyses were performed on low, mid and high-rise reinforced concrete and steel moment resisting frames using various invariant lateral load patterns utilized in current engineering practice to study the effects of lateral load pattern on global structure behavior, thus on the capacity curve and on the demand prediction of pushover analysis. The accuracy of any invariant lateral load pattern in predicting the seismic demands of frame structures experiencing individual ground motion excitations that cause elastic and certain levels of nonlinear deformation were identified. For this purpose, six deformation levels represented as peak roof displacements on the capacity curve of the frames were firstly predetermined and the response parameters such as story displacements, inter-story drift ratios, story shears and plastic hinge locations were then estimated from the results of pushover analyses for any lateral load pattern at the considered deformation level. Pushover predictions were compared with the 'exact' values of response parameters obtained from the nonlinear time history analyses using scaled

ground motion records corresponding to the considered deformation levels. The accuracy and the effects of invariant lateral load patterns utilized in traditional pushover analysis to determine the actual seismic behavior of planar structures were evaluated. No adaptive lateral load pattern was considered in this study because the main aim of this study is to determine the discrepancies in the predictions of practical pushover analysis with any invariant lateral load pattern. The adaptive lateral load patterns make the pushover analysis computationally demanding and conceptually complicated.

Chopra and Goel [9] developed an improved pushover analysis procedure named Modal Pushover Analysis (MPA) to account for the effects of higher modes on structural response and it was suggested that by considering the contributions of a sufficient number of modes, MPA generally predicts the height-wise distribution of any response parameter similar to the 'exact' results obtained from nonlinear time history analysis. The MPA was performed on case study frames and a comparative evaluation of MPA and traditional pushover analysis with invariant lateral load patterns in predicting the seismic demands was conducted.

4.2 DESCRIPTION OF CASE STUDY FRAMES

The effects of lateral load patterns and higher modes on global structural behavior and on the accuracy of pushover predictions were studied on reinforced concrete and steel moment resisting frames. Four reinforced concrete frames with 2, 5, 8 and 12-stories and three steel frames with 2, 5 and 13-stories were utilized to cover a broad range of fundamental periods.

The case study frames were designed for California using the Uniform Building Code-1982 [24]. Two dimensional models of case study frames were prepared using SAP2000 [14] and DRAIN-2DX [44] by considering the necessary geometric and strength characteristics of all members that affect the nonlinear seismic response. The structural models were based on centerline dimensions that beams and columns span between the nodes at the intersections of beam and column centerlines and beam-column joints were not modeled. Rigid floor diaphragms were assigned at each story level and the seismic mass of the frames were lumped at the mass center of each story. Gravity loads consisting of dead loads and 25% of live loads were considered in pushover and nonlinear time history analyses. Free vibration analyses were performed to determine elastic periods and mode shapes of the frames. The free vibration analyses of the frames using SAP2000 [14] and DRAIN-2DX [44] yielded exactly same dynamic properties. The dynamic properties

of the case study frames are summarized in Table 4.1. Modes are normalized to have unit modal amplitude at roof level.

Table 4.1 : Dynamic Properties of Case Study Frames

Frame	Period (T_n, sec)			Modal Participation Factor (Γ_n)			Modal Mass Factor (α_n)		
	T_1	T_2	T_3	Γ_1	Γ_2	Γ_3	α_1	α_2	α_3
2-Story R/C	0.488	0.148	-	1.336	0.336	-	0.834	0.166	-
5-Story R/C	0.857	0.272	0.141	1.348	0.528	0.258	0.794	0.116	0.054
8-Story R/C	1.064	0.374	0.192	1.409	0.613	0.319	0.727	0.144	0.050
12-Story R/C	1.610	0.574	0.310	1.398	0.615	0.372	0.730	0.130	0.052
2-Story Steel	0.535	0.155	-	1.272	0.272	-	0.972	0.028	-
5-Story Steel	1.039	0.379	0.196	1.412	0.594	0.266	0.862	0.104	0.022
13-Story Steel	1.922	0.692	0.403	1.364	0.571	0.358	0.781	0.125	0.048

The configuration, member details and dynamic properties of case study frames are presented in Appendix A. The details of shear reinforcement were not considered since controlling behavior of frame members was assumed to be flexure. Both pushover and nonlinear time history analyses were performed using gross section properties and P-Delta effects were neglected. Nonlinear member behavior of concrete and steel sections was modeled as discussed in Chapter 3 for SAP2000 [14] and DRAIN-2DX [44].

4.3 NONLINEAR TIME HISTORY ANALYSES

The nonlinear response of structures is very sensitive to the structural modeling and ground motion characteristics. Therefore, a set of representative ground motion records that accounts for uncertainties and differences in severity, frequency and duration characteristics has to be used to predict the possible deformation modes of the structures for seismic performance evaluation purposes. However, for simplicity, seismic demand prediction is generally performed by pushover analysis which mostly utilizes smoothened response spectra. In this study, the accuracy of demand prediction of pushover analyses for various invariant lateral load patterns was evaluated for the response obtained from randomly selected ground motion excitations.

The ground motion records used in this study include El Centro (Imperial Valley, 18 May 1940, NS component), Parkfield (27 June 1966, N65E component), Pacoima Dam (San Fernando, 9 February 1971, S16E component) and Düzce (12 November 1999, EW component) earthquakes. The peak ground accelerations (PGAs) of the selected ground motions are within 0.319g-1.17g. The El Centro is a widely known ground motion utilized

in many studies. The Pacoima Dam and the Düzce are near-field ground motions and the Düzce was selected to represent a local ground motion.

In this study, the response of case study frames were studied in the elastic and various degrees of inelastic deformation levels that were represented by peak roof displacements on the capacity (pushover) curve of the frames. Six deformation levels were considered as illustrated in Figure 4.1 for each frame and each ground motion record was scaled to obtain the predetermined peak roof displacement for the frame considered.

5% damped elastic pseudo-acceleration response spectra of ground motions are given in Figure 4.2. The acceleration- time histories of ground motion records are also shown in Figure 4.3.

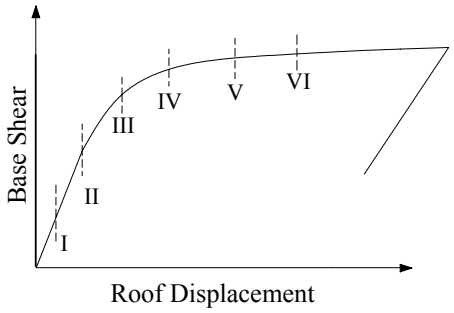

Figure 4.1 : Deformation Levels Considered for Case Study Frames

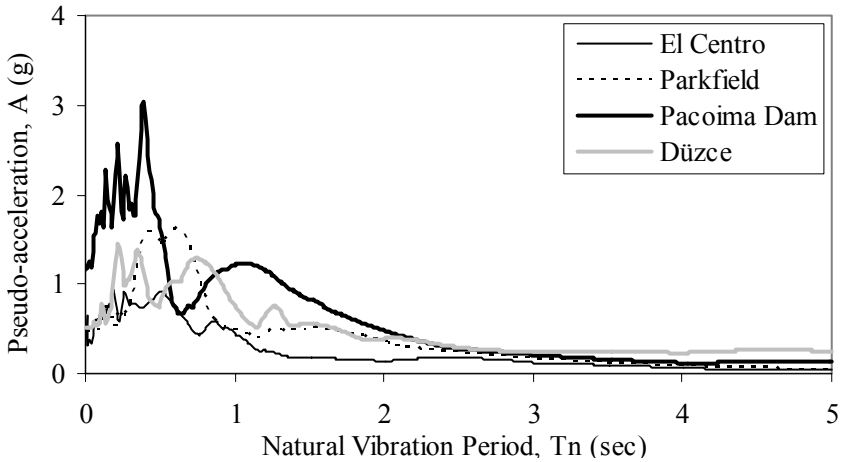

Figure 4.2 : Pseudo-Acceleration Response Spectra of Ground Motions (5% Damped)

The ground motion scale factors used to obtain the predetermined peak roof displacements corresponding to the considered deformation levels and the predetermined peak roof

displacements are presented for reinforced concrete and steel moment resisting frames in Table 4.2 and Table 4.3, respectively.

Nonlinear time history analyses were performed by using DRAIN-2DX [44] for the scaled ground motion records and maximum absolute values of response parameters such as story displacements, inter-story drift ratios and story shears were determined at the considered deformation level for each ground motion record. It is also worth mentioning that the maximum values of any response parameter over the height of the frames generally occurred at different instants of time. Also, plastic hinge locations were identified in nonlinear time history analyses.

4.4 PUSHOVER ANALYSES

Pushover analyses were performed on reinforced concrete and steel moment resisting frames using DRAIN-2DX [44] and SAP2000 [14] as discussed in Chapter 3. In pushover analyses, five different invariant lateral load patterns were utilized to represent the likely distribution of inertia forces imposed on the frames during an earthquake and the utilized lateral load patterns are described as follows (Note that the story forces are normalized with the base shear to have a total base shear equals to unity):

- **'Uniform' Lateral Load Pattern**

The lateral force at any story is proportional to the mass at that story, i.e.,

$$F_i = m_i / \Sigma m_i \quad (4.1)$$

where F_i : lateral force at i-th story

m_i : mass of i-th story

- **'Elastic First Mode' Lateral Load Pattern**

The lateral force at any story is proportional to the product of the amplitude of the elastic first mode and the mass at that story, i.e.,

$$F_i = m_i \emptyset_i / \Sigma m_i \emptyset_i \quad (4.2)$$

where $\emptyset_i$: amplitude of the elastic first mode at i-th story

- **'Code' Lateral Load Pattern**

The lateral load pattern is defined in Turkish Earthquake Code (1998) [53] and the lateral force at any story is calculated from the following formula:

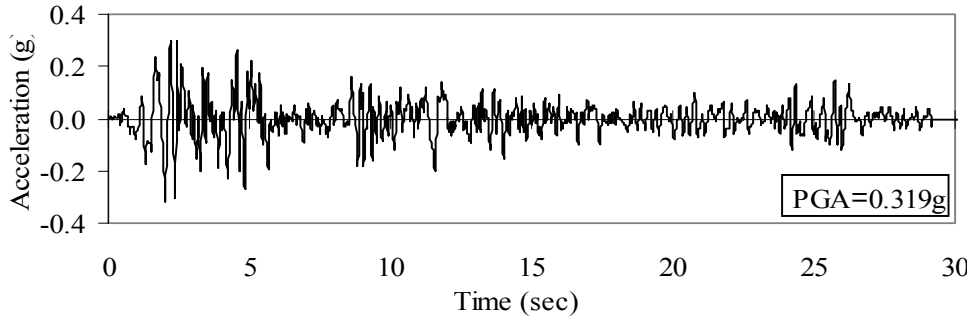

a) El Centro (Imperial Valley, 18 May 1940, NS component)

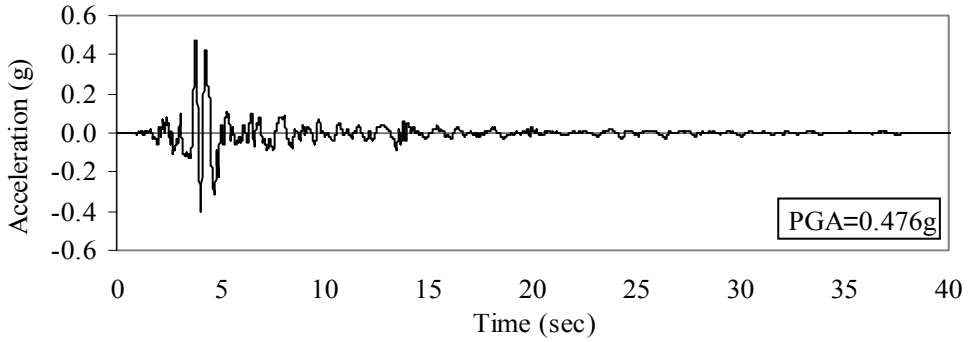

b) Parkfield (27 June 1966, N65E component)

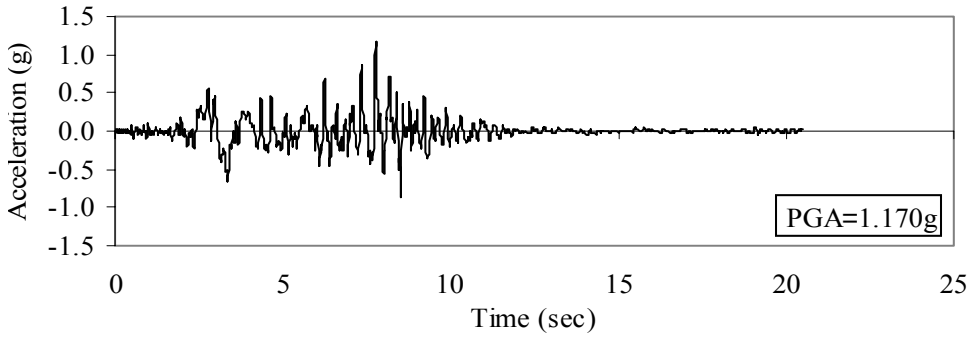

c) Pacoima Dam (San Fernando, 9 February 1971, S16E component)

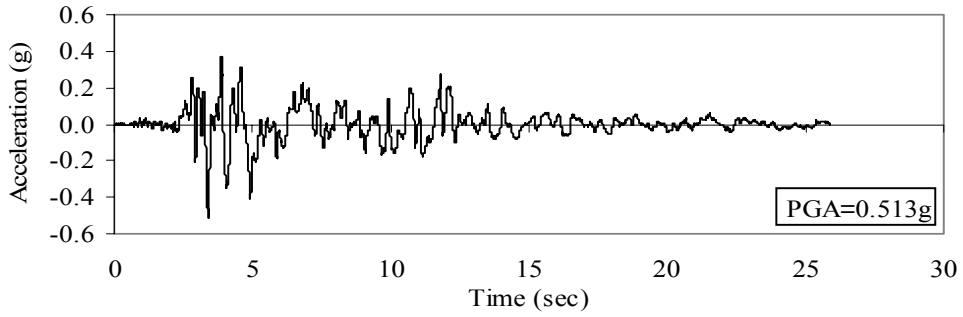

d) Düzce (12 November 1999, EW component)

Figure 4.3 : Acceleration-Time Histories of Ground Motion Records

Table 4.2 : Ground Motion Scale Factors and Predetermined Peak Roof Displacements Corresponding the Deformation Levels Considered (R/C Frames)

El Centro (Imparial Valley 1940, NS)								
Deformation Level	**2-Story**		**5-Story**		**8-Story**		**12-Story**	
	SF	**Ur (m)**	**SF**	**Ur (m)**	**SF**	**Ur (m)**	**SF**	**Ur (m)**
I	0.15	0.011	0.50	0.073	0.45	0.071	0.50	0.083
II	0.50	0.031	1.00	0.109	0.65	0.101	1.00	0.182
III	0.75	0.045	1.50	0.139	1.00	0.127	1.50	0.315
IV	1.35	0.067	2.00	0.189	1.50	0.205	2.00	0.417
V	1.75	0.091	2.50	0.212	2.00	0.281	2.50	0.521
VI	2.25	0.119	3.00	0.233	2.50	0.367	3.00	0.607
Parkfield (27 June 1966, N65E)								
Deformation Level	**2-Story**		**5-Story**		**8-Story**		**12-Story**	
	SF	**Ur (m)**	**SF**	**Ur (m)**	**SF**	**Ur (m)**	**SF**	**Ur (m)**
I	0.09	0.011	0.50	0.077	0.37	0.071	0.25	0.115
II	0.30	0.033	0.70	0.108	0.55	0.105	0.50	0.196
III	0.45	0.044	0.87	0.136	0.75	0.128	0.80	0.300
IV	0.68	0.067	1.12	0.183	0.96	0.203	1.00	0.434
V	0.87	0.091	1.30	0.212	1.13	0.283	1.15	0.536
VI	1.05	0.115	1.50	0.255	1.30	0.366	1.30	0.617
Pacoima Dam (San Fernando 1971, S16E)								
Deformation Level	**2-Story**		**5-Story**		**8-Story**		**12-Story**	
	SF	**Ur (m)**	**SF**	**Ur (m)**	**SF**	**Ur (m)**	**SF**	**Ur (m)**
I	0.075	0.010	0.29	0.075	0.15	0.073	0.15	0.104
II	0.27	0.031	0.41	0.108	0.22	0.105	0.30	0.208
III	0.40	0.044	0.52	0.136	0.28	0.126	0.45	0.316
IV	0.74	0.067	0.67	0.184	0.43	0.209	1.00	0.447
V	0.95	0.090	0.76	0.213	0.95	0.281	1.15	0.539
VI	1.15	0.115	0.92	0.256	1.12	0.365	1.30	0.638
Düzce (1999, EW)								
Deformation Level	**2-Story**		**5-Story**		**8-Story**		**12-Story**	
	SF	**Ur (m)**	**SF**	**Ur (m)**	**SF**	**Ur (m)**	**SF**	**Ur (m)**
I	0.18	0.010	0.27	0.076	0.30	0.070	0.20	0.097
II	0.53	0.032	0.38	0.108	0.45	0.103	0.40	0.193
III	0.67	0.045	0.55	0.137	0.55	0.130	0.80	0.306
IV	0.90	0.068	0.92	0.183	0.85	0.208	1.10	0.423
V	1.03	0.092	1.13	0.212	1.02	0.280	1.77	0.526
VI	1.12	0.118	1.39	0.256	1.26	0.367	1.92	0.613

SF : Ground Motion Scale Factor

U_r : Peak Roof Displacement

Table 4.3 : Ground Motion Scale Factors and Predetermined Peak Roof Displacements Corresponding the Deformation Levels Considered (Steel Frames)

El Centro (Imparial Valley 1940, NS)						
Deformation Level	**2-Story**		**5-Story**		**13-Story**	
	SF	**Ur (m)**	**SF**	**Ur (m)**	**SF**	**Ur (m)**
I	0.30	0.024	0.50	0.075	0.50	0.102
II	0.50	0.041	1.00	0.150	1.50	0.306
III	0.68	0.050	1.50	0.192	2.00	0.362
IV	0.85	0.060	2.00	0.252	2.50	0.453
V	1.35	0.072	2.50	0.308	3.00	0.635
VI	1.65	0.090	3.00	0.374	3.60	0.869
Parkfield (27 June 1966, N65E)						
Deformation Level	**2-Story**		**5-Story**		**13-Story**	
	SF	**Ur (m)**	**SF**	**Ur (m)**	**SF**	**Ur (m)**
I	0.30	0.024	0.50	0.075	0.50	0.102
II	0.30	0.040	1.00	0.177	0.55	0.305
III	0.38	0.050	1.25	0.225	1.00	0.399
IV	0.45	0.059	1.50	0.268	1.15	0.489
V	0.60	0.073	1.75	0.306	1.40	0.654
VI	0.95	0.090	2.00	0.418	1.75	0.862
Pacoima Dam (San Fernando 1971, S16E)						
Deformation Level	**2-Story**		**5-Story**		**13-Story**	
	SF	**Ur (m)**	**SF**	**Ur (m)**	**SF**	**Ur (m)**
I	0.30	0.024	0.50	0.075	0.50	0.102
II	0.34	0.040	0.35	0.160	0.45	0.304
III	0.45	0.051	0.50	0.223	0.55	0.372
IV	0.65	0.060	0.58	0.264	1.00	0.495
V	0.76	0.073	0.67	0.308	1.30	0.642
VI	0.94	0.090	1.00	0.420	1.70	0.855
Düzce (1999, EW)						
Deformation Level	**2-Story**		**5-Story**		**13-Story**	
	SF	**Ur (m)**	**SF**	**Ur (m)**	**SF**	**Ur (m)**
I	0.30	0.024	0.50	0.075	0.50	0.102
II	0.47	0.040	0.68	0.166	0.60	0.298
III	0.67	0.051	1.07	0.215	0.80	0.388
IV	0.80	0.061	1.23	0.257	1.00	0.480
V	0.92	0.073	1.38	0.308	1.85	0.658
VI	1.04	0.090	1.65	0.412	2.30	0.869

SF : Ground Motion Scale Factor

U_r : Peak Roof Displacement

$$F_i = (V_b - \Delta F_N) \frac{m_i h_i}{\sum_{j=1}^{N} (m_j h_j)} \quad (4.3)$$

where V_b : base shear

h : height of i-th story above the base

N : total number of stories

ΔF_N : additional earthquake load added to the N-th story when h_N>25 m

(For $h_N \leq 25$ m. ΔF_N=0 otherwise; $\Delta F_N = 0.07 T_1 V_b \leq 0.2 V_b$ where T_1 is the fundamental period of the structure)

- **'FEMA-273' Lateral Load Pattern**

The lateral load pattern defined in FEMA-273 [18] is given by the following formula that is used to calculate the internal force at any story:

$$F_i = m_i h^k_i / \Sigma m_i h^k_i \quad (4.4)$$

where h : height of the i-th story above the base

k : a factor to account for the higher mode effects (k=1 for $T_1 \leq 0.5$ sec and k=2 for T_1>2.5 sec and varies linearly in between)

- **'Multi-Modal (or SRSS)' Lateral Load Pattern**

The lateral load pattern considers the effects of elastic higher modes of vibration for long period and irregular structures and the lateral force at any story is calculated as Square Root of Sum of Squares (SRSS) combinations of the load distributions obtained from the modal analyses of the structures as follows:

1. Calculate the lateral force at i-th story for n-th mode from Equation (4.5).

$$F_{in} = \Gamma_n m_i \Phi_{in} A_n \quad (4.5)$$

where Γ_n : modal participation factor for the n-th mode

Φ_{in} : amplitude of n-th mode at i-th story

A_n : pseudo-acceleration of the n-th mode SDOF elastic system

2. Calculate the story shears, $V_{in} = \sum_{j \geq i}^{N} F_{jn}$ where N is the total number of stories

3. Combine the modal story shears using SRSS rule, $V_i = \sqrt{\sum_n (V_{in})^2}$.

4. Back calculate the lateral story forces, F_i, at story levels from the combined story shears, V_i starting from the top story.

5. Normalize the lateral story forces by base shear for convenience such that

$F_i' = F_i / \sum F_i$.

The contribution of first three elastic modes of vibration was considered to calculate the 'Multi-Modal (or SRSS)' lateral load pattern in this study.

'Elastic First Mode', 'Code', 'FEMA-273' and 'Multi-Modal (or SRSS)' lateral load patterns represent different versions of triangular lateral load patterns. 'Uniform' and triangular lateral load patterns represent the extreme cases for invariant lateral load distributions. The height-wise distribution of lateral load patterns for case study frames are illustrated in Figure 4.4.

The variation in the height-wise distribution between the 'Elastic First Mode', 'Code', 'FEMA-273' lateral load patterns are almost negligible for 2, 5, 8-story R/C and 2, 5-story steel frames while the variation being more observable for steel frames. Also, it is observed that the height-wise distribution of 'Multi-Modal (or SRSS)' lateral load pattern starts to vary from 'Elastic First Mode', 'Code', 'FEMA-273' distributions for frames having fundamental periods larger than about 1.0 seconds while the difference is very small for 2, 5, 8-story R/C frames and for 2, 5-story steel frames. However, the variations in the height-wise distribution of triangular lateral load patterns ('Elastic First Mode', 'Code', 'FEMA-273' and 'Multi-Modal (or SRSS)') are significant for long-period frames (12-story R/C and 13-story steel frames).

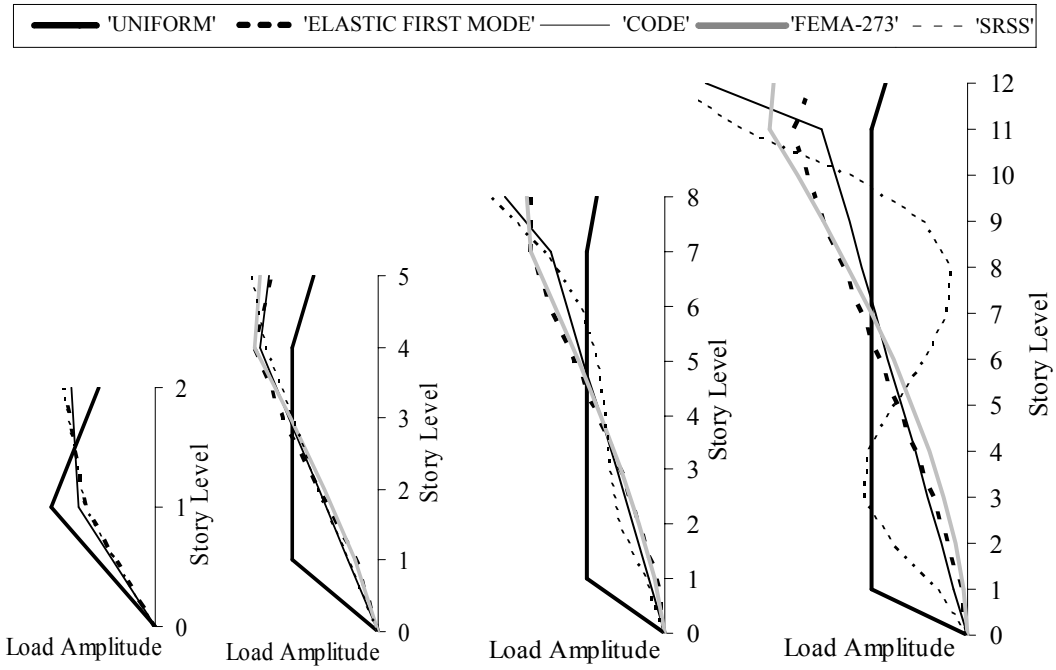

Figure 4.4 : Height-Wise Distribution of Lateral Load Patterns for R/C Case Study Frames

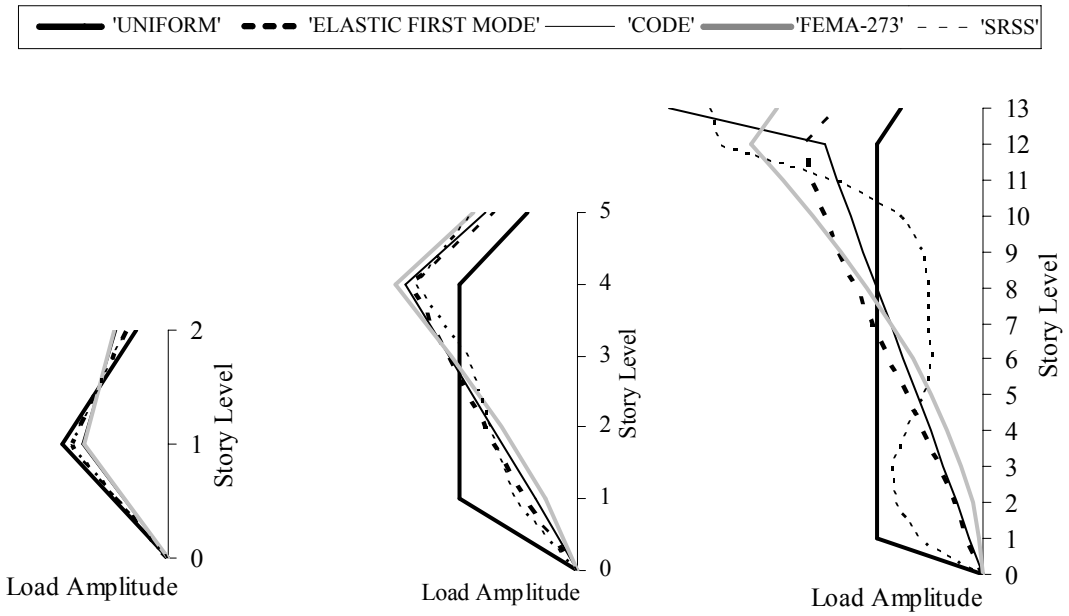

a) Steel Frames (2, 5 and 13-Story)

Figure 4.5 : Height-Wise Distribution of Lateral Load Patterns for Steel Case Study Frames

4.5 MODAL PUSHOVER ANALYSIS (MPA) PROCEDURE

Chopra and Goel [9] developed an improved pushover analysis procedure named Modal Pushover Analysis (MPA) to account for the effects of higher modes on structural response and for the redistribution of inertial forces during progressive yielding. The procedure is conceptually simple and easy to implement like the pushover analysis with invariant lateral load patterns.

Firstly, Chopra and Goel [9] applied the procedure to linearly elastic buildings and it was shown that the procedure is equivalent to the well known response spectrum analysis. Then, Chopra and Goel [9] extended the procedure to estimate the seismic demands of inelastic systems by identifying the assumptions and the approximations involved. The procedure consists of the following steps:

1. Determine the natural frequencies, ω_n, and modes, $\Ø_n$, for linearly elastic vibration of the structure.
2. For the n-th mode, develop the 'modal' capacity curve (base shear versus roof displacement) of the overall structure for the lateral force pattern $\mathbf{s}_n^* = \mathbf{m}\Ø_n$ where **m** is the mass matrix.

3. Obtain the force-displacement relationship of the n-th mode inelastic SDOF from the corresponding 'modal' capacity curve by performing one of the procedures described in Section 5.2.
4. Perform a nonlinear dynamic analysis for the ground motion excitation by utilising the force-displacement relationship of n-th mode inelastic SDOF system to obtain the peak deformation, D_n, of n-th mode inelastic SDOF system.
5. Calculate the peak roof displacement, u_{rno}, associated with the n-th mode inelastic SDOF system from

$$u_{rno} = \Gamma_n \, \emptyset_{rn} \, D_n \tag{4.6}$$

where

Γ_n : modal participation factor for the n-th mode

$\emptyset_{rn}$: amplitude of n-th mode at roof level

D_n : peak spectral roof displacement

6. Extract any response , r_{no}, from the pushover results at roof displacement u_{rno}.
7. Repeat Steps 2-6 for as many modes required for sufficient accuracy; usually the first two or three modes will suffice.
8. Determine the peak value of total response by combining the peak modal responses, r_{no}, using any appropriate modal combination rule, usually Square Root of Sum of Squares (SRSS) is used.

The procedure involves certain approximations and assumptions that coupling among modal coordinates due to yielding of the structure is neglected while calculating the peak roof displacement, u_{rno} and superposition of peak modal responses to obtain the total peak response is utilized although superposition is valid only for elastic systems. Also, the total response is approximated by using an appropriate modal combination rule to combine the peak modal responses.

The procedure was applied on 2, 5, 8- and 12-story reinforced concrete and 2, 5- and 13-story steel frames by considering the contribution of first three modes of vibration to the total response and a comparative evaluation of MPA and traditional pushover analysis with invariant lateral load patterns in predicting the seismic demands was conducted (Figures B.1-B.112 in the attached CD). The 'modal' capacity curves for case study frames considering the first two and/or three modes of vibration are presented in Figures 4.6-4.7.

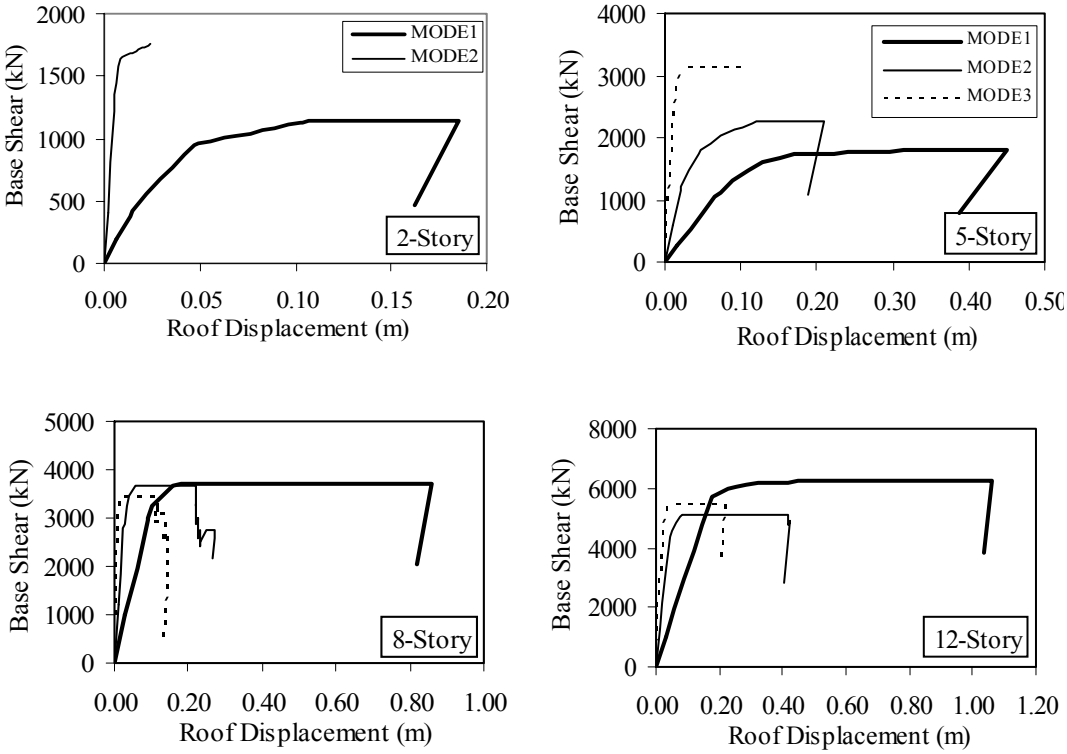

Figure 4.6 : 'Modal' Capacity Curves for R/C Frames (2, 5, 8- and 12-Story)

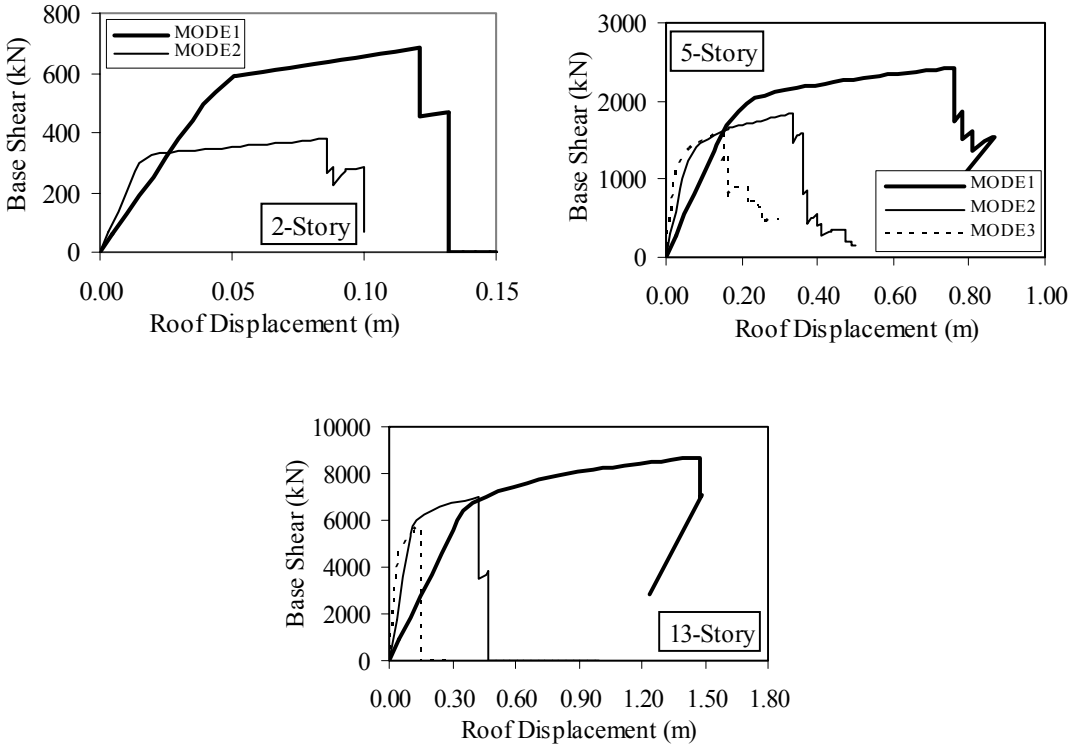

Figure 4.7 : 'Modal' Capacity Curves for Steel Frames (2, 5- and 13-Story)

4.6 COMPARISON AND INTERPRETATION OF RESULTS

The effects and the accuracy of invariant lateral load patterns utilized in pushover analysis to predict the behavior imposed on the structure due to randomly selected individual ground motions causing elastic and various levels of nonlinear response were evaluated in this study. For this purpose, global structure behavior, story displacements, inter-story drift ratios, story shears and plastic hinge locations were selected as response parameters.

Pushover curves were obtained by performing pushover analyses using SAP2000 [14] and DRAIN-2DX [44]. Story displacements, inter-story drift ratios, story pushover curves and plastic hinge locations for any lateral load pattern were extracted from the pushover database at the predetermined maximum roof displacement consistent with the deformation level considered and were compared with absolute maximum values of 'exact' response parameters obtained from nonlinear time history analyses for each deformation level for each ground motion. It should be mentioned that maximum story displacements and inter-story drift ratios for any story level generally occurred at different times in nonlinear time history analyses. Also, story displacements, inter-story drift ratios and plastic hinge locations were estimated by performing Modal Pushover Analysis (MPA) on case study frames. The error involved in story displacement and inter-story drift ratio prediction of each pushover method was calculated with respect to the 'exact' demands to assess the accuracy of pushover predictions. Story displacement, inter-story drift ratio and corresponding error profiles for case study frames for each pushover method at each deformation level for all ground motions are illustrated in Figures B.1-B.112 in the attached CD.

4.6.1 Global Structure Behavior

Capacity curves (base shear versus roof displacement) are the load-displacement envelopes of the structures and represent the global response of the structures. Capacity curves for case study frames were obtained from the pushover analyses using aforementioned lateral load patterns and are shown in Figures 4.8-4.10. The absolute maximum values of roof displacements and base shears experienced under ground motion excitations were determined for each deformation level to approximate a dynamic capacity curve for the frames. The approximate dynamic capacity curves for each ground motion were included in those figures to make a comparison of approximate dynamic capacity curves with the ones obtained from pushover analyses. Roof displacement is normalized

with respect to the total height of the frame while base shear is normalized with respect to the total seismic weight of the frame.

The examination of the height-wise distribution of lateral load patterns shown in Figure 4.4 together with the capacity curves obtained using these lateral load patterns (Figures 4.8-4.10) reveals that the shape of capacity curve directly depends on the height-wise distribution of lateral load pattern as well as the nonlinear structural characteristics.

The trend in the similarities and/or in the variations of the height-wise distribution of lateral load patterns is reflected on the capacity curves such that pushover analyses using 'Uniform' lateral load pattern yielded capacity curves with higher initial stiffness and base shear capacity but lower maximum roof displacement than those of the triangular lateral load patterns ('Elastic First Mode', 'Code', 'FEMA-273' and 'Multi-Modal (or SRSS)') for almost all frames considered (except 2-story steel frame since 'Uniform' lateral load pattern is similar to the triangular lateral load patterns). This is expected because capacity curve is a function of the point of application of the resultant of lateral load as well as the nonlinear structural characteristics. 'Uniform' loading gives the lowest point while the triangular lateral load patterns give a higher point for the application of the resultant load as the story forces at the upper stories are higher for triangular lateral load patterns. Thus, triangular lateral load patterns yield higher roof displacements for the same base shear value or the base shear needed to develop the same roof displacement with triangular lateral load patterns becomes higher for 'Uniform' load pattern in both elastic and inelastic ranges.

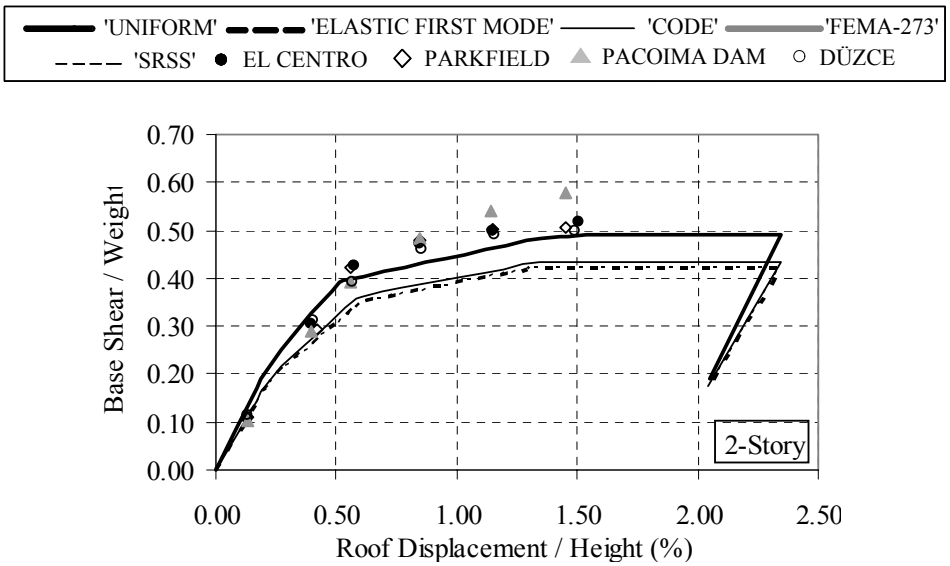

Figure 4.8 : Capacity (Pushover) Curves (2-Story R/C Frame)

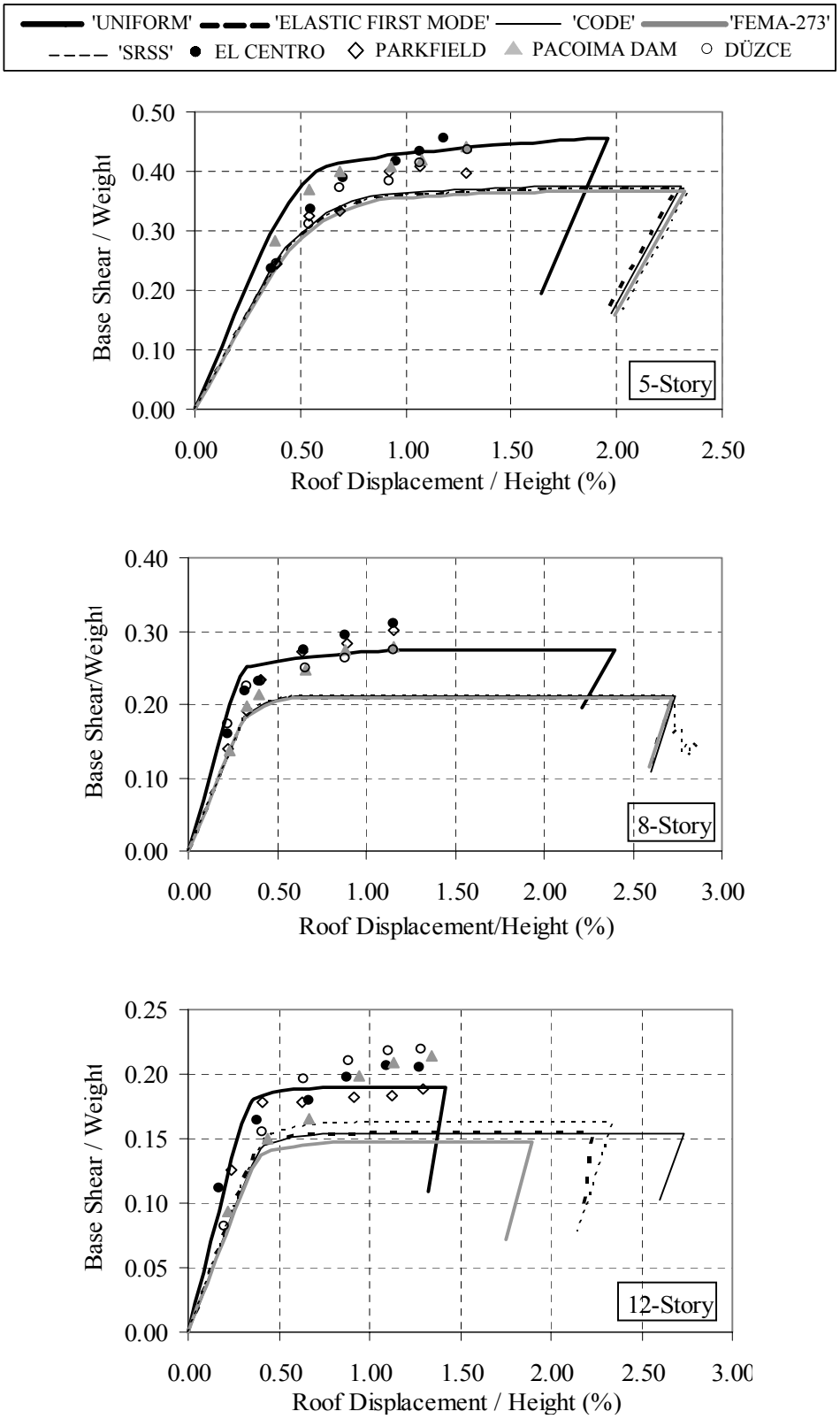

Figure 4.9 : Capacity (Pushover) Curves (5, 8- and 12-Story R/C Frames)

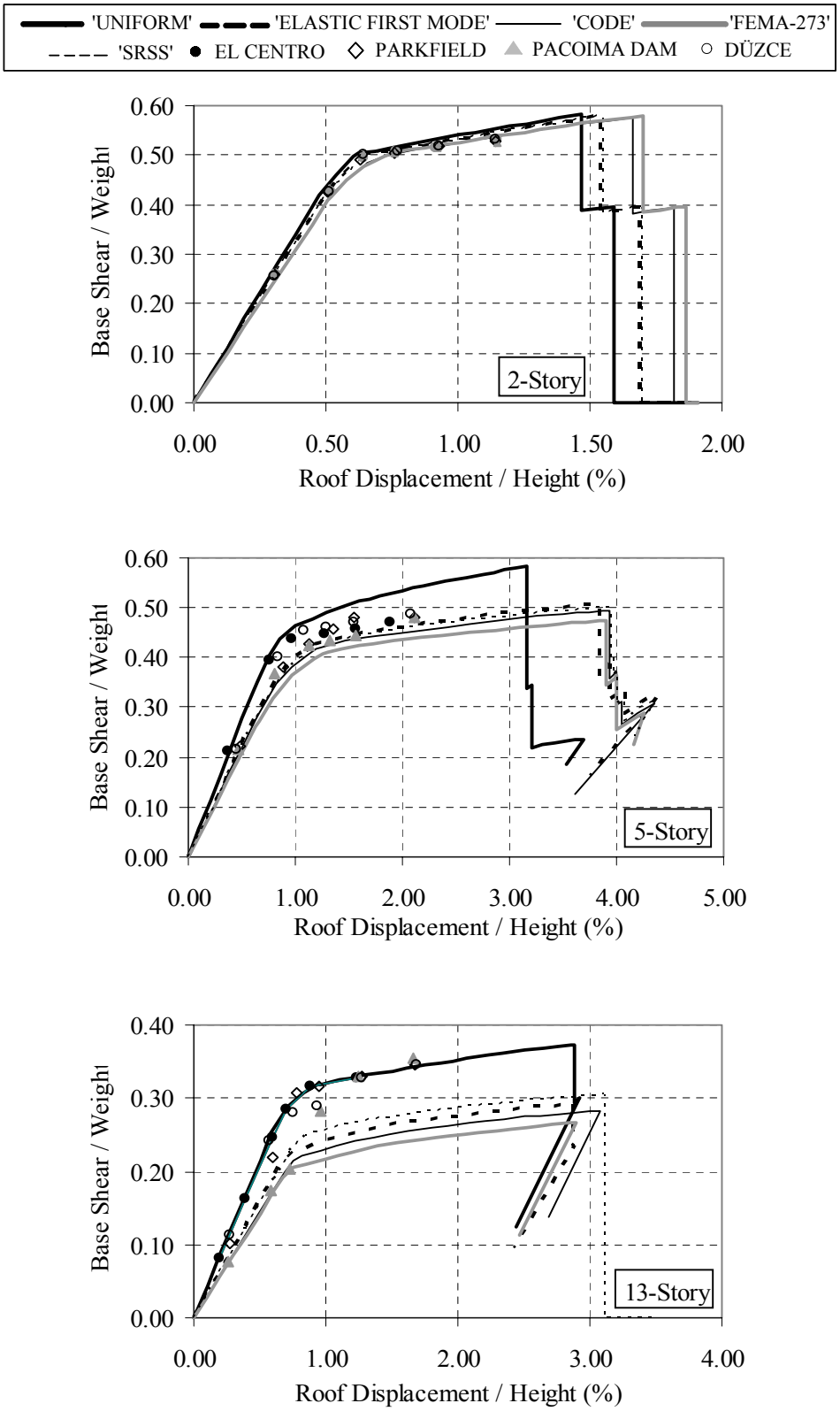

Figure 4.10 : Capacity (Pushover) Curves (2, 5- and 13-Story Steel Frames)

The difference in the point of application of the resultant load between triangular lateral load patterns are negligible for short-period frames (2, 5- and 8-story R/C and 2, 5-story steel frames) and all triangular lateral load patterns yielded almost same capacity curves for low to mid-rise frames (the difference being more for 5-story steel frame). However, for high-rise frames (12-story R/C and 13-story steel frames) the point of application of the resultant load for triangular lateral load patterns differs significantly as reflected on the capacity curves. 'FEMA-273' and 'Multi-Modal (or SRSS)' lateral load patterns yielded the lower and upper bounds of base shear capacities obtained from triangular lateral load patterns for long-period frames, respectively. However, maximum global displacement demand prediction of 'Code' lateral load pattern was observed to be more conservative. Therefore, the use of 'Elastic First Mode' or 'Code' lateral load patterns is better to represent an average capacity curve determined by triangular lateral load patterns for long period frames.

The global structural behavior predicted by triangular lateral load patterns is conservative with respect to the 'exact' dynamic behavior and the overall structural response prediction of triangular lateral load patterns is better than 'Uniform' lateral load pattern for almost all frames since 'Uniform' lateral load pattern is mostly unconservative that it overestimates base shear capacity and underestimates the maximum global displacement demand with respect to triangular lateral load patterns.

On the other hand, none of the invariant lateral load patterns could capture the approximate dynamic global behavior. The 'Uniform' and triangular lateral load patterns seem to be the upper and the lower bounds of the approximate dynamic global behavior, respectively.

4.6.2 Story Displacements

The story displacement and corresponding error profiles of case study frames are illustrated in Figures B.1-B.56 in the attached CD while story displacement and corresponding error profiles of 12-story R/C frame are also given in Figures 4.11-4.18.

The story displacement and corresponding error profiles of the case study frames studied under randomly selected individual ground motions did not reveal a particular trend because structural response is affected by the variations in ground motion characteristics and structural properties that each frame under each ground motion should be considered as a case. However, following observations could be made from the overall interpretation of story displacement and corresponding error profiles:

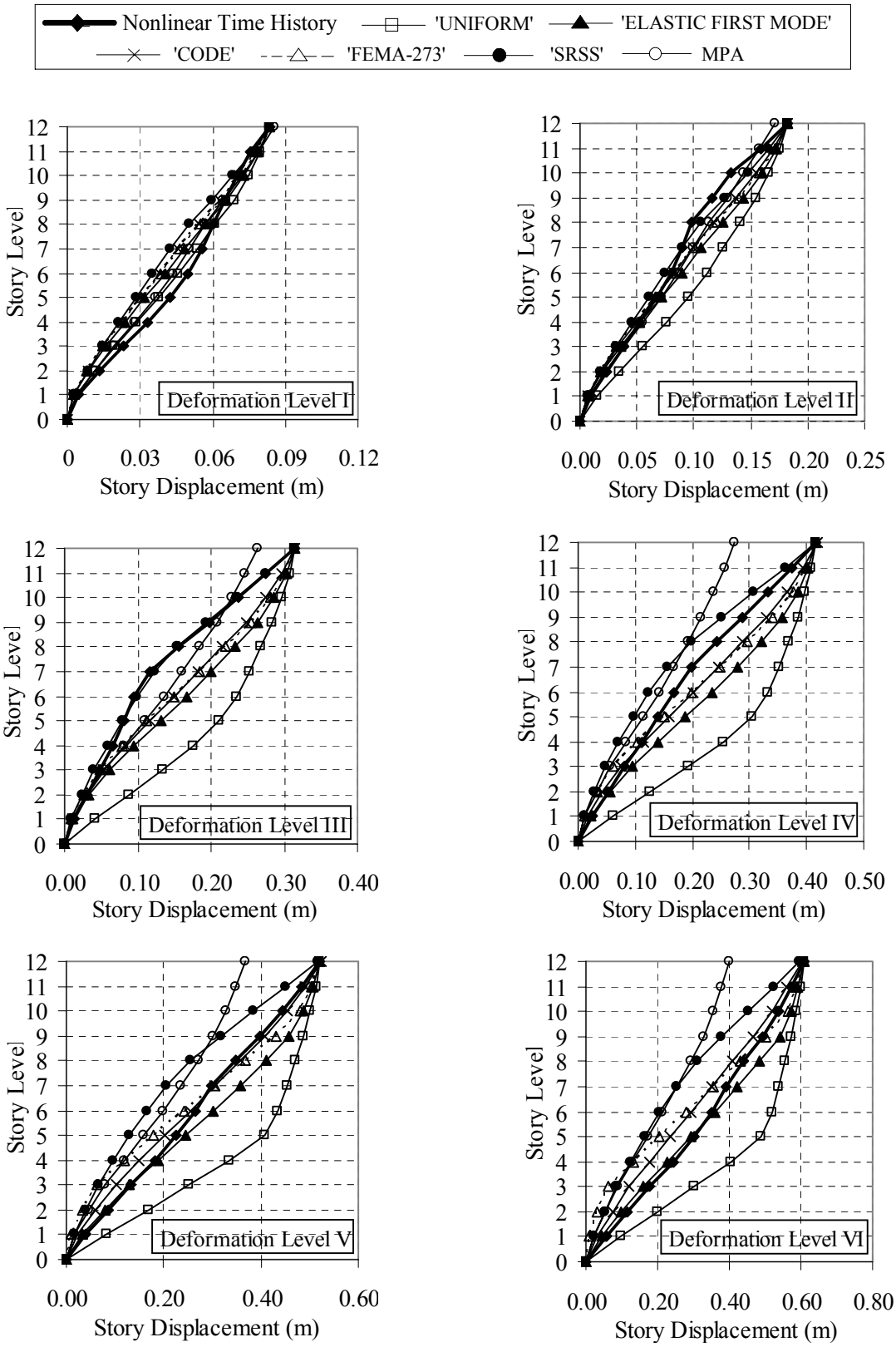

Figure 4.11 : Story Displacement Profile for 12-Story R/C Frame (El Centro)

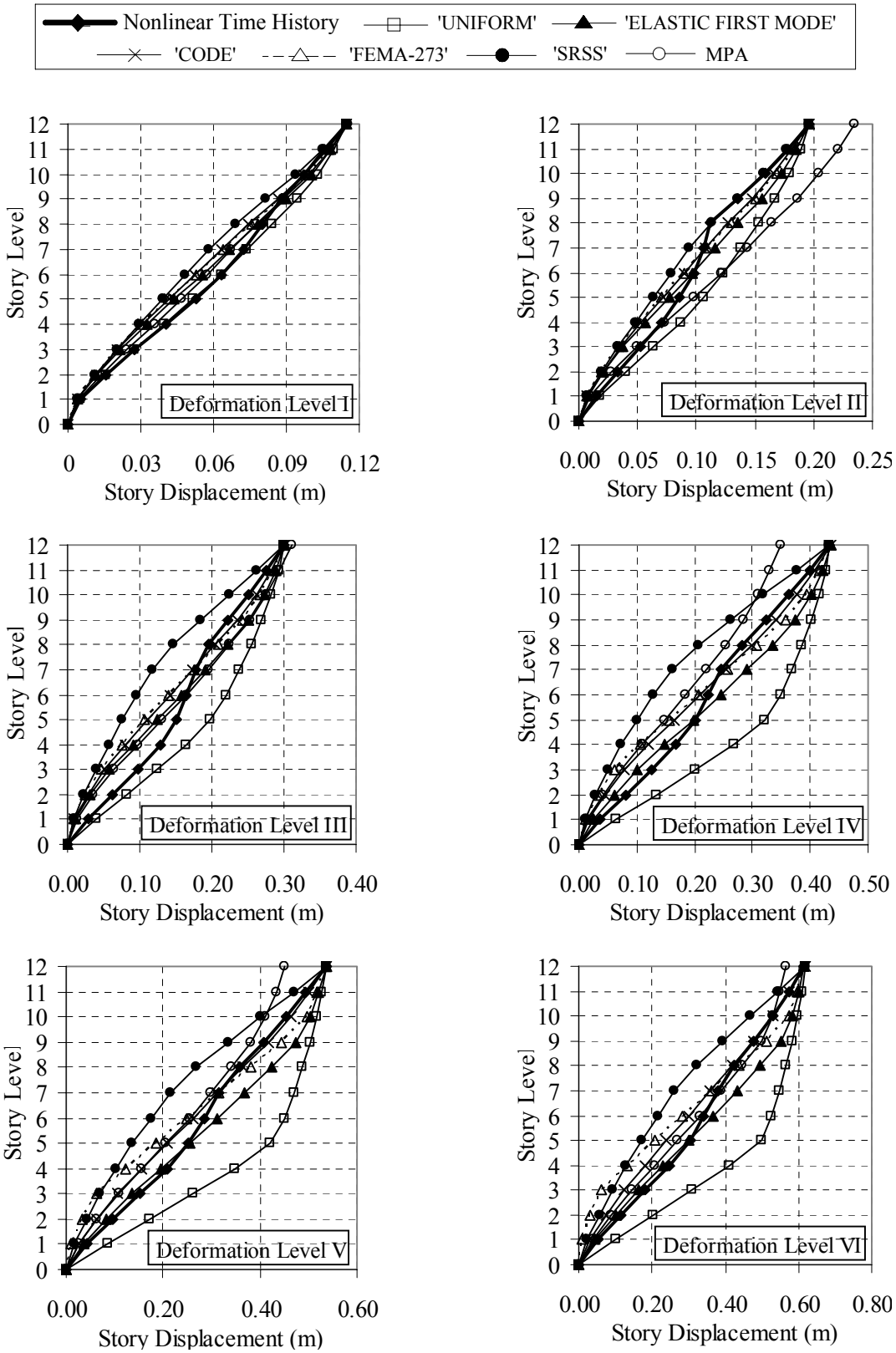

Figure 4.12 : Story Displacement Profile for 12-Story R/C Frame (Parkfield)

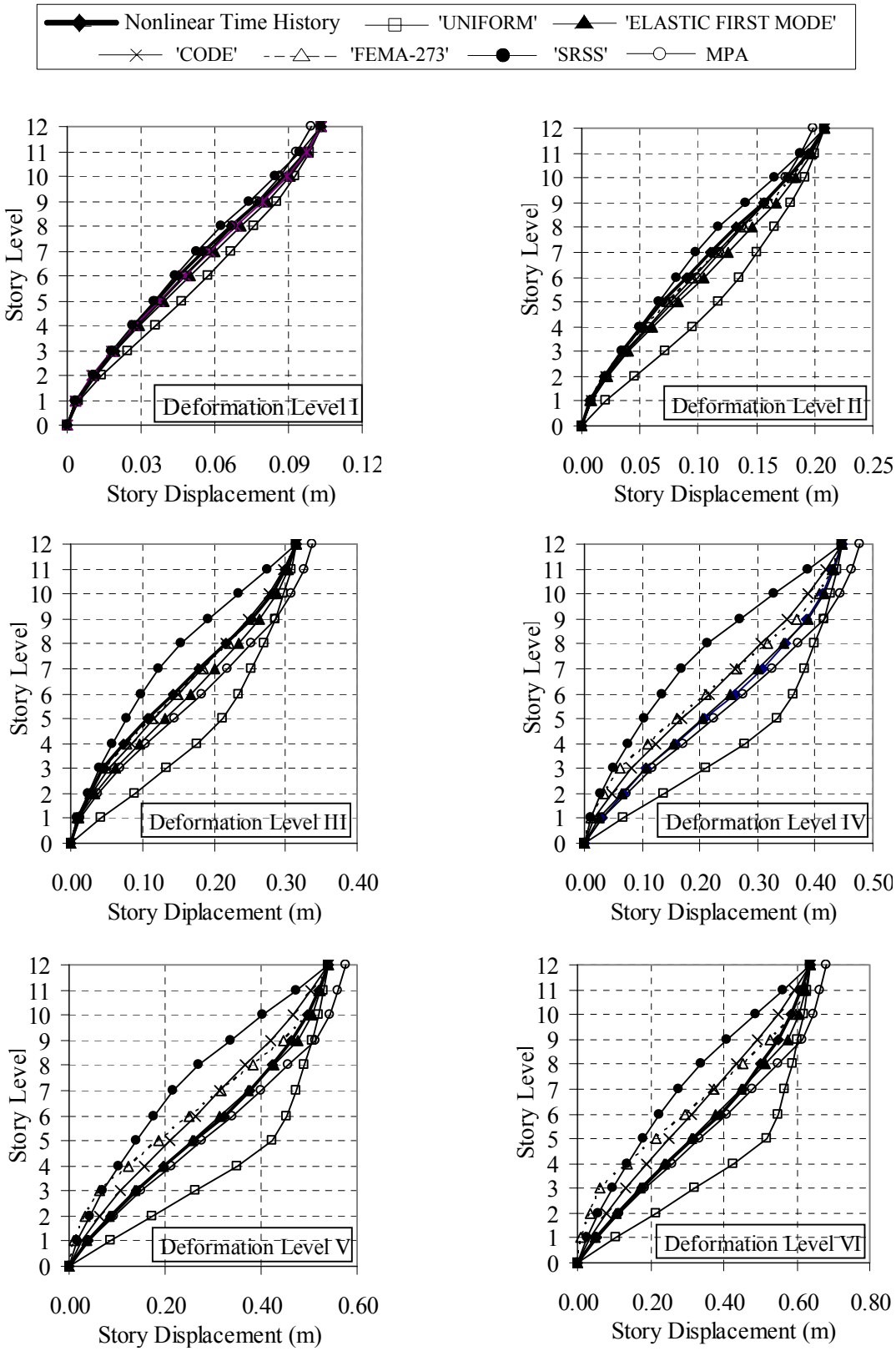

Figure 4.13 : Story Displacement Profile for 12-Story R/C Frame (Pacoima Dam)

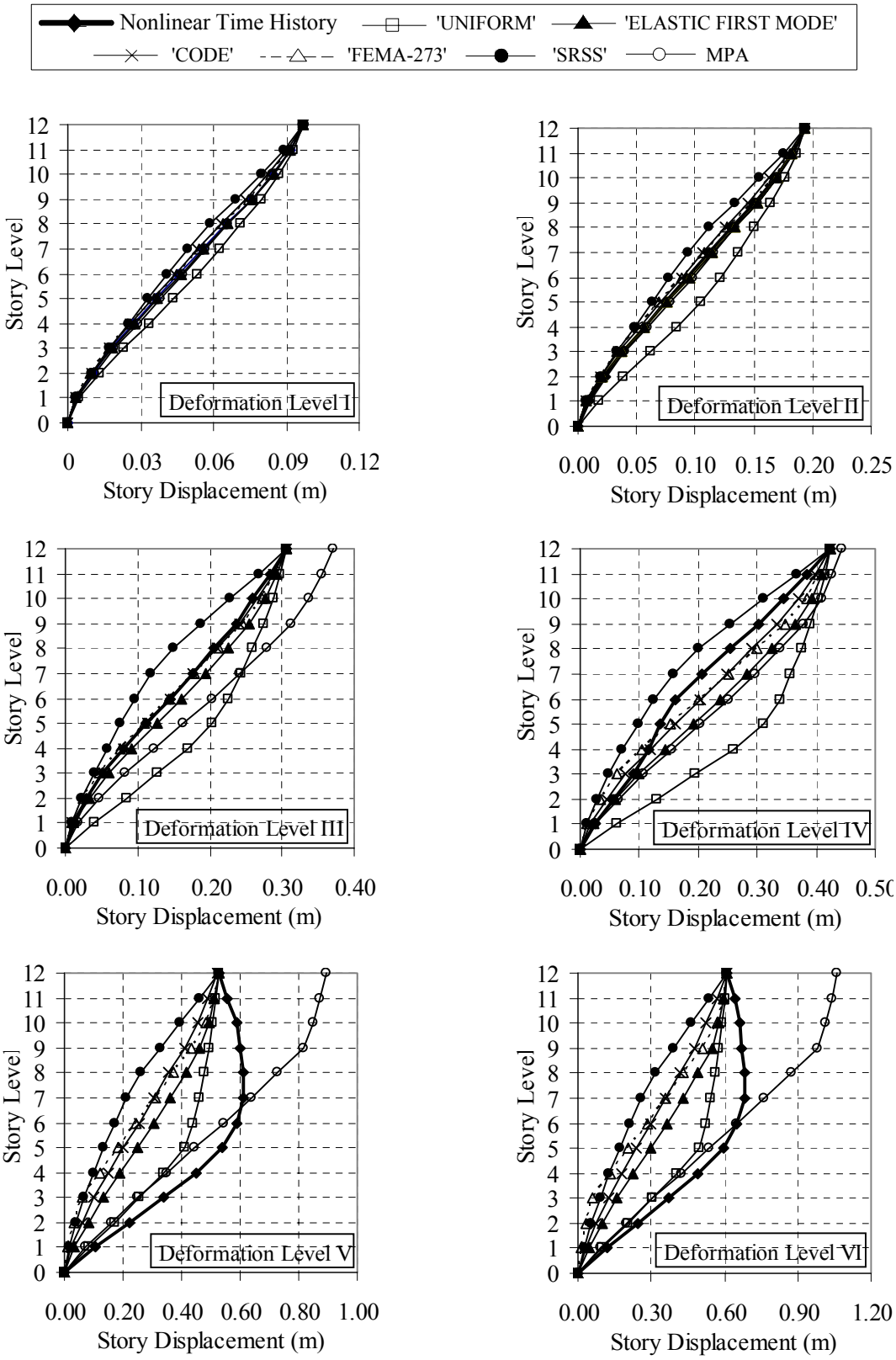

Figure 4.14 : Story Displacement Profile for 12-Story R/C Frame (Düzce)

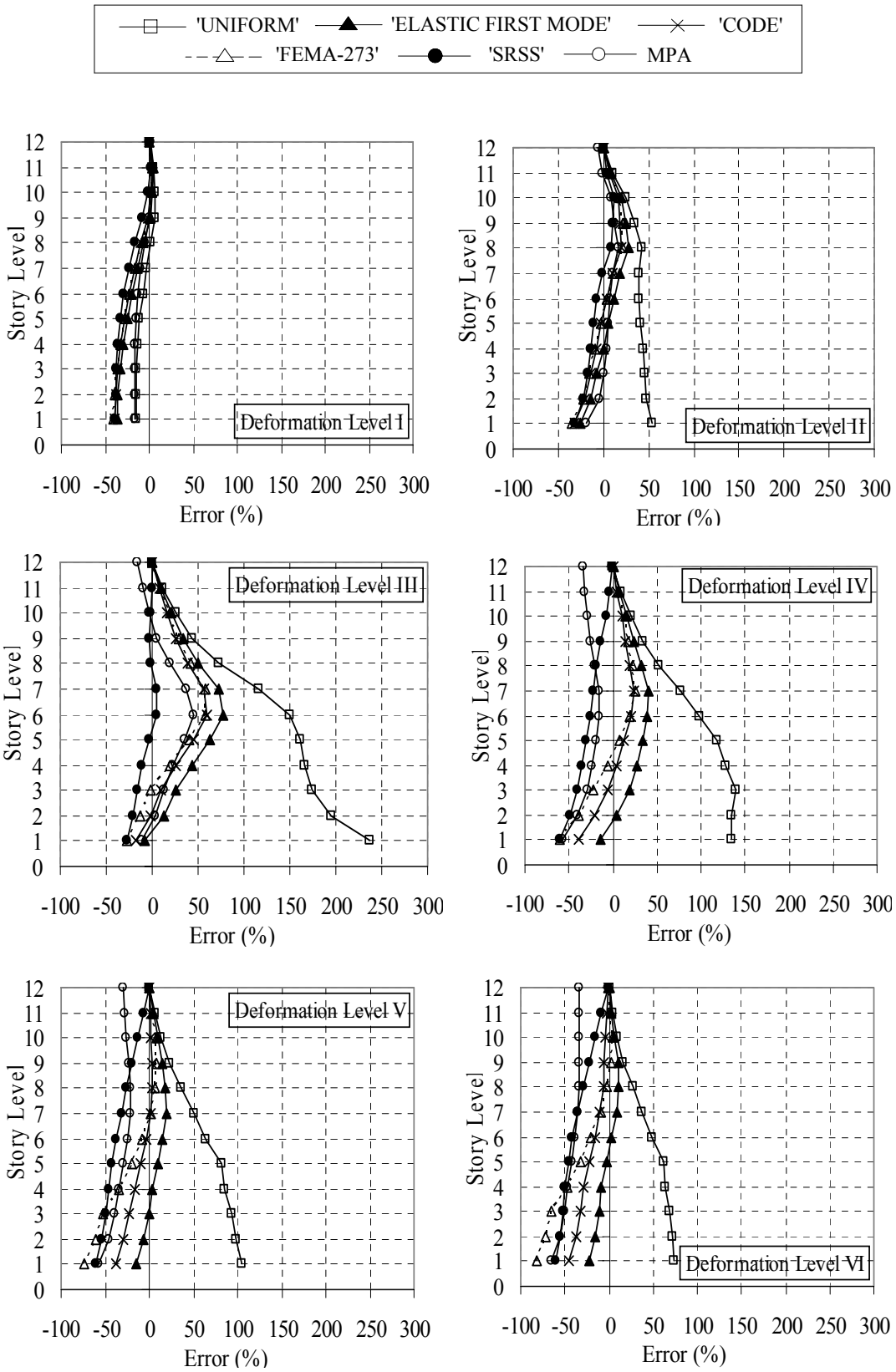

Figure 4.15 : Story Displacement Error Profile for 12-Story R/C Frame (El Centro)

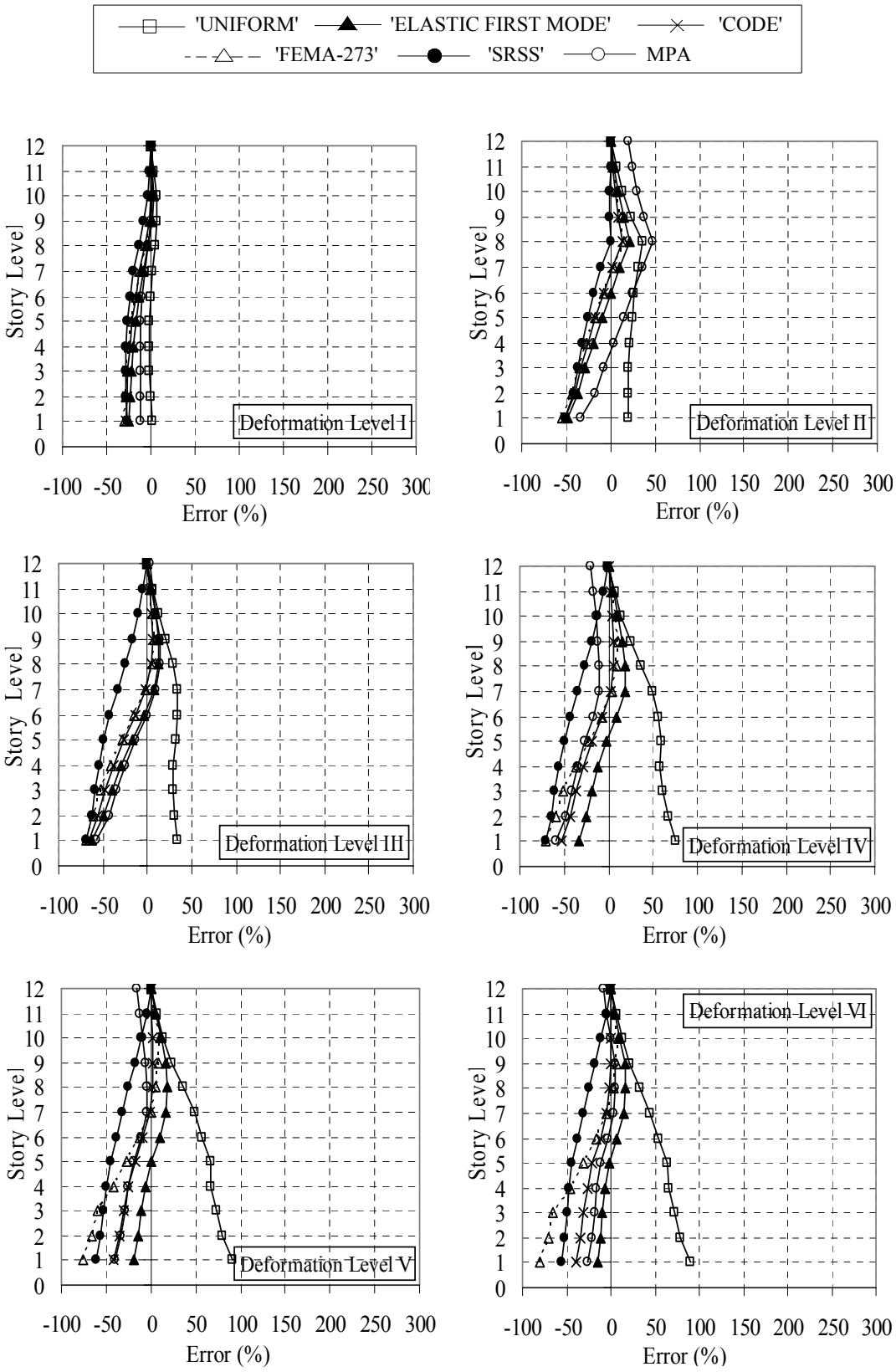

Figure 4.16 : Story Displacement Error Profile for 12-Story R/C Frame (Parkfield)

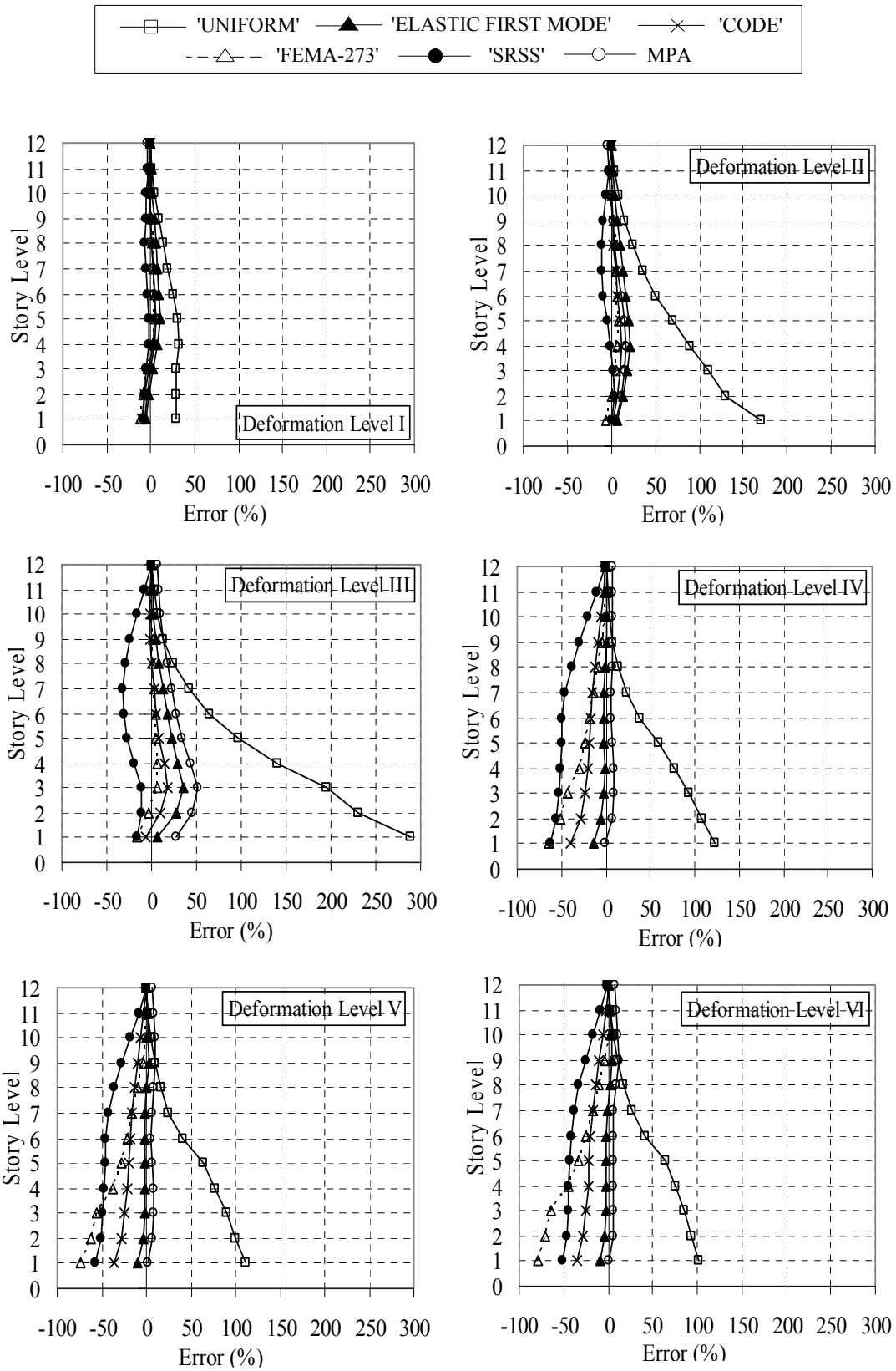

Figure 4.17 : Story Displacement Error Profile for 12-Story R/C Frame (Pacoima Dam)

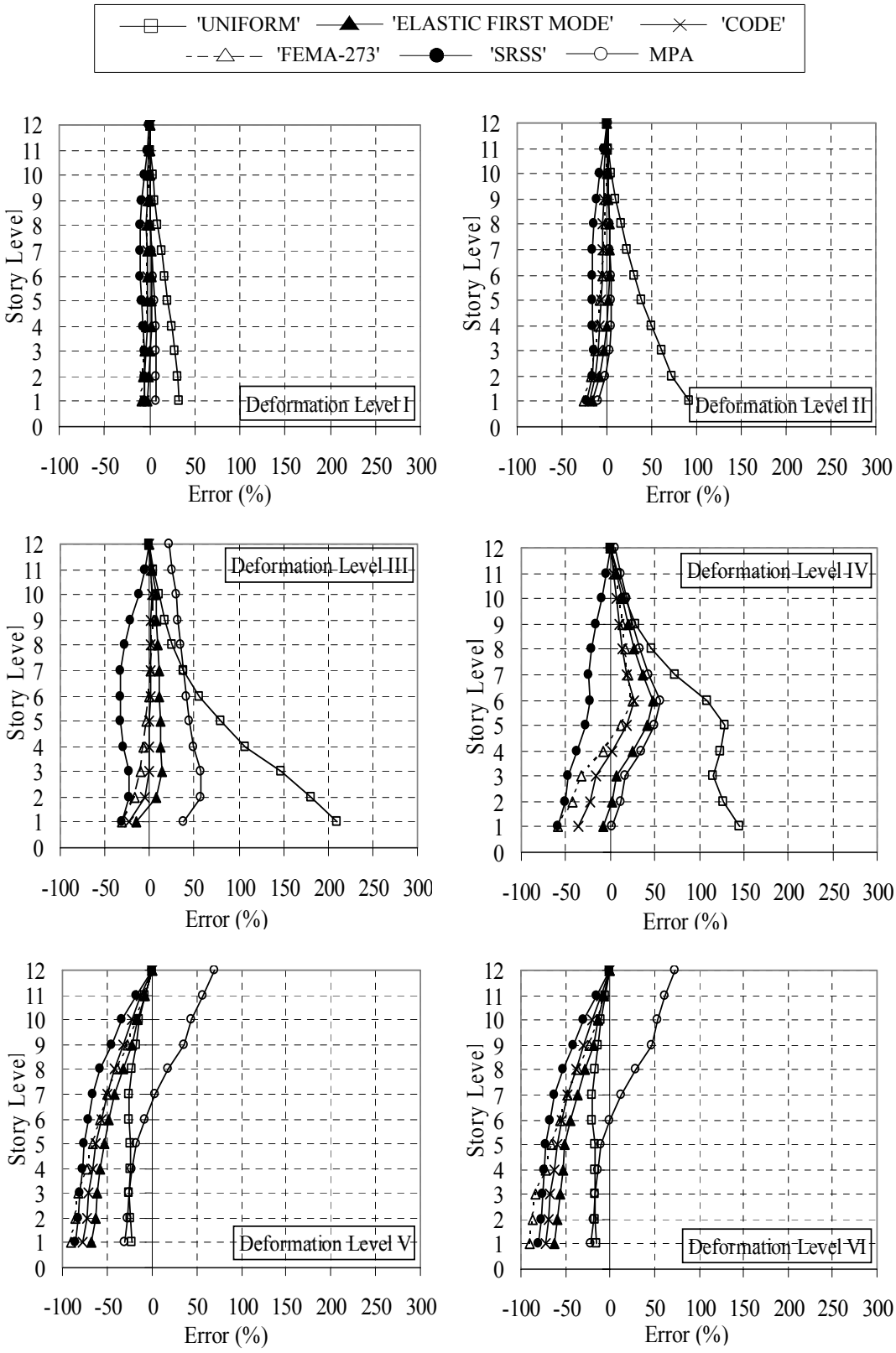

Figure 4.18 : Story Displacement Error Profile for 12-Story R/C Frame (Düzce)

1. None of the lateral load patterns could capture adequately the 'exact' story displacement profile obtained from nonlinear time history analysis at any deformation level.
2. The error involved in story displacement prediction of any lateral load pattern was observed to be larger in nonlinear deformation levels. However, the change in error with nonlinearity was mostly insignificant.
3. The error involved in story displacement prediction of any lateral load pattern was mostly observed to become larger as the number of stories (i.e. as the fundamental period of the frame) increases.
4. Pushover analyses with triangular lateral load patterns ('Elastic First Mode', 'Code', 'FEMA-273', 'Multi-Modal (SRSS)') yielded both overestimations and underestimations of story displacements while 'Uniform' lateral load pattern mostly overestimated the story displacement demand for all frames with few exceptional cases. Also, the error involved in story displacement demand prediction of 'Uniform' lateral load pattern was observed to reach very high levels compared to triangular lateral load patterns at any deformation level.
5. The trend in the similarities and/or in the variations of the height-wise distribution of lateral load patterns was also reflected on the story displacement profile of case study frames. The story displacement profiles for triangular lateral load patterns almost coincided in elastic deformation levels while insignificant discrepancies were observed at nonlinear deformation levels for 2, 5, 8-story R/C and 2, 5-story steel frames as the variation in the height-wise distribution of triangular lateral load patterns are almost negligible for these frames. However, the variation in height-wise distribution and in story displacement profile for triangular lateral load patterns was more apparent for steel frames. On the other hand, significant discrepancies in story displacement profiles existed in both elastic and inelastic deformation levels for long-period frames (12-story R/C and 13-story steel frame) as the variations in the height-wise distribution of triangular lateral load patterns are significant.
6. The discrepancies in story displacement profiles for triangular lateral load patterns were observed to be larger in nonlinear range however the discrepancies did not change appreciably with nonlinearity.

7. The story displacement demand was mostly estimated with about 0-5% accuracy for triangular lateral load patterns for 2-story R/C and steel frames while 'Uniform' load pattern predictions were within 5-10% for almost all cases considered.
8. For 5-story R/C frame, triangular lateral load patterns captured the 'exact' behavior with about 0-5% accuracy in elastic range for all ground motions except Pacoima Dam. Also, triangular lateral load patterns predicted the displacement demand with about 15-20% accuracy while 'Uniform' lateral load pattern predictions reached about 40-60% overestimations at nonlinear deformation levels.
9. Triangular lateral load patterns captured the 'exact' behavior within 20% accuracy while 'Uniform' lateral load pattern yielded about 50-100% overestimations until global yield for 8-story R/C frame. After global yield, the predictions of triangular lateral load patterns mostly lied between 'Multi-Modal (SRSS)' and 'Elastic First Mode' predictions with insignificant discrepancies. Although the error reaches as much as 50%, the behavior was mostly estimated with 20-50% accuracy for triangular lateral load patterns and 'Uniform' load pattern predictions resulted about 100-200% overestimations.
10. The displacement prediction of triangular lateral load patterns mostly lay between 'Multi-Modal (SRSS)' and 'Elastic First Mode' predictions with significant discrepancies at all deformation levels for 12-story R/C frame. The triangular loading predictions were within maximum 30-40% for elastic and low levels of inelastic behavior while 'Uniform' loading predictions reached 50-100% overestimations. Although the error reached 50-100% for triangular load patterns at nonlinear deformation levels, 'Elastic First Mode' and 'Code' predictions were within 20-30% for most of the cases while 'Uniform' loading yielded about 100-150%and sometimes 200% overestimations.
11. The predictions of triangular lateral load patterns were within maximum 20% accuracy while 'Elastic First Mode' yielded the best estimates with about maximum 10% accuracy in most of the cases for 5-story steel frame. 'Uniform' load pattern yielded about 20% in elastic and 20-40% overestimations in nonlinear range.
12. The displacement prediction of triangular lateral load patterns lay between 'Multi-Modal (SRSS)' and 'Elastic First Mode' predictions with significant discrepancies at all deformation levels for 13-story steel frame. The triangular loading predictions were within maximum 20-30% for elastic and low levels of inelastic

behavior while 'Uniform' loading predictions reached 20-40% overestimations. Triangular load patterns predicted displacement demand with about 40% error while 'Uniform' reached as much as 60% at nonlinear deformation levels. An average of the 'Multi-Modal (SRSS)' and 'Elastic First Mode' predictions could capture the 'exact' behavior for 13-story steel frame for all deformation levels.

13. Although 'FEMA-273' and 'Multi-Modal (SRSS)' lateral load patterns considers higher mode effects, these load patterns yielded no improved predictions of displacement demand for long-period frames.

4.6.3 Inter-Story Drift Ratios

The accurate estimation of inter-story drift ratio and its distribution along the height of the structure is very critical for seismic performance evaluation purposes since the structural damage is directly related to the inter-story drift ratio. The inter-story drift ratios and corresponding error profiles of case study frames are illustrated in Figures B.57-B.112 in the attached CD while inter-story drift ratios and corresponding error profiles of 12-story R/C frame are also given in Figures 4.19-4.26.

As this is the case, the overall interpretation on the accuracy of the inter-story drift ratio prediction of pushover analyses on case study frames for considered pushover methods and ground motions yields the following observations:

1. The observations mentioned at items 1, 2, 3, 5 and 6 in Section 4.6.2 are also valid for inter-story drift ratios.
2. The distribution of inter-story drift ratio over the frame height becomes non-uniform as frame height increases.
3. The 'Uniform' lateral load pattern overestimated the inter-story drift ratios at lower stories (about 1/3 of frame height from the base) and underestimated the response at higher stories at all deformation levels. On the other hand, triangular lateral load pattern yielded both overestimations and underestimations of inter-story drift ratio over the frame height while the predictions of both 'Uniform' (for all frames) and triangular lateral load patterns (for frames except 2-story R/C and steel) at upper stories were lower than the 'exact' response at all deformation levels that the effect of even the elastic higher modes were not represented by the lateral load patterns considered.
4. The magnitude of maximum inter-story drift ratio and the distribution of inter-story drift ratio over the frame height for all four ground motions are very similar

for 2 and 5-story R/C and steel frames and all lateral load patterns predicted the 'exact' inter-story drift ratio profile quite well for these frames since the effects of higher modes are negligible and the response is primarily at the fundamental mode.

5. The magnitude of maximum inter-story drift ratio and inter-story drift ratio profiles obtained from time history analyses show the effects of higher modes for 8, 12-story R/C and 13-story steel frames, especially at nonlinear deformation levels. Each ground motion excites different higher modes resulting in different structural response.
6. The inter-story drift ratio was mostly estimated with about 0-5% accuracy for triangular lateral load patterns and 5-10% for 'Uniform' load pattern for 2-story R/C frame for almost all cases considered. However, triangular lateral load patterns predicted inter-story drift ratio with 0-5% accuracy and 'Uniform' load pattern predictions were within 5-10% in elastic and low levels of inelastic behavior for 2-story steel frame while those predictions increased to about 5-10% and 10-20% accuracy respectively for higher levels of nonlinear behavior.
7. For 5-story R/C and steel frames, triangular lateral load patterns predicted the 'exact' behavior with about 10-20% accuracy and 'Uniform' load pattern predictions were within 20-40% in elastic and low levels of nonlinear deformation levels while those predictions reached to 20-40% and 40-60% accuracy respectively for higher nonlinear deformation levels.
8. Triangular lateral load patterns captured the 'exact' behavior within 20-30% accuracy while 'Uniform' lateral load pattern predictions were about 50% accuracy until global yield for 8-story R/C frame. After global yield, the behavior was mostly estimated with 20-30% accuracy for triangular lateral load patterns although the error reached as much as 50% and 'Uniform' load pattern predictions were mostly about 50-100% accuracy although error larger than 100% were observed in some cases.
9. The inter-story drift ratio prediction of triangular lateral load patterns mostly lay between 'Multi-Modal (SRSS)' and 'Elastic First Mode' predictions over the frame height for 12-story R/C frame. Triangular loading predictions were within 30-50% for elastic and low levels of nonlinear behavior while 'Uniform' load pattern predictions were mostly with about 50% accuracy. Although the error reached 50-100% for triangular load patterns at nonlinear deformation levels, 'Code'

predictions were within 30-50% for most of the cases while 'Uniform' loading mostly predicted with 50-100% accuracy altough its predictions involved about 200-300 % error in some cases. An average of the 'Multi-Modal (SRSS)' and 'Elastic First Mode' predictions or 'Code' load pattern which corresponds to that average in most cases could capture the 'exact' behavior with appreciable accuracy for 12-story R/C frame for all deformation levels.

10. The inter-story drift ratio prediction of triangular lateral load patterns mostly lay between 'Multi-Modal (SRSS)' and 'Elastic First Mode' predictions along the frame height for 13-story steel frame. The triangular loading predictions were within maximum 25-50% for elastic and low levels of inelastic behavior while 'Uniform' loading mostly predicted with about 50% accuracy. Triangular load patterns predicted with about 50% error while 'Uniform' loading reached as much as 60-80% at nonlinear deformation levels. An average of the 'Multi-Modal (SRSS)' and 'Elastic First Mode' predictions or 'Code' load pattern which corresponds to that average in most cases could capture the 'exact' behavior with appreciable accuracy for 13-story steel frame at all deformation levels.

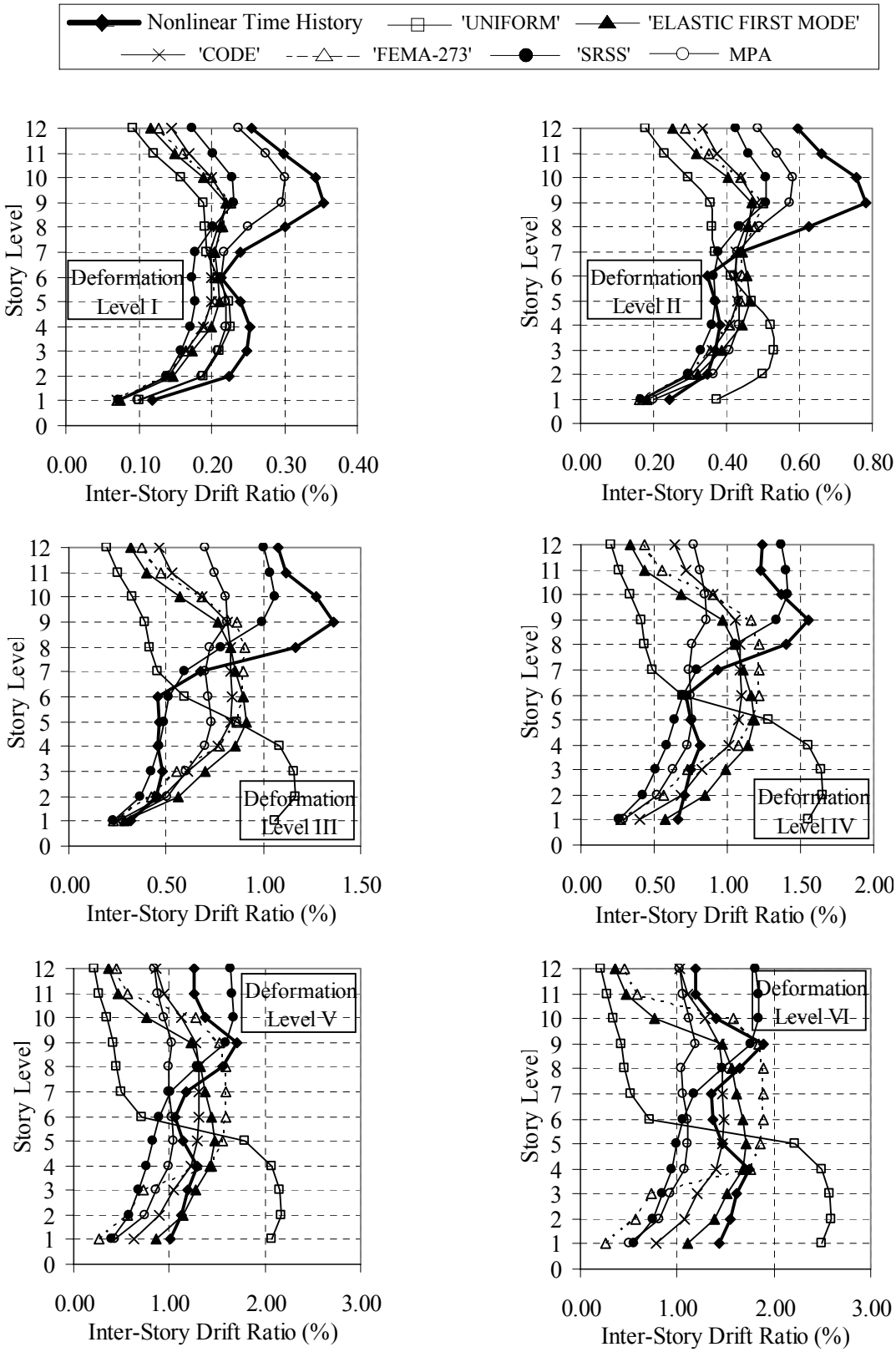

Figure 4.19 : Inter-Story Drift Ratio Profile for 12-Story R/C Frame (El Centro)

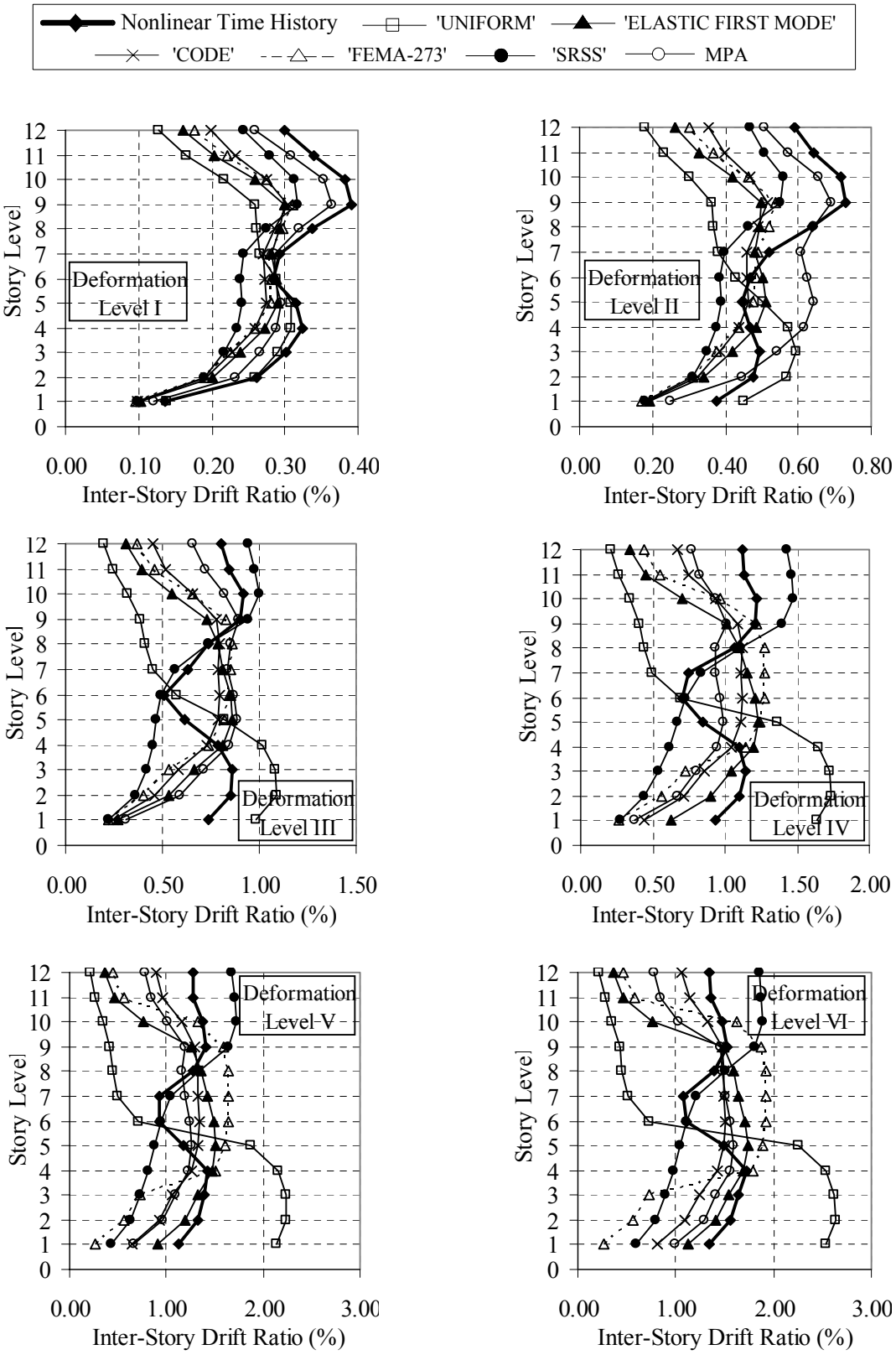

Figure 4.20 : Inter-Story Drift Ratio Profile for 12-Story R/C Frame (Parkfield)

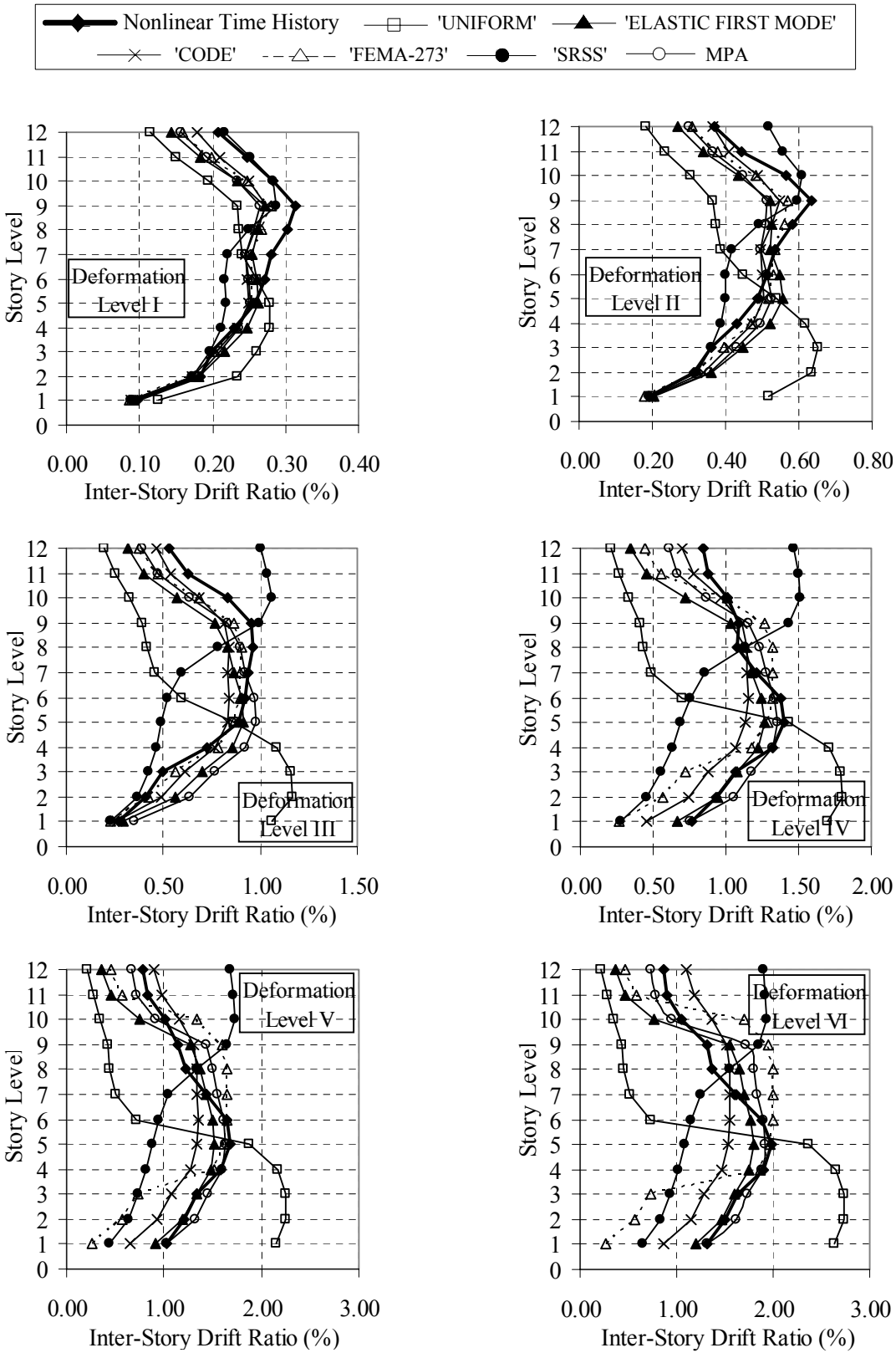

Figure 4.21 : Inter-Story Drift Ratio Profile for 12-Story R/C Frame (Pacoima Dam)

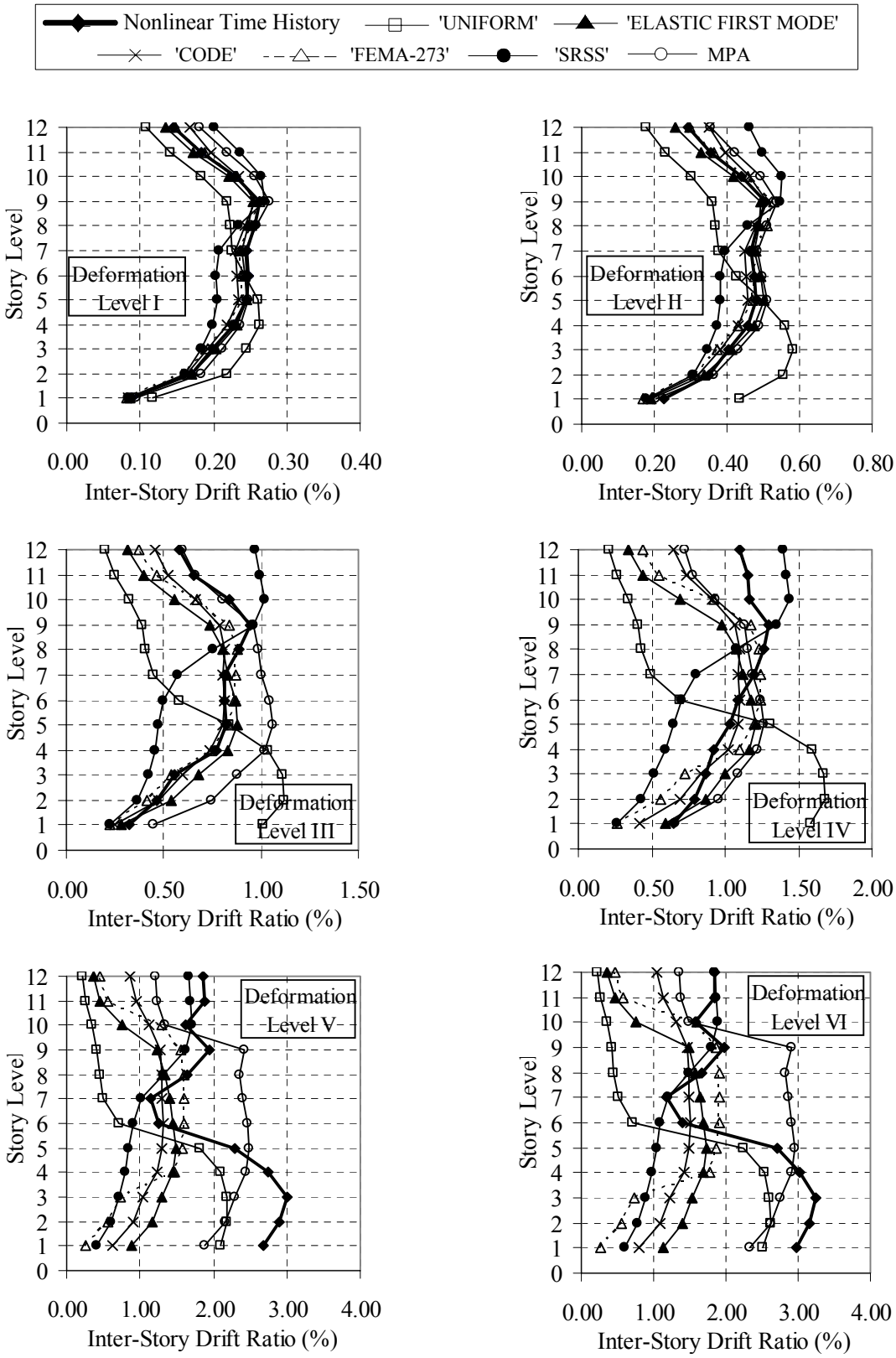

Figure 4.22 : Inter-Story Drift Ratio Profile for 12-Story R/C Frame (Düzce)

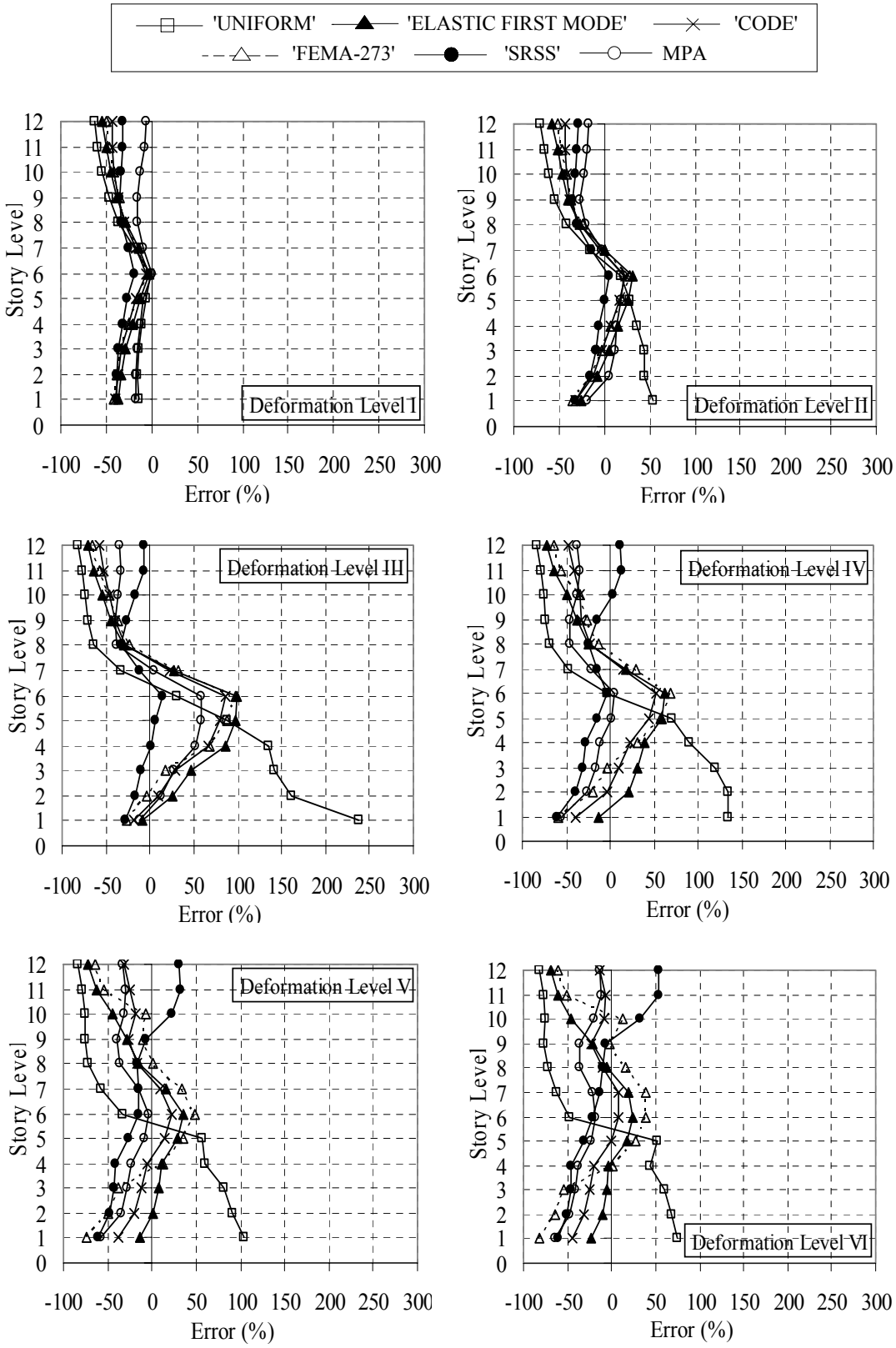

Figure 4.23 : Inter-Story Drift Ratio Error Profile for 12-Story R/C Frame (El Centro)

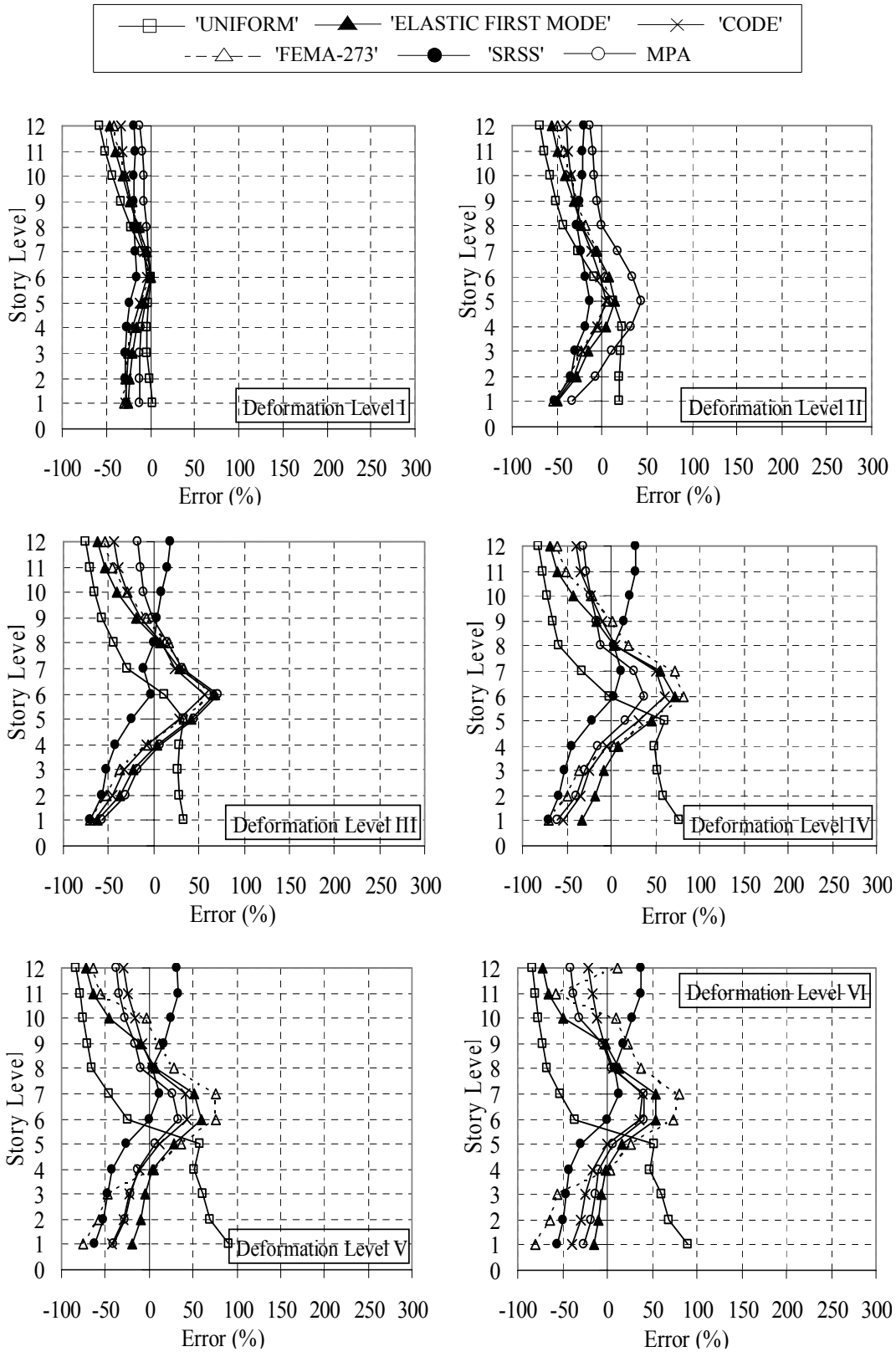

Figure 4.24 : Inter-Story Drift Ratio Error Profile for 12-Story R/C Frame (Parkfield)

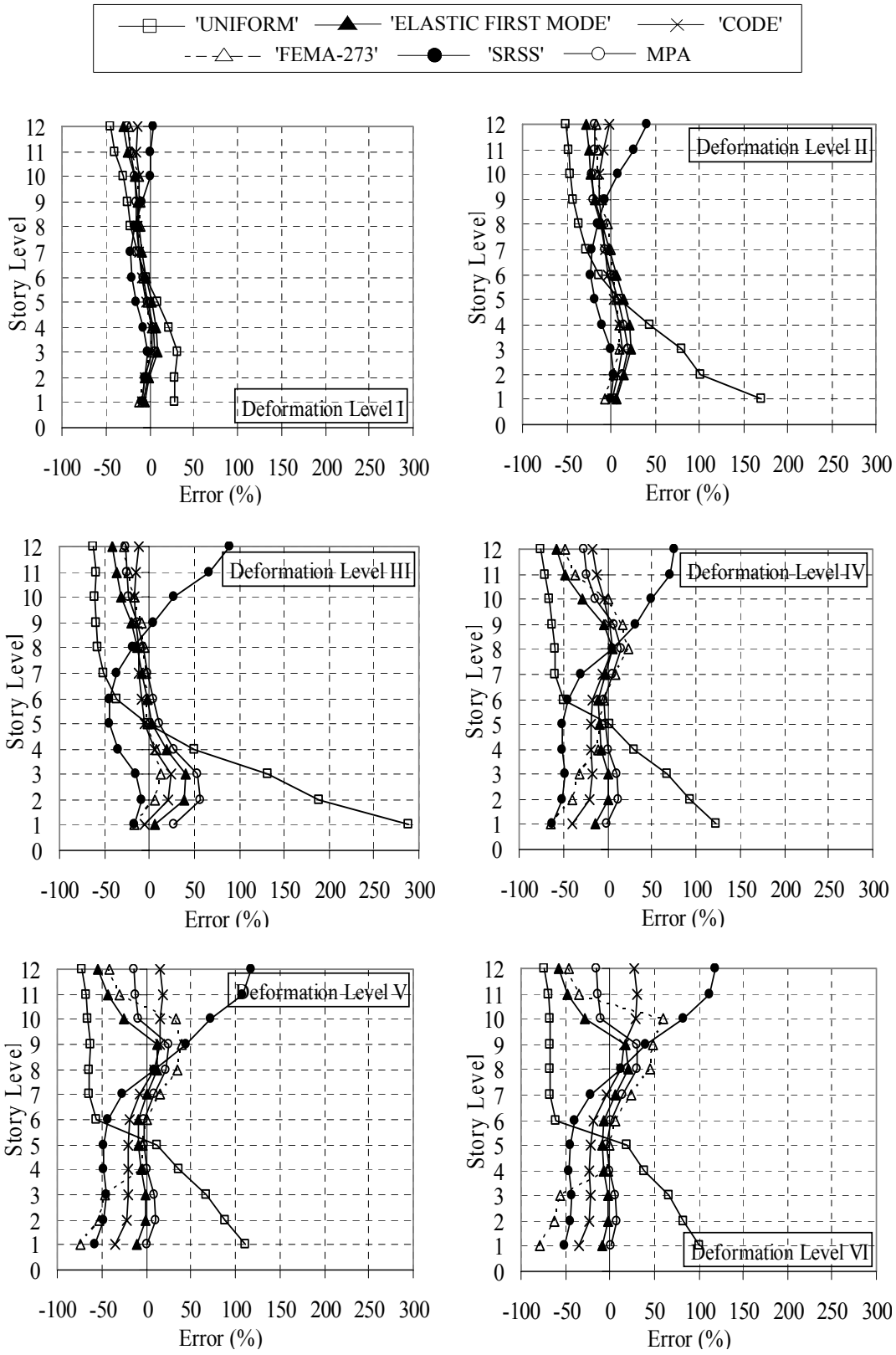

Figure 4.25 : Inter-Story Drift Ratio Error Profile for 12-Story R/C Frame (Pacoima Dam)

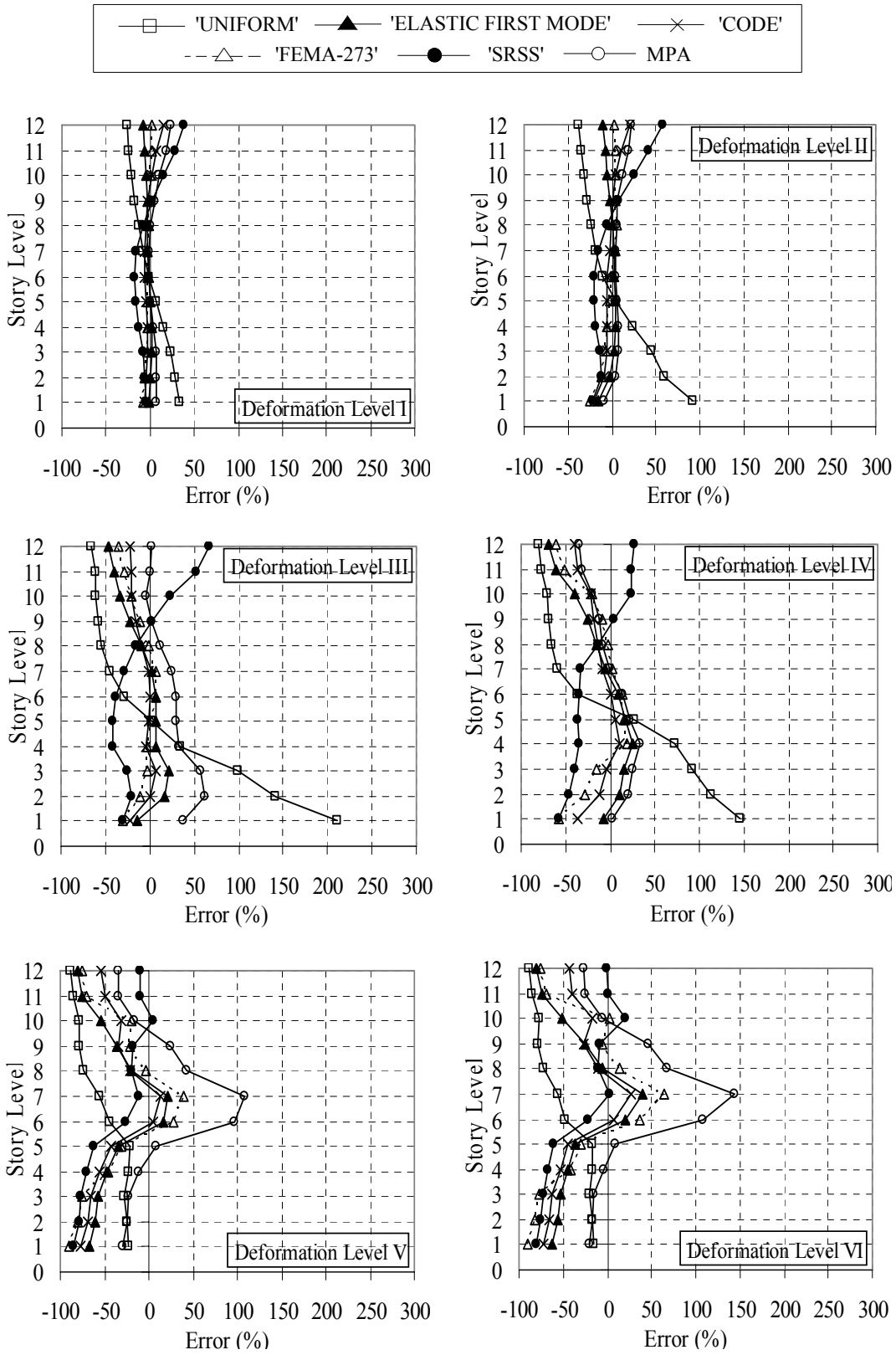

Figure 4.26 : Inter-Story Drift Ratio Error Profile for 12-Story R/C Frame (Düzce)

4.6.4 Story Pushover Curves

Story shears and story displacements were extracted from pushover database at each step of pushover analyses for all lateral load patterns and story pushover curves (story shear vs story displacement) were developed to illustrate the variation in story shears due to the height-wise distribution of lateral load pattern. Also, the absolute maximum values of story shears and story displacements experienced under ground motion excitations were determined for each deformation level to approximate a dynamic story pushover curve for case study frames. Story pushover curves for 2, 5, 8- and 12-stories R/C frames are shown in Figures 4.27-4.31 while story pushover curves for 2, 5- and 13-stories steel frames are illustrated in Figures A.8-A.11.

The variation in the shape of story pushover curves is a function of base shear capacity of the frames and the height-wise distribution of story forces which develops that base shear as well as the nonlinear structural characteristics. The base shear capacity of frames under 'Uniform' lateral load pattern is higher than that of triangular lateral load patterns as discussed in Section 4.6.1 so 'Uniform' load pattern yields higher story shear values for lower stories (up to about one third of frame height, h/3). On the other hand, higher story forces are developed at upper stories for frames under triangular lateral load patterns that triangular lateral load patterns yield higher story shears at upper stories (about above h/3). It is also observed that all lateral load patterns yield approximately same story shear values at about h/3.

Moreover, as the variation in the height-wise distribution of triangular lateral load patterns ('Uniform', 'Elastic First Mode', 'Code', 'FEMA-273' and 'Multi-Modal (SRSS)') increases the difference in story shears becomes more significant. There exists a significant variation in the height-wise distribution of triangular lateral load patterns for long-period frames and the difference in story shears developed under triangular lateral load patterns is significant for those frames at all story levels. The variation in the height-wise distribution of triangular lateral load patterns for low to mid-rise frames is negligible and the difference in story shears is only significant for uppermost stories due to the significant difference in the amplitude of story forces developed at uppermost stories.

On the other hand, none of the invariant lateral load patterns captures the approximate dynamic behavior at story level. The invariant lateral load patterns resulted in underestimated story pushover curves at almost all story levels for case study frames.

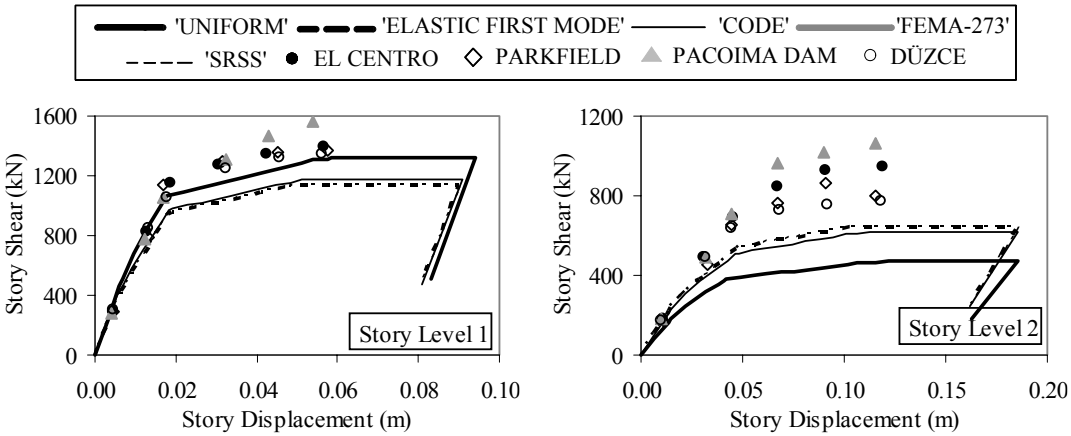

Figure 4.27 : Story Pushover Curves for 2-Story R/C Frame (Story Levels 1-2)

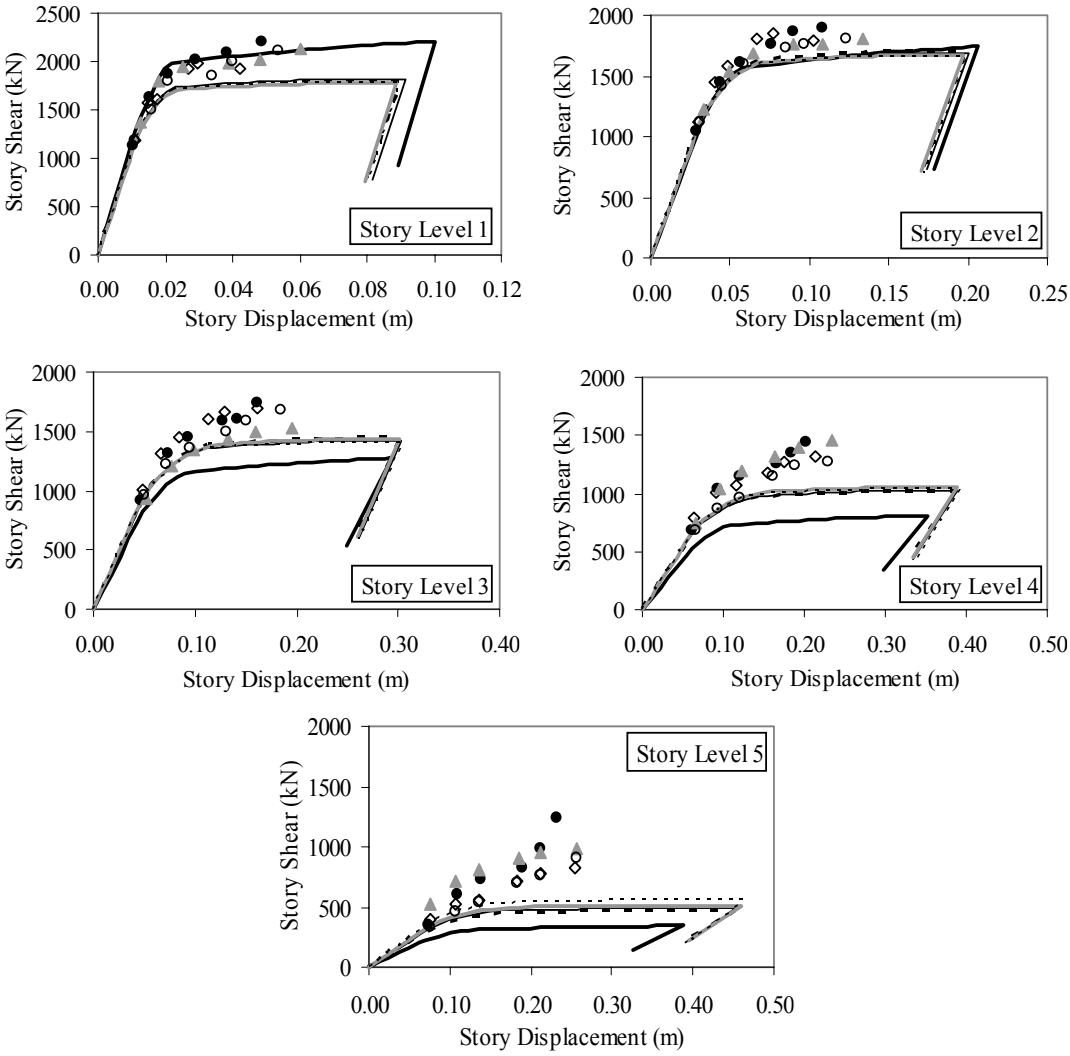

Figure 4.28 : Story Pushover Curves for 5-Story R/C Frame (Story Levels 1-5)

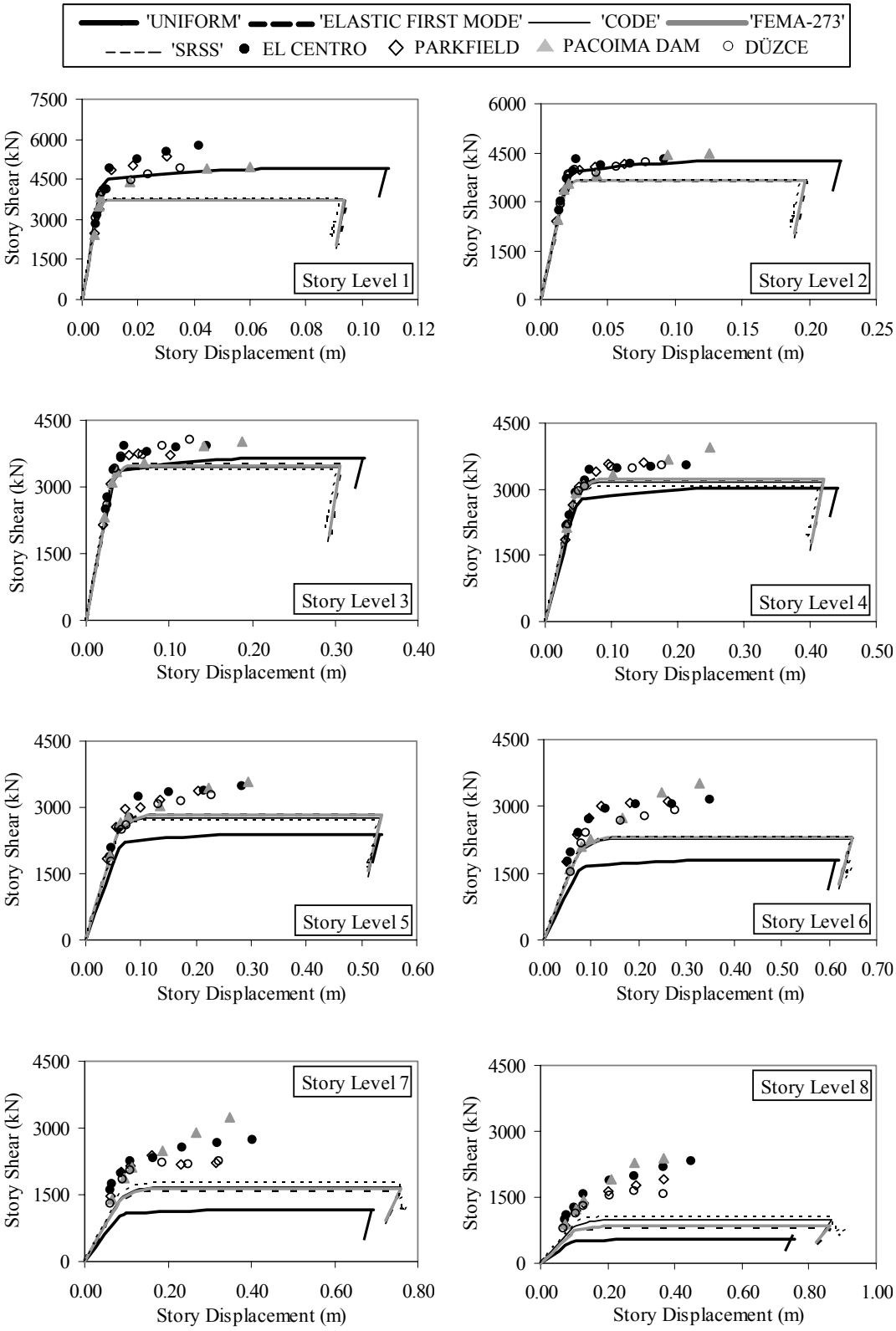

Figure 4.29 : Story Pushover Curves for 8-Story R/C Frame (Story Levels 1-8)

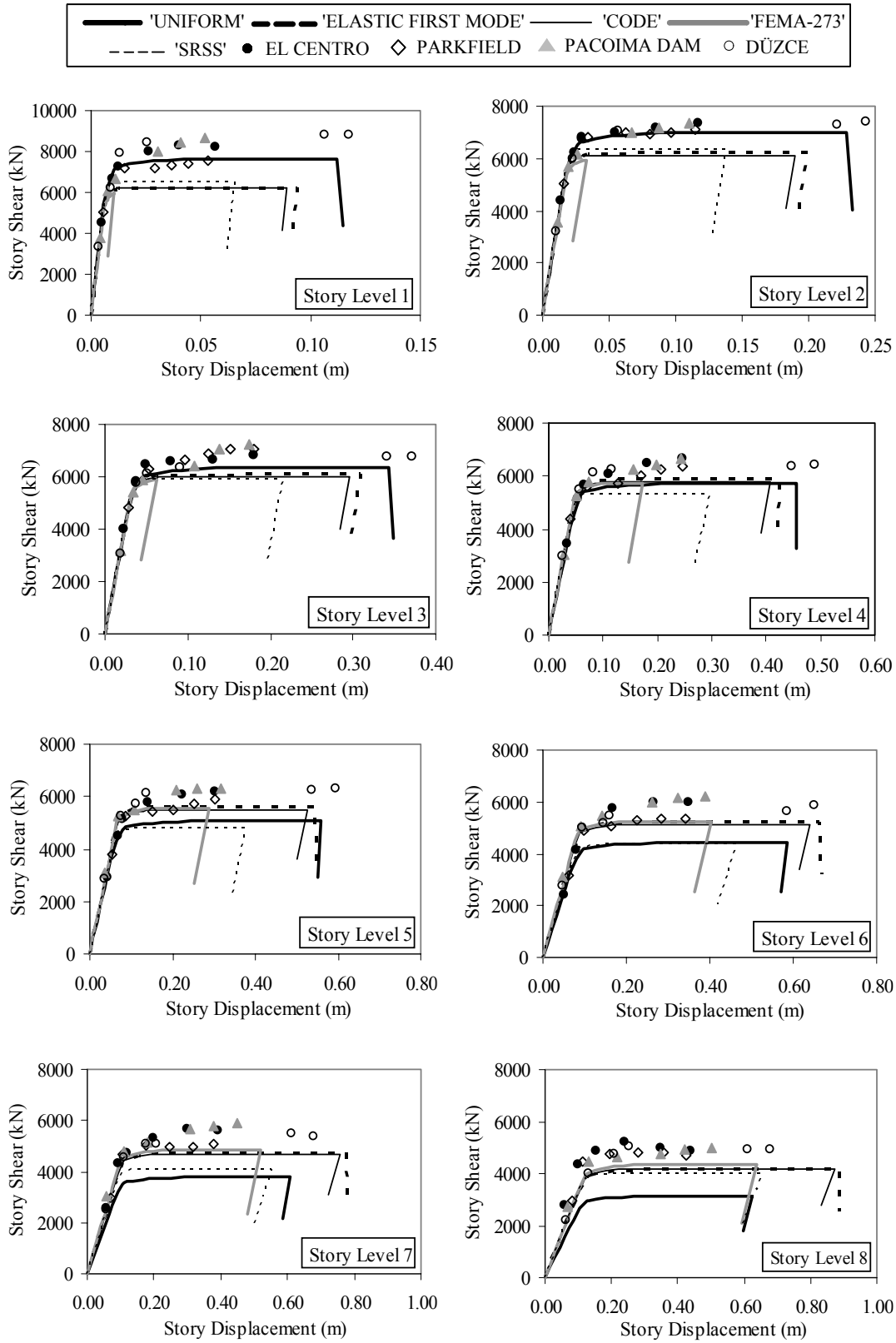

Figure 4.30 : Story Pushover Curves for 12-Story R/C Frame (Story Levels 1-8)

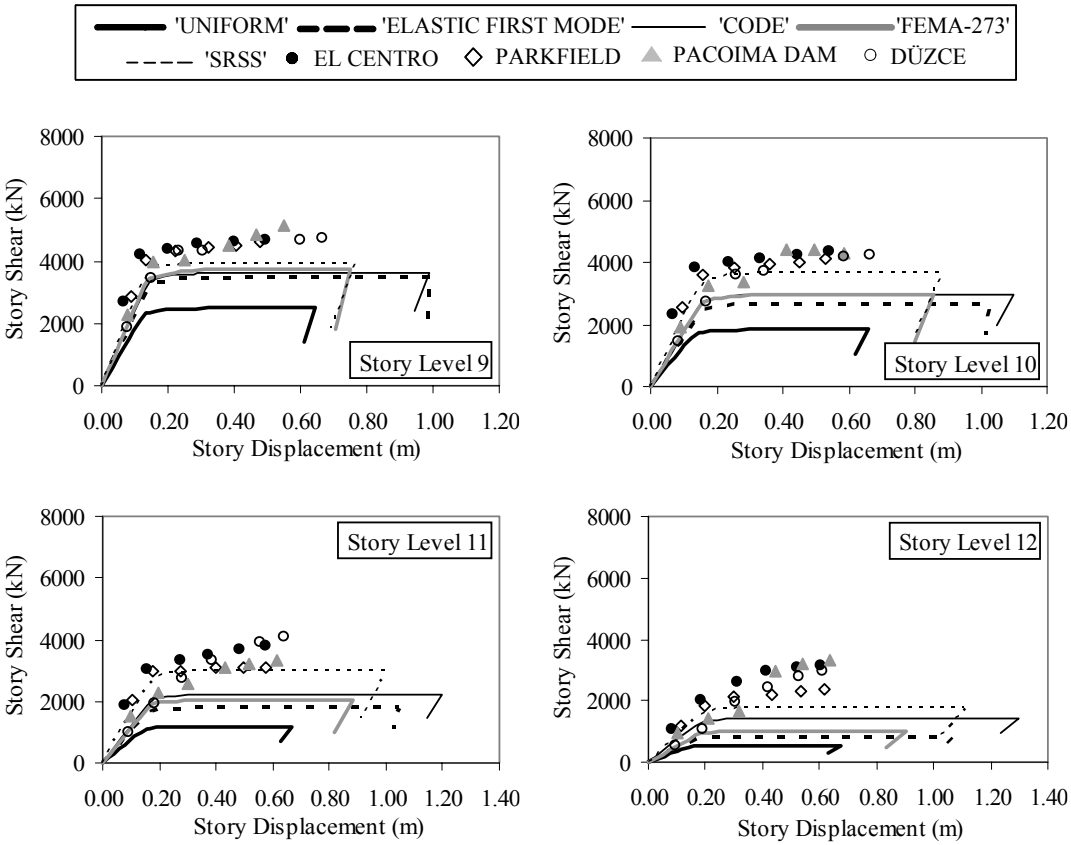

Figure 4.31: Story Pushover Curves for 12-Story R/C Frame (Story Levels 9-12)

4.6.5 Plastic Hinge Locations

Location of weak points and potential failure modes that structure would experience in case of a seismic event is expected to be identified by pushover analyses. The accuracy of various lateral load patterns utilized in traditional pushover analyses and Modal Pushover Analysis (MPA) to predict the plastic hinges similar to those predicted by nonlinear time history analyses was evaluated in this study.

The location of plastic hinges for case study R/C frames were predicted by pushover analyses performed considering the lateral load patterns used in this study at roof displacements corresponding to the nonlinear time history Deformation Levels II, III and VI. These deformation levels represent low levels of nonlinear behavior, global yield and high levels of nonlinear behavior. The pushover and nonlinear time history hinge patterns were compared. The plastic hinge locations were also estimated for R/C frames by MPA. The location of plastic hinges for R/C frames predicted by each pushover method and nonlinear time history analyses for each ground motion at considered

deformation levels are illustrated in Figures A.12-A.20 in Appendix A. The results for the 8-story R/C frame are shown in Figures 4.32-4.34.

Following observations can be made from the comparison of plastic hinge locations determined by pushover analyses and nonlinear time history analyses:

1. Locations of plastic hinges obtained from nonlinear time history analyses are generally different for each ground motion for each frame at all deformation levels considered as each ground motion excites the structure differently.
2. None of the lateral load patterns could capture adequately the 'exact' plastic hinge locations obtained from nonlinear time history analyses at any considered deformation level even for 2-story R/C frame.
3. Pushover analyses could not predict the plastic hinging in same sequence with nonlinear time history analyses predictions.
4. 'Uniform' lateral load pattern mostly predicts the plastic hinging at lower stories but could not produce any plastic hinging at upper stories especially for long-period frames.
5. Triangular lateral load patterns yield similar plastic hinge locations for 2, 5- and 8-story R/C frames but significant differences are observed for 12-story R/C frame.
6. Although triangular lateral load patterns yield more homogenous prediction of plastic hinge locations over the entire frame than 'Uniform' loading, they could not predict the plastic hinges at upper stories and/or at story column ends for 5, 8- and 12-story R/C frames.
7. Plastic hinge patterns obtained from nonlinear time history analyses for 8- and 12-story R/C frames reveal the effects of higher modes on structural behavior. However, none of the lateral load patterns capture this behavior even the 'Multi-Modal (SRSS)' lateral load pattern which considers at least elastic higher modes.

Lateral load patterns utilized in traditional pushover analyses give some idea about the locations where inelastic behavior is expected but their prediction of plastic hinge locations is generally inadequate for the deformation levels considered. Although these lateral load patterns miss important weak points and could not represent the higher mode effects, the predictions of triangular lateral load patterns were observed to be better than 'Uniform' loading predictions for 5, 8- and 12-story R/C frames but the difference in the accuracy of any triangular lateral load pattern was observed to be insignificant.

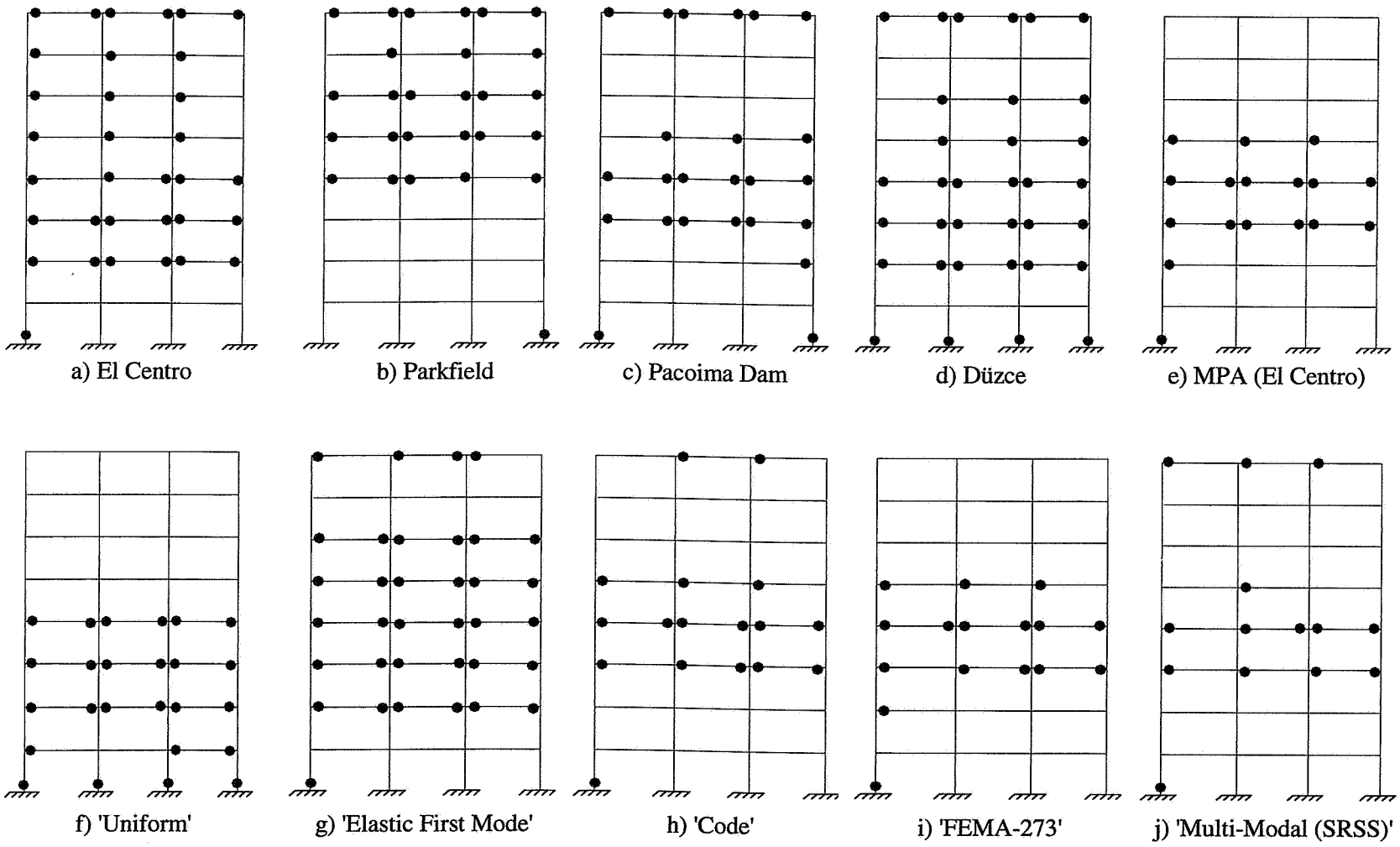

Figure 4.32 : Plastic Hinges for 8-Story R/C Frame (Deformation Level II)

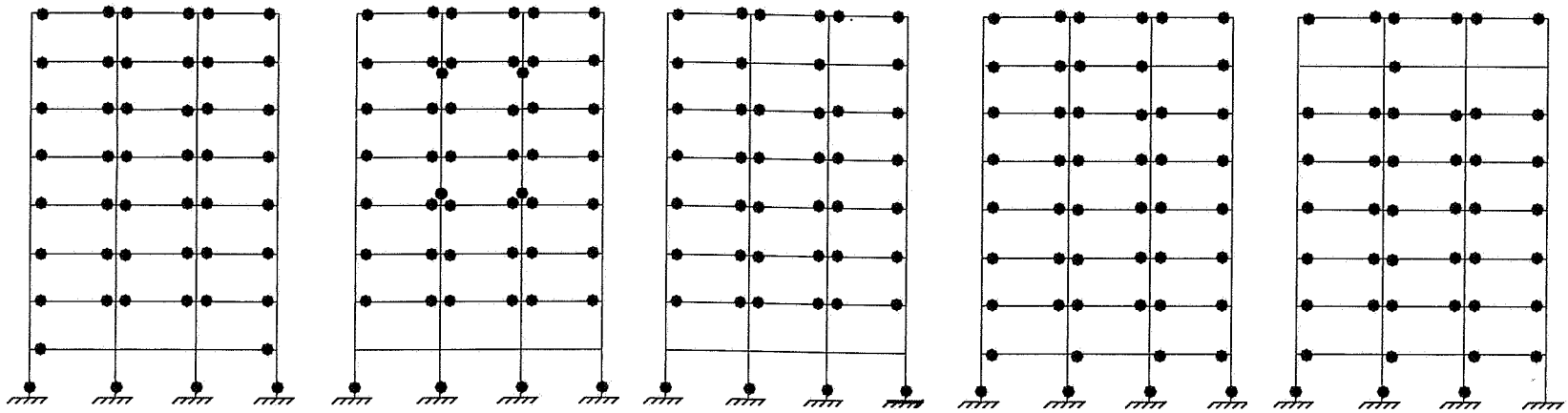

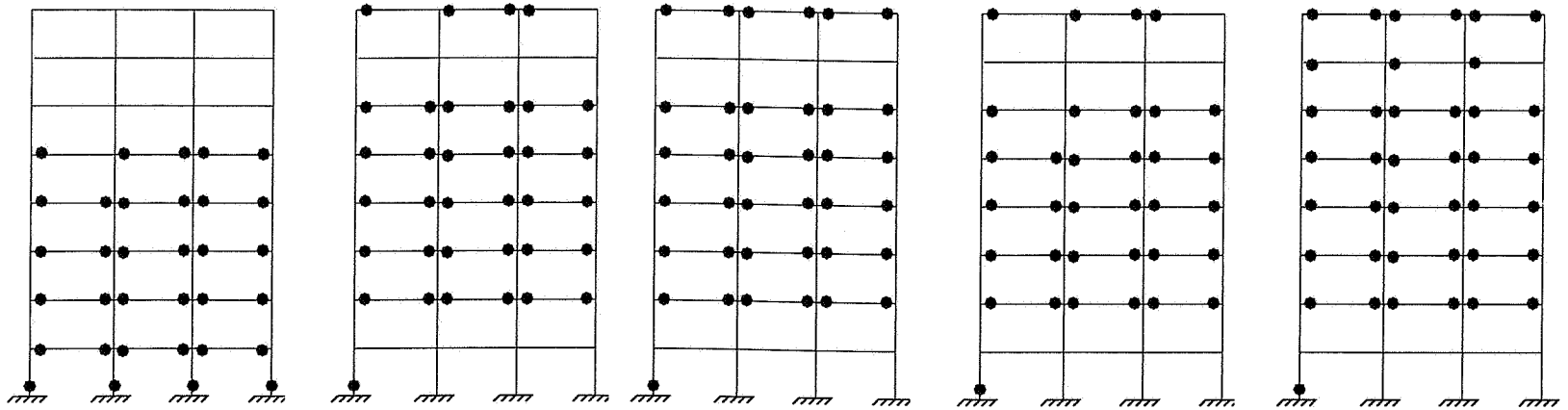

Figure 4.33 : Plastic Hinges for 8-Story R/C Frame (Deformation Level III)

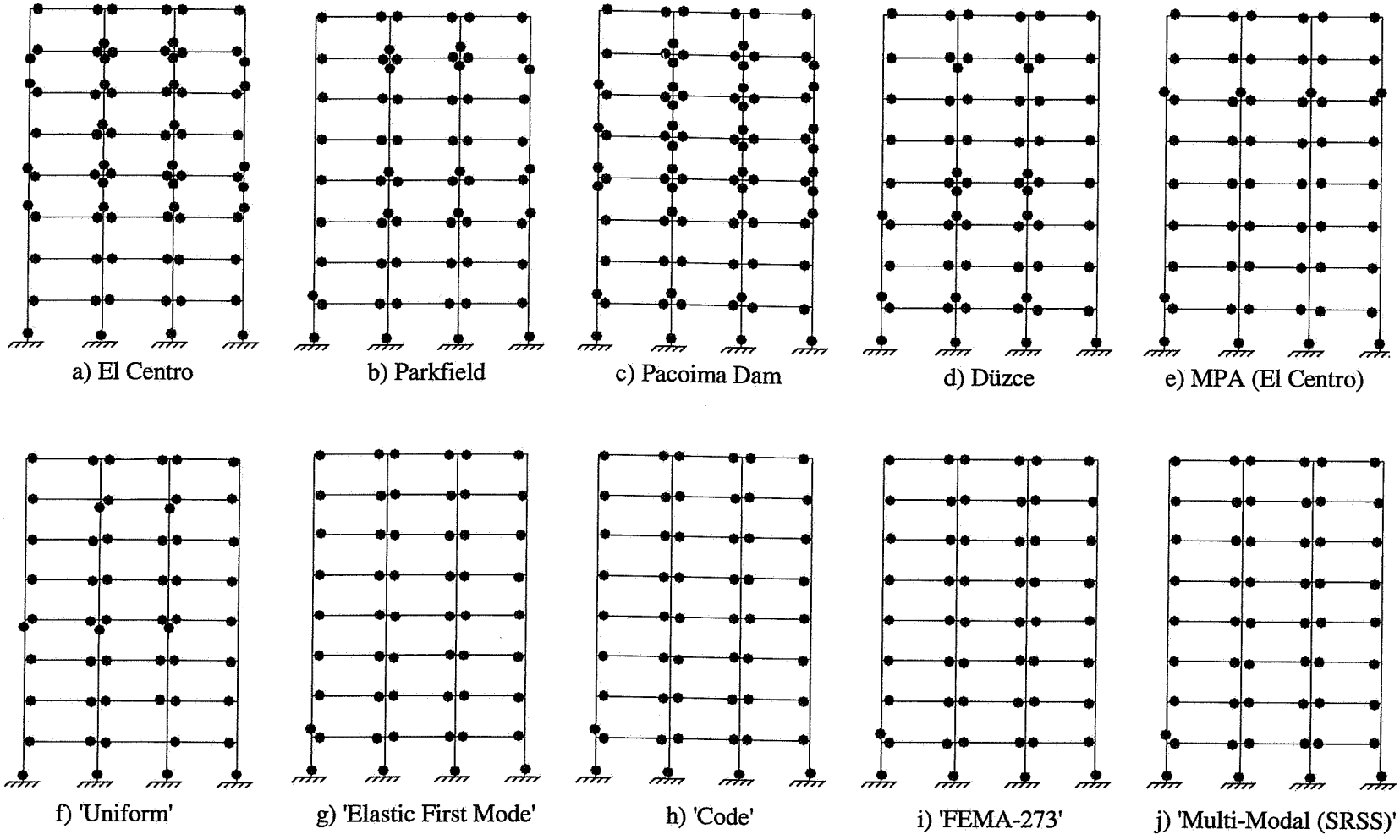

Figure 4.34 : Plastic Hinges for 8-Story R/C Frame (Deformation Level VI)

4.6.1 Accuracy of Modal Pushover Analysis (MPA) Predictions

The seismic demands were estimated by pushover analyses using various invariant lateral load patterns at peak roof displacements obtained from nonlinear time history analyses corresponding to the deformation levels considered. However, seismic demands were estimated by Modal Pushover Analysis (MPA) at peak roof displacements different than 'exact' peak roof displacements due to the implementation of the procedure. Although this is the case, the accuracy of MPA predictions was investigated for case study frames and a comparative evaluation on the accuracy of seismic demand predictions of lateral load patterns and MPA was conducted.

MPA could not capture the 'exact' story displacement and inter-story drift ratio demands obtained from nonlinear time history analysis at any deformation level and the error in story displacement and inter-story drift ratio prediction of MPA was observed to become larger at nonlinear deformation levels. The demand prediction of MPA was observed to be less accurate as the frame height increases.

No clear trend was observed in the story displacement prediction of MPA such that MPA mostly predicted the displacement demand for almost all frames with similar accuracy as triangular lateral load pattern predictions at any deformation level. However, MPA mostly overestimated the displacement demand of 2-story R/C frame about 20-40%. Both overestimated and underestimated displacement predictions of about 30-50% were observed in some cases for both mid and high-rise frames.

MPA predicted inter-story drift ratio with a similar degree of accuracy as triangular load patterns for 2-story frames and overestimated the 'exact' results by 20-40%. No clear trend was observed in the inter-story drift ratio prediction of MPA for 5- and 8-story R/C and 5-story steel frames such that MPA mostly yielded very similar inter-story drift ratio profiles as those obtained from triangular lateral load patterns while about 20-30% overestimated or underestimated inter-story drift ratio profiles were also obtained from MPA in some cases. On the other hand, MPA mostly predicted the inter-story drift ratio demands at lower stories similar to triangular lateral load patterns while improved predictions were observed at upper stories for 12-story R/C and 13-story steel frames that higher mode effects are represented better by MPA for long-period frames. The height-wise distribution of inter-story drift ratio determined by MPA was much closer to the trend observed from nonlinear time history analysis for long period frames.

MPA could not capture the 'exact' plastic hinge locations either at any considered deformation level even for 2-story R/C frame although MPA takes into the effects of

higher modes. However, the plastic hinge location predictions of MPA were generally observed to be better than triangular lateral load pattern predictions for 5, 8- and 12-story R/C frames.

2.1 SUMMARY AND DISCUSSION OF RESULTS

As the structural response is affected from the lateral load patterns utilized in pushover analysis, the accuracy of lateral load patterns in predicting seismic demands should be evaluated. Pushover analyses were performed on reinforced concrete and steel moment resisting frames covering a broad range of fundamental periods using traditional invariant lateral load patterns such as 'Uniform', 'Elastic First Mode', 'Code', 'FEMA-273' and 'Multi-Modal (SRSS)'. The effects and the accuracy of lateral load patterns in predicting the behavior imposed on the structure due to randomly selected individual ground motions causing elastic and various levels of nonlinear response were also evaluated in this study. For this purpose, capacity curves representing global structure behavior, story displacements, inter-story drift ratios, story shears and plastic hinge locations were selected as response parameters. The story displacements, inter-story drift ratios and plastic hinge locations were estimated by performing the Modal Pushover Analysis (MPA) on the case study frames as well. The applicability and the accuracy of each pushover method in predicting seismic demands were investigated for low, mid and high-rise frame structures.

The main conclusion derived from the observations on the response prediction of each pushover method considered is that the response prediction of pushover analysis is directly related to the height-wise distribution of lateral load pattern utilized as well as nonlinear structural properties of the frames and the seismological features of the excitation. The trend in the similarities and/or in the variations of the height-wise distribution of lateral load patterns are reflected on the global capacity curve, story displacement, inter-story drift ratio, story shear and plastic hinge location prediction of pushover analyses for case study frames.

The variation in height-wise distribution of triangular lateral load patterns ('Elastic First Mode', 'Code', 'FEMA-273' and 'Multi-Modal (SRSS)') is negligible for low to mid-rise frames (fundamental period less than about 1.0 s). For these frames the triangular lateral load patterns predicted similar global capacity curves, story displacement and inter-story drift ratio profiles, story shears and plastic hinge locations and the results were general in good agreement with the 'exact' ones. Therefore, any triangular lateral load

pattern could be used in practice to predict response parameters for these frames (2, 5-story R/C and steel frames) as the difference in the accuracy of any triangular lateral load pattern demand prediction was observed to be insignificant.

On the other hand, the variation in the height-wise distribution of triangular lateral load patterns is observed to be significant for high-rise frames (8, 12-story R/C and 13-story steel frames) that appreciable differences in the prediction of response parameters were observed. The story displacement and inter-story drift ratio prediction of triangular lateral load patterns mostly lied between the predictions of 'Multi-Modal (SRSS)' and 'Elastic First Mode' for long-period frames. Therefore, it would be better to estimate the story displacement and inter-story drift ratio demand of long-period structures by considering the average of the 'Multi-Modal (SRSS)' and 'Elastic First Mode' predictions or 'Code' load pattern which corresponds to that average in most cases. Although 'FEMA-273' and 'Multi-Modal (SRSS)' lateral load patterns consider higher mode effects, these load patterns yielded no improved predictions of seismic demand for long-period frames. Also, 'FEMA-273' and 'Multi-Modal (or SRSS)' lateral load patterns yielded the lower and upper bounds of base shear capacities obtained from triangular lateral load patterns for long-period frames, respectively and it was observed that the use of 'Elastic First Mode' or 'Code' lateral load patterns is better to represent an average global capacity curve determined by triangular lateral load patterns for long period frames.

The predictions of triangular lateral load patterns were observed to be better than 'Uniform' loading predictions for all frames at all deformation levels since 'Uniform' lateral load pattern mostly emphasized demands in lower stories over demands in upper stories as observed in the story displacement, inter-story drift ratio, story shear and plastic hinge location predictions. On the other hand, triangular lateral load patterns predicted the response more homogenously over the frame height that both overestimated and underestimated predictions were observed over the frame height for story displacements and inter-story drift ratios. Triangular lateral load patterns predicted the story displacement and inter-story drift ratio profiles of low-to mid rise frames with more or less same accuracy. On the other hand, inter-story drift ratio was predicted with less accuracy for long-period frames as story drifts are much affected by higher modes. Also, the error involved in 'Uniform' loading predictions of story displacement and inter-story drift ratio demands were observed to reach unacceptably large values compared to the predictions of triangular lateral load patterns.

However, none of the invariant lateral load patterns could capture the approximate dynamic behavior globally and at story levels. The 'Uniform' and triangular lateral load patterns seem to be the upper and lower bounds of approximate dynamic global behavior while all invariant lateral load patterns underestimated the dynamic behavior at almost all story levels as illustrated in story pushover curves. Similarly, none of the invariant lateral load patterns and MPA could predict the 'exact' plastic hinge locations and plastic hinge location prediction of each pushover method was observed to be inadequate and non-conservative for all frames. Plastic hinge location predictions of triangular lateral load patterns were observed to be better than those of 'Uniform' loading for 5, 8- and 12-story R/C frames while the difference in the accuracy of any triangular loading prediction was observed to be insignificant. However, MPA yielded improved predictions of plastic hinge locations.

On the other hand, no clear trend was observed in the predictions of MPA due to the approximations inherent in the procedure. MPA mostly estimated the story displacement and inter-story drift ratio demands with a similar degree of accuracy as triangular lateral load patterns for low to mid-rise frames although some exceptions were observed. However, MPA mostly predicted the inter-story drift demands at lower stories similar to triangular lateral load patterns while improved predictions were observed at upper stories for long-period frames as MPA considers higher mode effects.

Although pushover analyses give an insight about nonlinear behavior imposed on structure by seismic action, any design and seismic evaluation process should be performed by keeping in mind that some amount of variation always exists in seismic demand prediction of pushover analysis for low, mid and high-rise frames.

The degree of accuracy attained by the pushover procedures was observed to be better in the elastic response range as compared to the inelastic range.

CHAPTER 5

ESTIMATION OF INELASTIC DISPLACEMENT DEMAND

5.1 GENERAL

The inelastic displacement demand referred as target displacement represents the probable maximum global displacement demand of the structure when exposed to the design earthquake. The accurate estimation of the target displacement associated with specific performance objective affects the accuracy of seismic demand predictions of pushover analysis since force and deformation demands at target displacement are compared with available capacities for a performance check.

The maximum displacement demand of structures can be accurately computed through a time history analysis when full ground motion record is available. However, the complexity of time history analysis is well known and seismic performance evaluation procedures are mostly employed for design evaluation purposes that seismic demands are generally estimated under smooth design spectra rather than individual ground motion records. Thus, many approximate procedures have been proposed to estimate seismic displacement demand of structures. The estimation of maximum inelastic displacement demand of MDOF structure from the maximum displacement demand of corresponding equivalent SDOF system forms the underlying principle of most of the proposed approximate procedures.

Four commonly known approximate procedures, Nonlinear Dynamic Analysis of Equivalent SDOF System, Capacity Spectrum Method (ATC-40 Procedure A) [3], Displacement Coefficient Method (FEMA-356) [20] and Constant Ductility Procedure (Chopra&Goel) [8], which make use of capacity (pushover) curve of the structure were evaluated under individual ground motion records. Capacity curves obtained using lateral

load pattern proportional to product of story masses and elastic first mode which is normalised to have unit modal amplitude at roof level were utilised in all procedures. Also, bilinear representation of capacity curve and/or capacity spectrum is required to be used in these procedures. The approach used in Displacement Coefficient Method [20] was utilised to construct the bilinear representation of capacity curve in all procedures.

The theoretical background for each procedure is presented in the following sections.

5.2 NONLINEAR DYNAMIC ANALYSIS OF EQUIVALENT SDOF SYSTEM

The maximum global displacement demand of MDOF structure is directly obtained through a time history analysis of corresponding equivalent SDOF system with properly modeled hysteretic characteristics. This procedure can be used only when the response against a ground motion is desired.

The basic properties of equivalent SDOF system can be obtained by using the approach proposed by ATC-40 [3]. In this approach, the deflected shape of MDOF structure is assumed to be represented by elastic first mode of the structure. MDOF structure is represented by an equivalent SDOF system having an effective mass (M^*) and an effective stiffness (K^*) where the effective period equals to $2\pi\sqrt{\frac{M^*}{K^*}}$ (Figure 5.1).

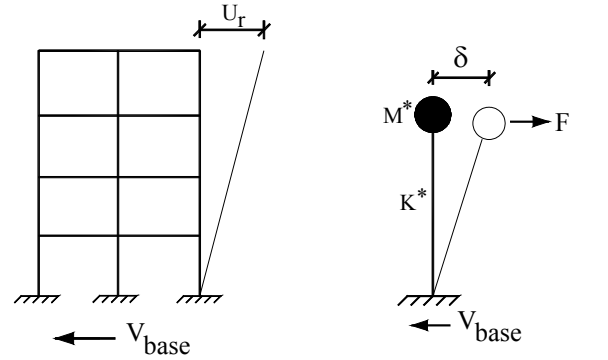

Figure 5.1 : MDOF Structure Represented by Equivalent SDOF System (Approach Proposed by ATC-40 [3])

Force-displacement relationship of equivalent SDOF system is determined from the capacity (pushover) curve of the MDOF structure. The procedure consists of the following steps:

1. Develop a capacity curve (base shear versus roof displacement) of the overall structure by pushover analysis.
2. Construct a bilinear representation of capacity curve. The approach used in Displacement Coefficient Method [20] was utilised to construct the bilinear representation of capacity curve. In this approach, a line representing the average post-elastic stiffness, K_s, of capacity curve is first drawn by judgement. Then, a secant line representing effective elastic stiffness, K_e , is drawn such that it intersects the capacity curve at 60% of the yield base shear. The yield base shear, V_y, is defined at the intersection of K_e and K_s lines. The process is iterative because the value of yield base shear is not known at the beginning. An illustrative capacity curve and its bilinear representation are shown in Figure 5.2. Note that there may be cases when initial stiffness (K_i) is equal to effective stiffness (K_e).

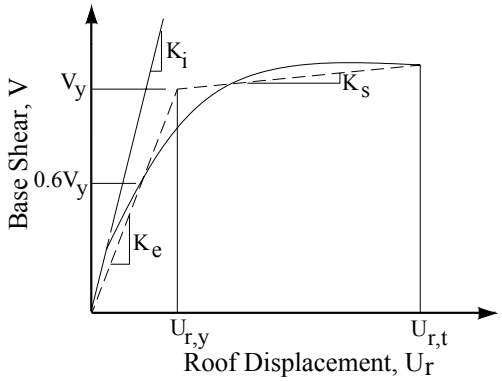

Figure 5.2 : Bilinear Representation of Capacity (Pushover) Curve

3. Convert the bilinear capacity curve into acceleration-displacement response spectrum (ADRS) format using the equations below (Figure 5.3):

$$Sa = \frac{V/W}{\alpha_1} \tag{5.1}$$

$$Sd = \frac{U_r}{\Gamma_1 \cdot \phi_{1,r}} \tag{5.2}$$

where W : total weight of building (kN)

V : base shear (kN)

U_r : roof displacement (m)

α_1 : modal mass coefficient for the fundamental mode

Γ_1 : modal participation factor for the fundamental mode

$Ø_{1,r}$: amplitude of first mode at roof level

Sa : spectral acceleration (m/s^2)

Sd : spectral displacement (m)

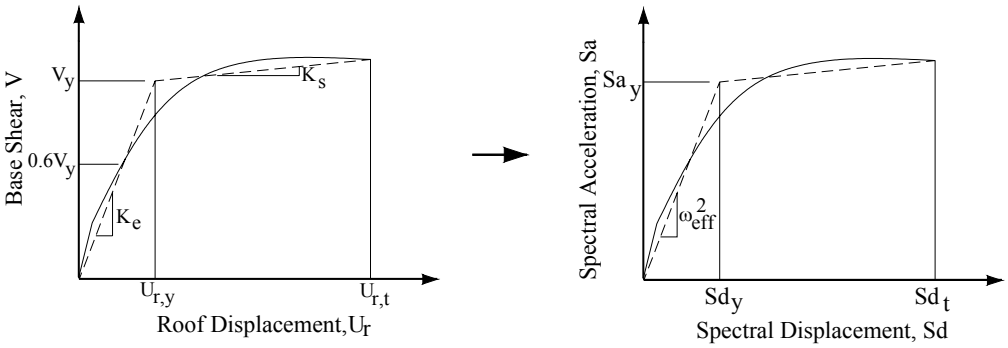

Figure 5.3 : Conversion of Capacity (Pushover) Curve to Capacity Spectrum

4. Determine the ω_{eff}^2 of equivalent SDOF system from the initial slope (elastic portion) of the bilinear capacity spectrum.
5. Obtain the force-displacement relationship of equivalent SDOF system using the equations below:

$$M^* = \alpha_1 \cdot M \tag{5.3}$$

$$K^* = \omega_{eff}^2 \cdot M^* \tag{5.4}$$

$$F_y = V_y = Sa_y \cdot W^* \tag{5.5}$$

where M : mass of the building (t)

M^* : effective mass of SDOF (t)

K^* : effective stiffness of SDOF (kN/m)

ω_{eff} : effective frequency of SDOF (sn^{-1})

W^* : effective weight of the building ($=M^*g$)

Sa_y : yield spectral acceleration (m/s^2)

F_y : yield force (kN)

V_y : yield base shear (kN)

6. Represent the force-displacement relationship of SDOF as shown in Figure 5.4 where α is the ratio of average post-elastic stiffness (K_s) of capacity curve to the effective elastic stiffness of capacity curve (K_e).

7. Perform a nonlinear dynamic analysis using any software (e.g. USEE [54], NONLIN [40], etc.) by utilising the force-displacement relationship of the equivalent SDOF system to obtain the inelastic displacement demand of the equivalent SDOF system.
8. Convert the displacement demand determined in Step 7 to global (roof) displacement by multiplying estimated spectral displacement demand of equivalent SDOF system with first modal participation factor at the roof level.

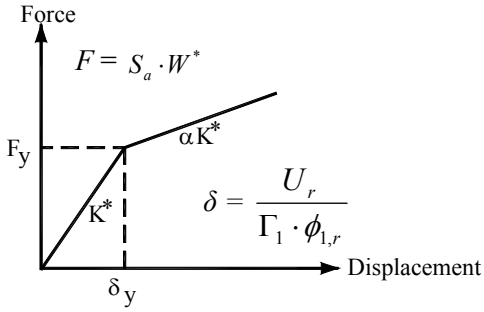

Figure 5.4 : Force-Displacement Relationship of Equivalent SDOF System (Approach Proposed by ATC-40 [3])

Although the approach proposed by ATC-40 [3] is frequently used to determine the force-displacement relationship of equivalent SDOF system, Chopra and Goel [9] proposed an alternative method. In the alternative method, the deflected shape of MDOF structure is also assumed to be represented by elastic first mode of the structure. MDOF structure is represented by an equivalent SDOF system having same stiffness properties of MDOF structure with an effective mass (M_{eff}) (Figure 5.5).

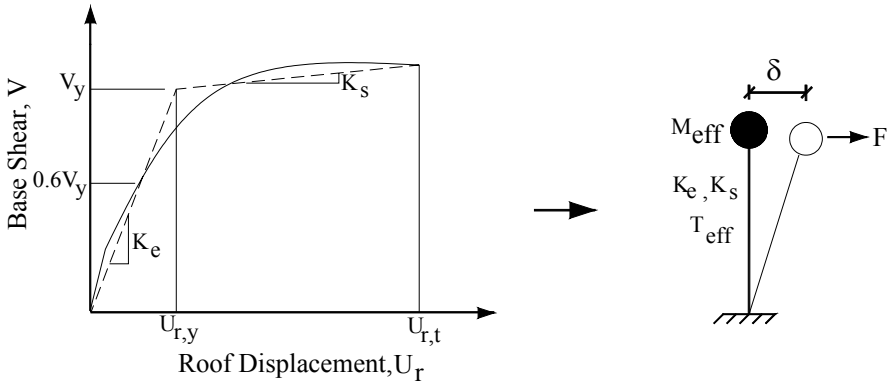

Capacity Curve of MDOF Structure Equivalent SDOF System

Figure 5.5 : MDOF Structure Represented by Equivalent SDOF System (Alternative Approach Proposed by Chopra and Goel [9])

The alternative method is basically composed of the following steps:

1. Perform the same Steps 1-4 described in the approach proposed by ATC-40 [3].
2. Determine the effective mass (M_{eff}) from the relationship given below:

$$\omega_{eff}^2 \cdot Sd_y = Sa_y \tag{5.6}$$

where

$$\omega_{eff}^2 = \frac{K_e}{M_{eff}} \tag{5.7}$$

$$Sd_y = \frac{U_{r,y}}{\Gamma_1 \cdot \phi_{1,r}} \tag{5.8}$$

$$Sa_y = \frac{Vy/W}{\alpha_1} \tag{5.9}$$

where M_{eff} : effective mass of SDOF (t)

$U_{r,y}$: roof displacement at yield (m)

3. Insert Equations 5.7, 5.8 and 5.9 into Equation 5.6 to obtain the relationship given below:

$$M_{eff} = \frac{\alpha_1 \cdot W}{\Gamma_1 \cdot \phi_{1,r}} \tag{5.10}$$

4. Force-displacement relationship of equivalent SDOF is represented in Figure 5.6 where yield force, F_y, is calculated as follows:

$$F_y = M_{eff} \cdot Sa_y \tag{5.11}$$

When Equations 5.9 and 5.10 are inserted into Equation 5.11, F_y becomes;

$$F_y = \frac{V_y}{\Gamma_1 \cdot \phi_{1,r}} \tag{5.12}$$

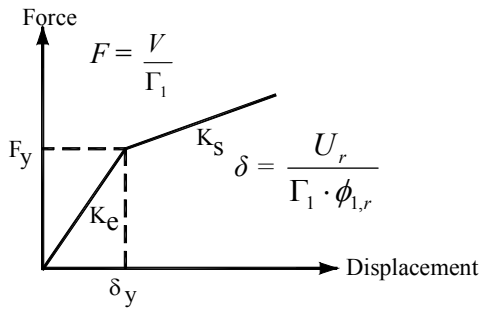

Figure 5.6 : Force-Displacement Relationship of Equivalent SDOF System (Alternative Approach Proposed by Chopra and Goel [9])

5.3 CAPACITY SPECTRUM METHOD (ATC-40 PROCEDURE A)

ATC-40 [3] presents the recent three versions of the Capacity Spectrum Method to estimate the earthquake induced displacement demand of inelastic systems. All three procedures are based on the same underlying principles that these procedures are approximate since they avoid the dynamic analysis of inelastic system. Instead, the displacement demand of inelastic system is estimated by dynamic analysis of a series of equivalent linear systems with successively updated values of T_{eq} and ζ_{eq}.

Procedures A and B are analytical and suitable to computer implementation while Procedure C is graphical and more suitable for hand analysis. In this study, the procedure which is equivalent to Procedure A in ATC-40 [3] except that it is specialized for bilinear systems was utilised. The procedure consists of the following steps:

1. Perform same Steps 1-3 described in the approach proposed by ATC-40 [3] in Section 5.2
2. Convert 5% elastic response (demand) spectrum from standard Sa vs T format to Sa vs Sd (ADRS) format. For this purpose, the spectral displacement, Sd, can be computed using Eqn. 5.13 for any point on standard response spectrum (See Figure 5.7).

$$Sd = \frac{1}{4\pi^2} SaT^2 \tag{5.13}$$

where Sa : spectral acceleration (m/s^2)

Sd : spectral displacement (m)

T : period (s)

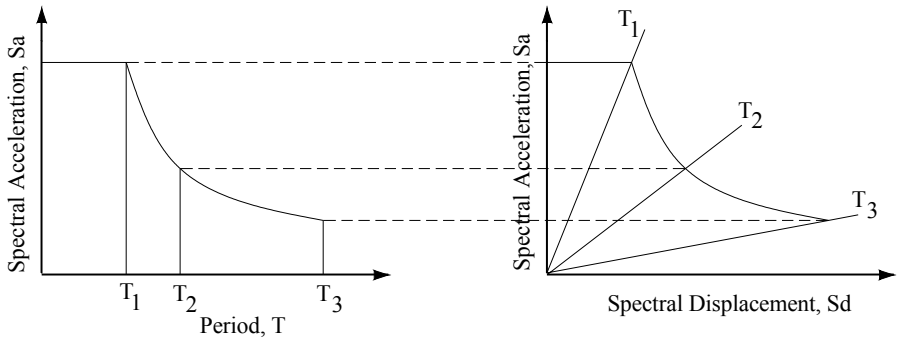

$$Sd = \frac{1}{4\pi^2} SaT^2 \qquad T = 2\pi\sqrt{\frac{Sd}{Sa}}$$

Standard Spectrum (Sa vs T) — ADRS Spectrum (Sa vs Sd)

Figure 5.7 : Response Spectrum in Standard and ADRS Formats

3. Initially, assume a peak spectral displacement demand Sd_i = Sd (T_1, ξ = 5%) determined for period T_1 from the elastic response spectrum.
4. Compute displacement ductility ratio $\mu = Sd_i / Sd_y$
5. Compute the equivalent damping ratio ξ_{eq} from the following equation:

$$\xi_{eq} = 0.05 + \kappa \cdot \xi_o \tag{5.14}$$

where ξ_{eq} : equivalent damping ratio

0.05 : 5% viscous damping inherent in the structure (assumed to be constant)

κ : damping modification factor to simulate the probable imperfections in actual building hysteresis loops

ζ_o : hysteretic damping ratio represented as equivalent viscous damping ratio

The most common method for defining equivalent viscous damping ratio is to equate the energy dissipated in a vibration cycle of the inelastic system and of the equivalent linear system. Based on this concept, Chopra [7] defines equivalent viscous damping ratio as;

$$\xi_o = \frac{1}{4\pi}\frac{E_D}{E_S} \tag{5.15}$$

where E_D : the energy dissipated in the inelastic system given by the area enclosed by the hysteresis loop

E_S : maximum strain energy

Substituting E_D and E_S in Equation (5.15) leads to

$$\xi_o = \frac{2}{\pi}\frac{(\mu-1)(1-\alpha)}{\mu(1+\alpha\mu-\alpha)} \tag{5.16}$$

where μ : displacement ductility ratio

α : ratio of average post-elastic stiffness of capacity curve to effective elastic stiffness of the capacity curve

The κ-factor depends on the structural behavior of the building which in turn depends on the quality of seismic resisting system and the duration of ground shaking. ATC-40 [3] defines three different structural behavior types. Type A represents hysteretic behavior with stable, reasonably full hysteresis loops while Type C represents poor hysteretic behavior with severely pinched and/or degraded loops. Type B denotes hysteresis behavior intermediate between Type A and Type C (Table 5.1)

Table 5.1 : Structural Behavior Types (ATC-40 [3])

Shaking Duration	Essentially New Building	Average Existing Building	Poor Existing Building
Short	Type A	Type B	Type C
Long	Type B	Type C	Type C

The ranges and limits for the values of κ assigned to the three structural behavior types are given in Table 5.2

Table 5.2 : Values for Damping Modification Factor, κ (ATC-40 [3])

Structural Behavior Type	ζ_o (percent)	κ
Type A	≤ 16.25	1.0
	> 16.25	$1.13 - \frac{0.51\left(Sa_y Sd_i - Sd_y Sa_i\right)}{\left(Sa_i Sd_i\right)}$
Type B	≤ 25	0.67
	> 25	$0.845 - \frac{0.446\left(Sa_y Sd_i - Sd_y Sa_i\right)}{\left(Sa_i Sd_i\right)}$
Type C	Any value	0.33

6. Plot elastic demand spectrum for ζ_{eq} determined in Step 7 and bilinear capacity spectrum on same chart and obtain the spectral displacement demand Sd_j at the intersection (Figure 5.8)
7. Check for convergence. If $\frac{\left(Sd_j - Sd_i\right)}{Sd_j} \leq$ tolerance (=0.05) then earthquake induced spectral displacement demand is $Sd=Sd_j$. Otherwise, set $Sd_i = Sd_j$ (or another estimated value) and repeat Steps 6-9.
8. Convert the spectral displacement demand determined in Step 9 to global (roof) displacement by multiplying estimated spectral displacement demand of equivalent SDOF system with first modal participation factor at the roof level.

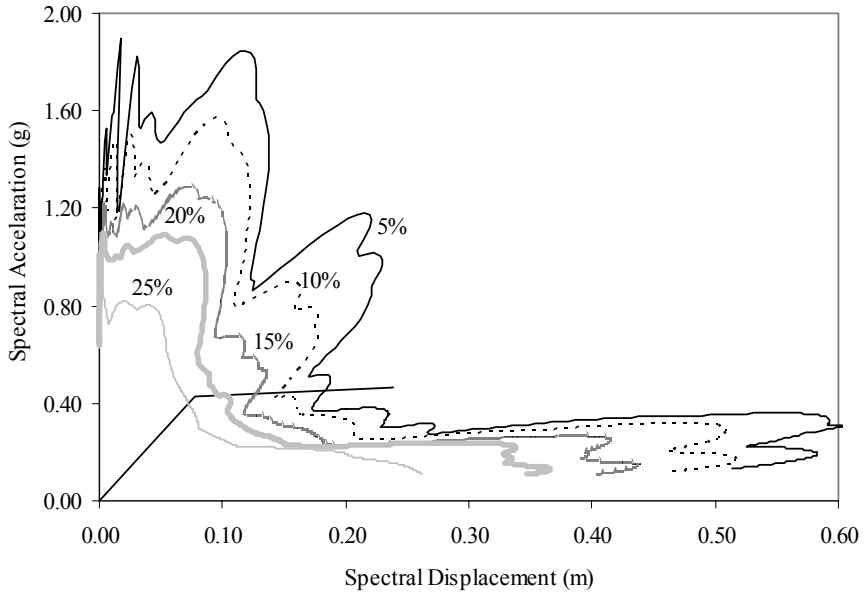

Figure 5.8 : Capacity Spectrum Method (ATC-40 Procedure A)

5.4 DISPLACEMENT COEFFICIENT METHOD (FEMA-356)

The Displacement Coefficient Method described in FEMA-356 [20] is an approximate method which provides a direct numerical calculation of maximum global displacement demand of structures. Inelastic displacement demand, δ_t , is calculated by modifying elastic displacement demand with a series of displacement modification factors.

Bilinear representation of capacity curve is required to be used in the procedure. The procedure described in Section 5.2 is recommended for bilinear representation. After the construction of bilinear curve, effective fundamental period (T_e) of the structure is calculated using Equation 5.17.

$$T_e = T_i \sqrt{\frac{K_i}{K_e}} \tag{5.17}$$

where T_e : effective fundamental period (in seconds)

T_i : elastic fundamental period (in seconds) in the direction under consideration

K_i : elastic lateral stiffness of the stucture in the direction under consideration

K_e : effective lateral stiffness of stucture in the direction under consideration

The target displacement, δ_t , is computed by modifying the spectral displacement of an equivalent SDOF system using the coefficients as shown below.

$$\delta_t = C_0 C_1 C_2 C_3 S_a \frac{T_e^2}{4\pi^2} g \tag{5.18}$$

where

C_0 : modification factor to relate spectral displacement and likely roof displacement of the structure. The first modal participation factor at the roof level is used.

C_1 : modification factor to relate expected maximum inelastic displacements to displacements calculated for linear elastic response.

C_2 : modification factor to represent the effect of hysteresis shape on the maximum displacement response. In this study, C_2 was taken as 1.1 for both elastic and inelastic deformation levels. As the estimates of Displacement Coefficient Method (FEMA-356) [20] depend on the coefficient C_2, the coefficient C_2 should be taken as unity in the elastic range and should take the specified value for the considered performance level in the inelastic range for seismic performance evaluation purposes.

C_3 : modification factor to represent increased displacements due to second-order effects.

S_a : response spectrum acceleration at the effective fundamental period of the structure.

T_e : effective fundamental period of the structure.

In this method, different target displacements can be obtained for different seismic performance levels. In this study, target displacements for each ground motion record were calculated for life safety performance level.

5.5 CONSTANT DUCTILITY PROCEDURE (CHOPRA&GOEL)

Chopra and Goel [8] proposed an improvement to Capacity Spectrum Method described in ATC-40 [3]. The improved capacity-demand diagram method uses constant ductility demand spectrum to estimate seismic deformation of equivalent SDOF system representation of MDOF structure.

There are three versions of the proposed improved procedure; Procedure A, Procedure B and Numerical procedure. Procedures A and B are graphically similar to ATC-40 Procedures A and B. In this study, Procedure A was used to estimate seismic displacement demand of inelastic SDOF systems. The procedure consists of the following steps:

1. Perform same Steps 1-3 described in the approach proposed by ATC-40 [3] in Section 5.2

2. Obtain elastic 5% damped response spectrum and a set of inelastic response spectra for various ductility levels (Figure 5.9)
3. Plot the bilinear capacity spectrum and demand spectra together.
4. Determine the displacement demand as follows: Compute the ductility value at the intersection of capacity spectrum and each demand spectrum (u_m / u_y). When the computed ductility matches the ductility of intersecting demand spectrum, that intersection point is selected as inelastic displacement demand of SDOF system.
5. Convert the spectral displacement demand determined in Step 4 to global (roof) displacement by multiplying estimated spectral displacement demand of equivalent SDOF system with first modal participation factor at the roof level.

In Step 2, the inelastic response spectra for various ductility levels can be developed from the elastic response spectrum by using the R_y-μ-T_n relations. Newmark and Hall [39], Nassar and Krawinkler [38], Vidic, Fajfar and Fischinger [55] suggested different R_y-μ-T_n relations. However, in this study, SeismoSignal [50] was utilised to develop elastic and inelastic response that the spectra are computed by means of time integration of the equation of motion of a series of SDOF systems from which the peak acceleration response quantities were then obtained.

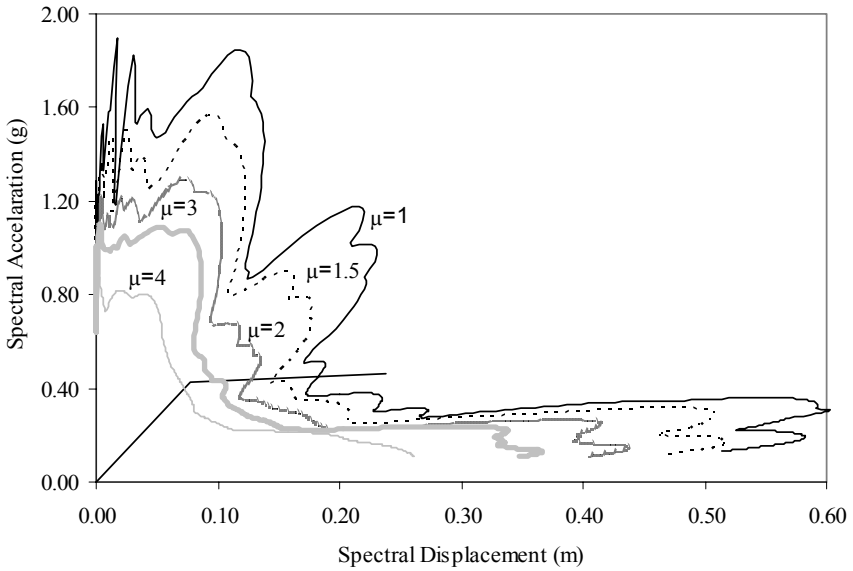

Figure 5.9 : Constant Ductility Procedure (Chopra&Goel [8])

The displacement demand is determined at the intersection of capacity and demand spectra in both Capacity Spectrum Method (ATC-40 Procedure A) [3] and Constant Ductility Procedure [8]. However, the demand is calculated by analysing an inelastic system in improved procedure instead of equivalent linear systems in Capacity Spectrum Method (ATC-40 Procedure A) [3].

5.6 COMPARISON AND INTERPRETATION OF RESULTS

The Nonlinear Dynamic Analysis of Equivalent SDOF System, Capacity Spectrum Method (ATC-40 Procedure A) [3], Displacement Coefficient Method (FEMA-356) [20] and Constant Ductility Procedure (Chopra&Goel) [8] were used to estimate maximum seismic displacement demands of 2, 5, 8 and 12-story reinforced concrete frames under El Centro (Imperial Valley, 18 May 1940, NS component), Parkfield (27 June 1966, N65E component), Pacoima Dam (San Fernando, 9 February 1971, S16E component) and Düzce (12 November 1999, EW component) earthquakes. The estimated displacement demands were compared with the 'exact' values obtained from nonlinear time history analyses to assess the accuracy of the procedures in predicting seismic demands. The ground motion records were scaled to obtain elastic and various levels of inelastic behavior from the structures and target displacements were estimated for each specified deformation level on the capacity curve of the frames (Figure 4.2).

USEE [54] was used to perform nonlinear dynamic analyses of equivalent SDOF systems and force-displacement relationships of equivalent SDOF representation of the frames considered are given in Table 5.3 with reference to Figure 5.4. The SeismoSignal [50] was utilised to construct response (demand) spectra for various damping and ductility levels. Nonlinear time history analyses of MDOF structures to determine 'exact' target displacements were performed by DRAIN-2DX [44]. Target displacements estimated using each procedure, 'exact' values determined from nonlinear time history analyses for all frames and ground motions are given in Tables 5.4-5.7. The error involved in approximate procedures with respect to 'exact' values are presented in Figures 5.9-5.12.

Table 5.3 : Force-Displacement Relationships of SDOF Representation of R/C Frames

Frame	T_{eff} (s)	Sa_y (g)	Sdy (m)	Fy (kN)	K* (kN/m)	α (%)
2-Story	0.529	0.458	0.032	1032.0	32371.5	4.22
5-Story	0.853	0.427	0.077	1640.0	21262.8	4.11
8-Story	1.066	0.282	0.079	3647.0	45873.6	0.47
12-Story	1.621	0.208	0.136	6120.7	45071.1	0.82

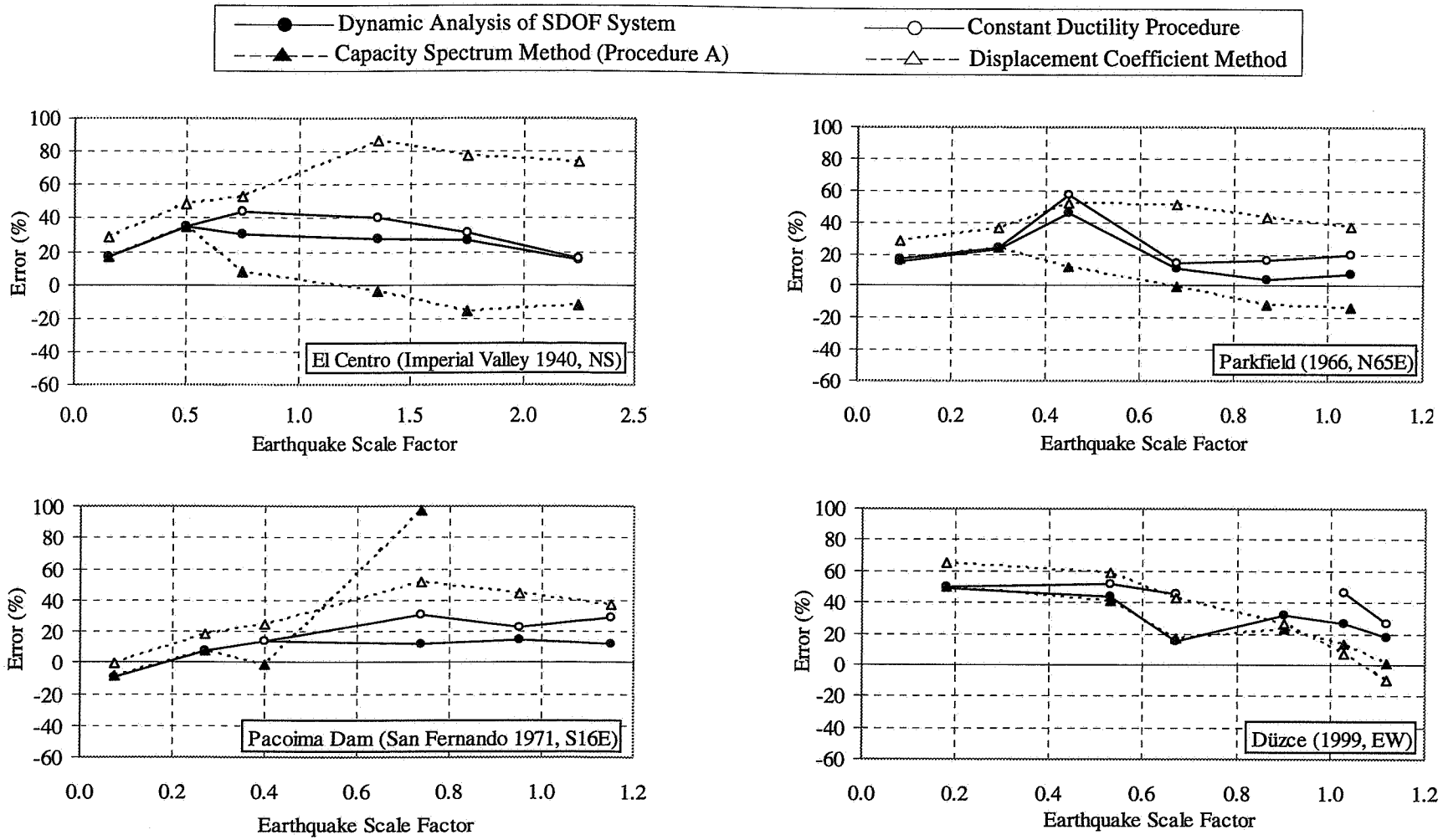

Figure 5.9 : Error in Target Displacement Estimation for 2-Story R/C Frame

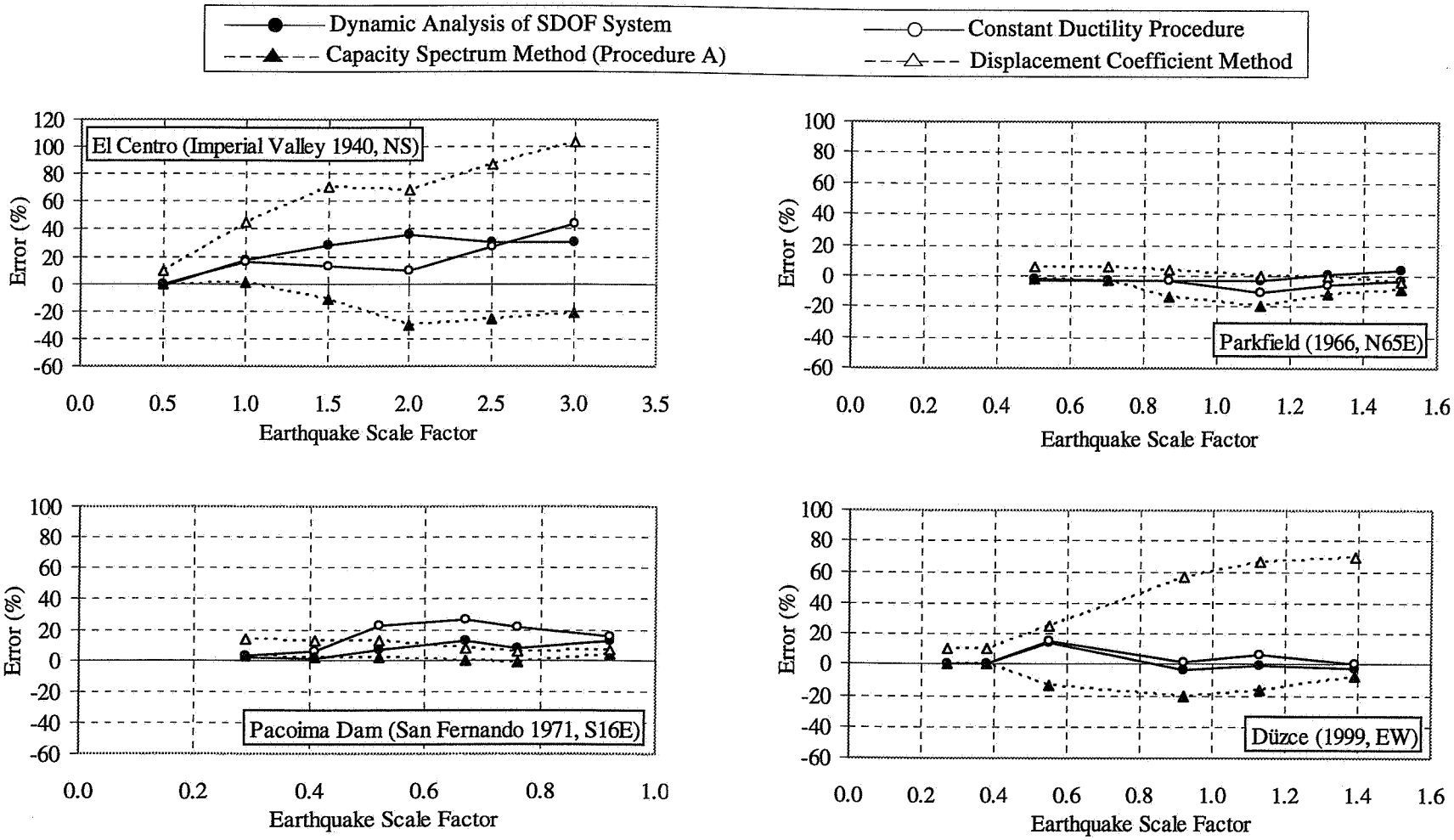

Figure 5.10 : Error in Target Displacement Estimation for 5-Story R/C Frame

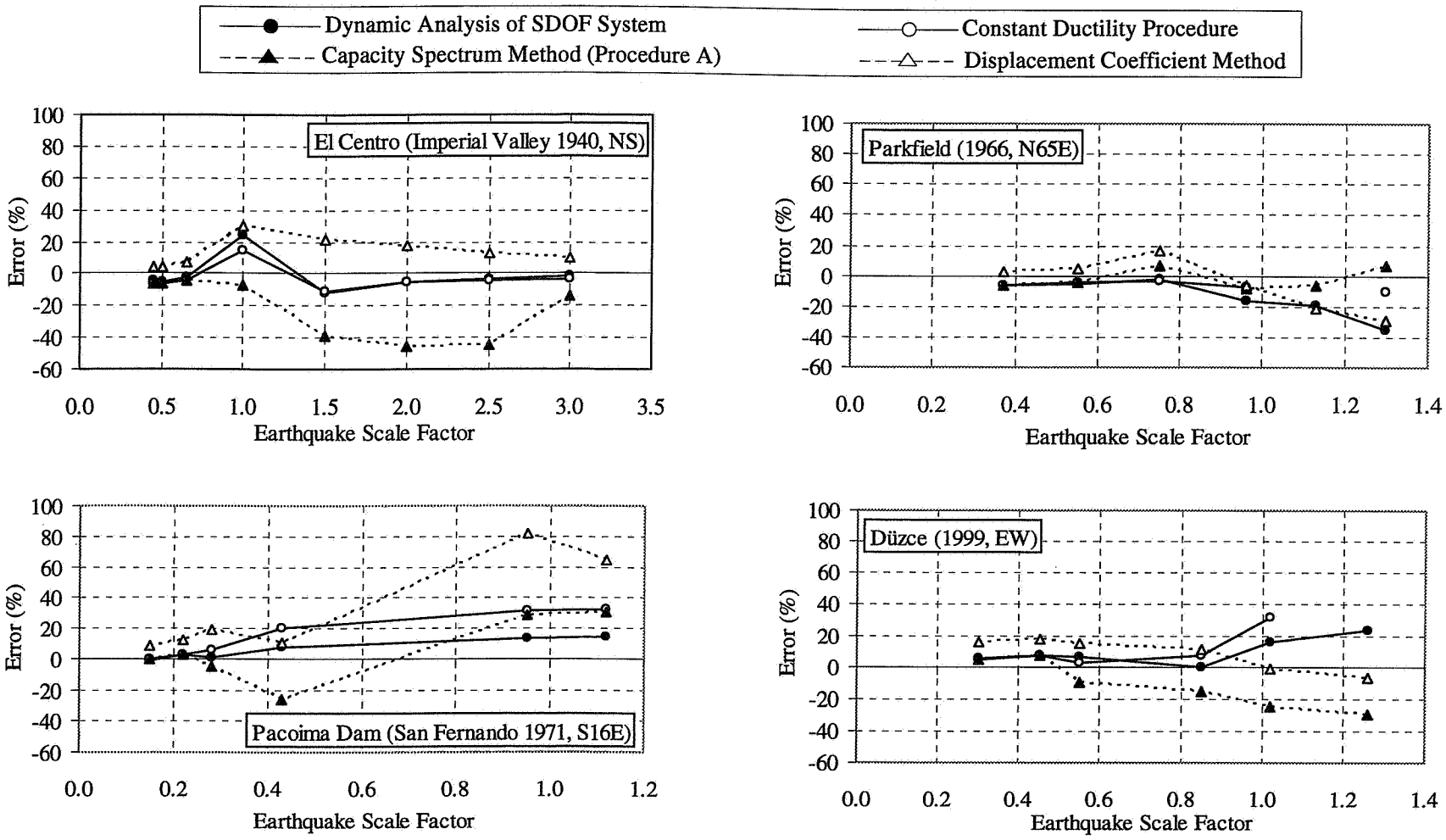

Figure 5.11 : Error in Target Displacement Estimation for 8-Story R/C Frame

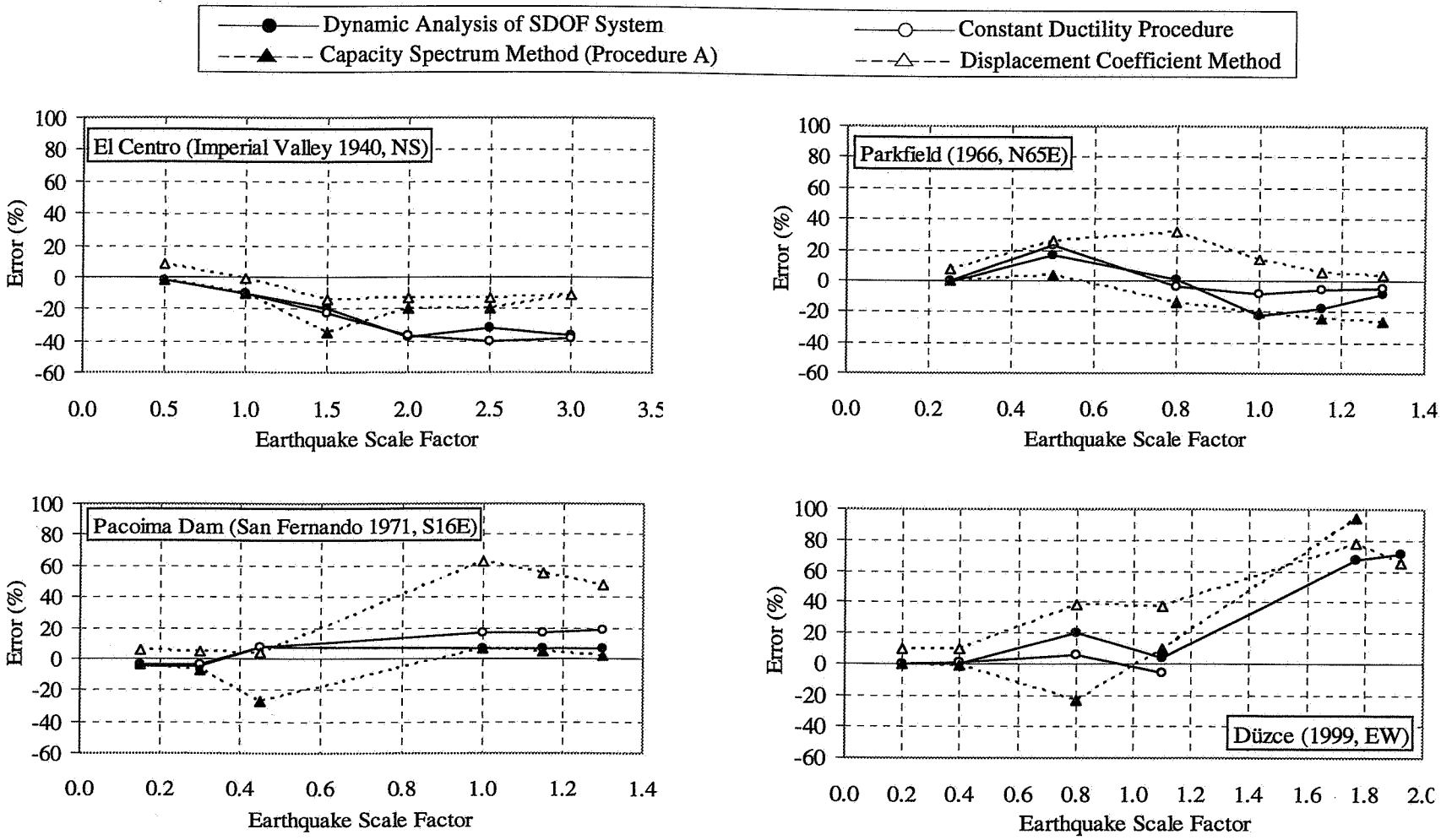

Figure 5.12 : Error in Target Displacement Estimation for 12-Story R/C Frame

Table 5.4 : Target Displacement Estimation for 2-Story R/C Frame

		Nonlinear Time History Analysis	Dynamic Analysis of SDOF System		Constant Ductility Procedure		Capacity Spectrum Method (Procedure A)		Displacement Coefficient Method	
Earthquake	**EQ Scale F.**	**Ur (m)**	**Ur (m)**	**Error (%)**	**Ur (m)**	**Error (%)**	**Ur (m)**	**Error (%)**	**Ur (m)**	**Error (%)**
El Centro (Imperial Valley 1940, NS)	0.15	0.011	0.013	16.71	0.013	17.15	0.013	17.15	0.014	28.85
	0.50	0.031	0.042	34.88	0.042	35.10	0.042	35.10	0.046	48.57
	0.75	0.045	0.059	30.66	0.065	44.14	0.049	7.81	0.069	53.02
	1.35	0.067	0.085	27.35	0.094	40.00	0.064	-4.18	0.125	86.12
	1.75	0.091	0.116	26.95	0.120	31.08	0.077	-15.64	0.162	77.27
	2.25	0.119	0.138	15.48	0.139	16.03	0.105	-11.92	0.208	74.17
Parkfield (27 June 1966, N65E)	0.09	0.011	0.012	15.58	0.012	16.52	0.012	16.52	0.013	28.08
	0.30	0.033	0.041	23.16	0.041	23.64	0.041	23.88	0.045	36.21
	0.45	0.044	0.065	45.79	0.070	57.25	0.050	12.12	0.067	51.59
	0.68	0.067	0.075	10.92	0.077	14.49	0.067	-0.12	0.102	51.21
	0.87	0.091	0.094	3.59	0.105	15.69	0.081	-11.57	0.130	43.05
	1.05	0.115	0.123	7.10	0.138	19.99	0.099	-13.91	0.157	36.68
Pacoima Dam (San Fernando 1971, S16E)	0.075	0.010	0.009	-9.58	0.009	-9.50	0.009	-8.81	0.010	-0.37
	0.27	0.031	0.034	7.31	0.034	7.40	0.034	7.40	0.037	18.19
	0.40	0.044	0.050	13.81	0.050	13.70	0.044	-1.47	0.055	24.15
	0.74	0.067	0.075	11.95	0.088	30.66	0.132	97.37	0.102	51.55
	0.95	0.090	0.103	14.27	0.111	22.91	NC	NC	0.131	44.40
	1.15	0.115	0.129	11.98	0.149	29.25	NC	NC	0.158	37.20
Düzce (1999, EW)	0.18	0.010	0.015	49.08	0.016	50.30	0.016	50.30	0.017	65.13
	0.53	0.032	0.046	43.67	0.048	51.68	0.045	40.57	0.051	58.97
	0.67	0.045	0.051	15.07	0.065	45.60	0.052	16.67	0.064	42.98
	0.90	0.068	0.089	31.95	NC	NC	0.084	23.38	0.086	26.74
	1.03	0.092	0.116	26.26	0.134	46.67	0.104	13.12	0.098	7.35
	1.12	0.118	0.139	17.37	0.150	26.91	0.119	0.56	0.107	-9.66

NC : no convergence

Table 5.5 : Target Displacement Estimation for 5-Story R/C Frame

		Nonlinear Time History Analysis	Dynamic Analysis of SDOF System		Constant Ductility Procedure		Capacity Spectrum Method (Procedure A)		Displacement Coefficient Method	
Earthquake	**EQ Scale F.**	**Ur (m)**	**Ur (m)**	**Error (%)**	**Ur (m)**	**Error (%)**	**Ur (m)**	**Error (%)**	**Ur (m)**	**Error (%)**
El Centro (Imperial Valley 1940, NS)	0.5	0.073	0.071	-1.67	0.073	-0.01	0.073	-0.01	0.079	9.07
	1.0	0.109	0.129	17.73	0.128	16.75	0.111	1.24	0.159	44.79
	1.5	0.139	0.179	28.25	0.158	12.98	0.123	-11.62	0.238	70.58
	2.0	0.189	0.257	35.65	0.208	9.94	0.131	-30.51	0.317	67.62
	2.5	0.212	0.278	30.93	0.269	27.00	0.157	-25.94	0.396	86.91
	3.0	0.233	0.305	30.72	0.336	44.12	0.183	-21.46	0.476	103.91
Parkfield (27 June 1966, N65E)	0.50	0.077	0.075	-2.66	0.075	-2.47	0.075	-2.45	0.082	6.10
	0.70	0.108	0.105	-2.81	0.104	-3.29	0.104	-3.40	0.114	6.06
	0.87	0.136	0.132	-3.17	0.132	-3.28	0.118	-13.54	0.142	4.12
	1.12	0.183	0.178	-2.73	0.162	-11.30	0.147	-19.42	0.183	0.01
	1.30	0.212	0.214	0.77	0.200	-5.52	0.186	-12.11	0.212	0.06
	1.50	0.255	0.264	3.79	0.247	-2.99	0.233	-8.65	0.245	-3.89
Pacoima Dam (San Fernando 1971, S16E)	0.29	0.075	0.077	1.84	0.077	2.54	0.077	2.54	0.086	13.59
	0.41	0.108	0.109	0.77	0.114	5.88	0.110	1.86	0.121	12.39
	0.52	0.136	0.145	6.30	0.167	22.66	0.138	1.62	0.154	12.84
	0.67	0.184	0.207	12.06	0.232	25.97	0.183	-0.48	0.198	7.45
	0.76	0.213	0.228	7.17	0.259	21.88	0.211	-0.91	0.225	5.73
	0.92	0.256	0.288	12.61	0.295	15.37	0.264	3.11	0.272	6.38
Düzce (1999, EW)	0.27	0.076	0.076	0.06	0.076	-0.25	0.076	-0.25	0.084	10.08
	0.38	0.108	0.108	-0.03	0.108	0.41	0.108	0.10	0.118	10.00
	0.55	0.137	0.156	14.46	0.157	14.87	0.118	-13.88	0.171	25.40
	0.92	0.183	0.176	-3.67	0.185	1.31	0.145	-20.68	0.287	57.03
	1.13	0.212	0.210	-0.90	0.225	6.34	0.177	-16.67	0.352	66.08
	1.39	0.256	0.248	-3.06	0.256	-0.16	0.235	-7.98	0.433	69.22

Table 5.6 : Target Displacement Estimation for 8-Story R/C Frame

		Nonlinear Time History Analysis	Dynamic Analysis of SDOF System		Constant Ductility Procedure		Capacity Spectrum Method (Procedure A)		Displacement Coefficient Method	
Earthquake	**EQ Scale F.**	**Ur (m)**	**Ur (m)**	**Error (%)**	**Ur (m)**	**Error (%)**	**Ur (m)**	**Error (%)**	**Ur (m)**	**Error (%)**
El Centro (Imperial Valley 1940, NS)	0.45	0.071	0.068	-4.84	0.067	-6.00	0.067	-6.00	0.075	4.47
	0.65	0.101	0.098	-2.92	0.097	-4.07	0.097	-4.07	0.108	6.59
	1.00	0.127	0.158	24.20	0.145	14.35	0.118	-7.36	0.166	30.26
	1.50	0.205	0.181	-11.83	0.183	-10.93	0.126	-38.61	0.248	21.20
	2.00	0.281	0.265	-5.75	0.265	-5.66	0.154	-45.28	0.331	17.95
	2.50	0.367	0.353	-3.94	0.350	-4.61	0.204	-44.39	0.414	12.85
Parkfield (27 June 1966, N65E)	0.37	0.071	0.067	-6.41	0.067	-6.20	0.067	-6.20	0.073	2.96
	0.55	0.105	0.099	-4.98	0.099	-4.83	0.099	-4.83	0.109	4.45
	0.75	0.128	0.125	-2.30	0.124	-3.04	0.136	6.28	0.149	16.27
	0.96	0.203	0.170	-16.08	0.188	-7.41	0.186	-8.25	0.191	-6.10
	1.13	0.283	0.228	-19.30	NC	NC	0.265	-6.37	0.223	-21.16
	1.30	0.366	0.236	-35.44	0.329	-10.16	0.389	6.35	0.258	-29.44
Pacoima Dam (San Fernando 1971, S16E)	0.15	0.074	0.074	-1.09	0.074	-0.41	0.074	-0.41	0.081	8.31
	0.22	0.105	0.108	2.27	0.109	3.05	0.109	3.05	0.118	12.08
	0.28	0.126	0.127	0.80	0.133	5.64	0.120	-5.27	0.150	19.00
	0.43	0.209	0.224	7.23	0.251	20.24	0.155	-25.94	0.231	10.39
	0.95	0.281	0.317	12.79	0.370	31.84	0.361	28.44	0.510	81.66
	1.12	0.365	0.416	13.91	0.484	32.32	0.478	30.81	0.601	64.54
Düzce (1999, EW)	0.30	0.070	0.074	4.92	0.073	4.36	0.073	4.36	0.081	15.58
	0.45	0.103	0.110	6.78	0.111	7.55	0.111	7.55	0.122	17.74
	0.55	0.130	0.138	6.19	0.134	2.89	0.117	-10.05	0.149	14.60
	0.85	0.208	0.207	-0.38	0.223	7.41	0.176	-15.40	0.230	10.58
	1.02	0.280	0.323	15.44	0.370	32.08	0.209	-25.31	0.276	-1.49
	1.26	0.367	0.453	23.39	NC	NC	0.258	-29.69	0.341	-7.09

NC : no convergence

Table 5.7 : Target Displacement Estimation for 12-Story R/C Frame

		Nonlinear Time History Analysis	Dynamic Analysis of SDOF System		Constant Ductility Procedure		Capacity Spectrum Method (Procedure A)		Displacement Coefficient Method	
Earthquake	**EQ Scale F.**	**Ur (m)**	**Ur (m)**	**Error (%)**	**Ur (m)**	**Error (%)**	**Ur (m)**	**Error (%)**	**Ur (m)**	**Error (%)**
El Centro (Imperial Valley 1940, NS)	0.50	0.083	0.082	-1.66	0.082	-1.67	0.082	-1.67	0.090	7.90
	1.00	0.182	0.164	-10.00	0.164	-9.98	0.164	-9.97	0.180	-1.20
	1.50	0.315	0.254	-19.46	0.245	-22.34	0.205	-34.92	0.270	-14.19
	2.00	0.417	0.262	-37.08	0.266	-36.18	0.335	-19.60	0.360	-13.48
	2.50	0.521	0.357	-31.47	0.313	-39.94	0.419	-19.52	0.451	-13.49
	3.00	0.607	0.383	-36.94	0.373	-38.57	0.537	-11.57	0.541	-10.97
Parkfield (27 June 1966, N65E)	0.25	0.115	0.113	-1.36	0.115	0.20	0.115	0.20	0.123	7.52
	0.50	0.196	0.229	17.01	0.240	22.82	0.203	3.66	0.246	25.96
	0.80	0.300	0.303	0.92	0.288	-3.94	0.257	-14.55	0.394	31.30
	1.00	0.434	0.338	-22.21	0.399	-8.25	0.345	-20.47	0.493	13.47
	1.15	0.536	0.442	-17.50	0.504	-6.02	0.404	-24.73	0.567	5.67
	1.30	0.617	0.561	-8.98	0.587	-4.80	0.456	-26.03	0.641	3.91
Pacoima Dam (San Fernando 1971, S16E)	0.15	0.104	0.099	-4.47	0.099	-4.28	0.099	-4.29	0.109	5.21
	0.30	0.208	0.198	-4.72	0.201	-3.59	0.193	-7.23	0.218	4.69
	0.45	0.316	0.338	6.95	0.338	7.01	0.229	-27.45	0.327	3.48
	1.00	0.447	0.476	6.62	0.520	16.48	0.477	6.72	0.726	62.55
	1.15	0.539	0.575	6.61	0.628	16.43	0.564	4.59	0.835	54.86
	1.30	0.638	0.679	6.39	0.754	18.15	0.648	1.56	0.944	48.03
Düzce (1999, EW)	0.20	0.097	0.096	-0.53	0.097	-0.48	0.097	-0.48	0.106	8.98
	0.40	0.193	0.193	-0.08	0.194	0.63	0.191	-1.17	0.211	9.48
	0.80	0.306	0.367	20.12	0.321	5.08	0.234	-23.30	0.423	38.41
	1.10	0.423	0.439	3.90	0.396	-6.36	0.463	9.46	0.582	37.62
	1.77	0.526	0.882	67.56	NC	NC	1.023	94.31	0.936	77.82
	1.92	0.613	1.049	71.19	NC	NC	NC	NC	1.015	65.64

NC : no convergence

The comparison of estimated target displacements with 'exact' results obtained from nonlinear time history analyses could not reveal a clear particular trend because structural response is affected by the variations in ground motion characteristics and structural properties that each frame under each ground motion should be considered as a case. However, the overall interpretation of results shows that the estimation of approximate procedures yield different target displacement values than the 'exact' results for almost all cases. The accuracy of the predictions depends on ground motion characteristics and structural properties as well as the inherent limitations of the procedures.

All of the four approximate procedures yield almost same displacement demand prediction in the elastic range provided that the coefficient C_2 is taken as unity in elastic range for Displacement Coefficient Method (FEMA-356) [20]. Capacity Spectrum Method (ATC-40 Procedure A) [3] and Constant Ductility Procedure [8] estimate exactly same target displacements in the elastic range because same elastic response spectrum intersects the capacity diagram in both procedures for ductility values less than 1.0. The target displacement estimates of approximate procedures are within 10% of the 'exact' values in the elastic range for all cases except for 2-story frame under Düzce where all procedures overestimate the displacement demand as much as 50%. This is probably due to the idealization of the capacity curve because the effective period is quite different from the period of the frame.

The predictions of approximate procedures have discrepancies in the inelastic deformation levels. Capacity Spectrum Method (ATC-40 Procedure A) underestimates the displacement demand in the inelastic range for most of the cases and the underestimations may be as much as 40 %. On the other hand, Displacement Coefficient Method (FEMA-356) [20] results in overestimations in the inelastic range for most of the cases and overestimations may be about 100%. The predictions of Nonlinear Dynamic Analysis of Equivalent SDOF System and Constant Ductility Procedure [8] follow a similar trend which lies between Displacement Coefficient Method (FEMA-356) [20] and Capacity Spectrum Method (ATC-40 Procedure A) [3] and are reasonably conservative for most of the cases considered while the predictions of Nonlinear Dynamic Analysis of Equivalent SDOF System being more accurate. However, Nonlinear Dynamic Analysis of Equivalent SDOF System and Constant Ductility Procedure [8] underestimate the displacement demand about 40% and 20% for 12-story frame under El Centro and Düzce ground

motions, respectively. It is also worth mentioning that the error involved in the estimations of approximate procedures are not dependent on the number of stories.

Nonlinear Dynamic Analysis of Equivalent SDOF System and Displacement Coefficient Method [20] directly give an estimation of target displacement without any iteration. However, Capacity Spectrum Method (ATC-40 Procedure A) [3] and Constant Ductility Procedure [8] involve an iterative solution and the iterations did not converge for some cases. Also, multiple intersections of response (demand) spectra with capacity curve were observed in both procedures due to the jagged shape of demand spectra. In such cases, the iterative solution was performed more carefully to determine the right demand point consistent with the demand spectra.

In Capacity Spectrum Method (ATC-40 Procedure A) [3], no target displacement could be estimated for 2-story frame under 0.95Pacoima and 1.15Pacoima earthquakes and for 12-story frame under 1.92Düzce earthquake because the demand spectra could only intersect the capacity curve at very large damping values that exceed the upper limit of equivalent damping ratio. Response spectra with damping values larger than 5% (reduced demand spectra) remained inside the elastic spectra with only one intersecting point in almost all cases (Figure 5.8). However, multiple intersections of response (demand) spectra with capacity curve were observed and only one intersecting point satisfying the solution could be determined in such cases (Figure 5.13). The jagged shape of demand spectra becomes smoother for damping values larger than about 15% that the probabilty of multiple intersection decreases for high levels of damping.

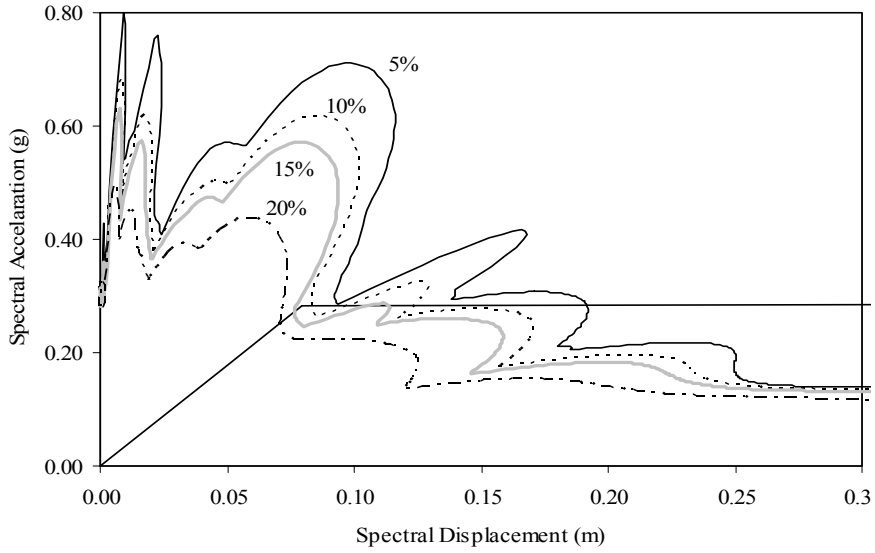

Figure 5.13 : Multiple Intersection of Response Spectra with Capacity Curve

In Constant Ductility Procedure [8], multiple intersections of response (demand) spectra with capacity curve were observed more frequently due to the shifting of jagged response spectra for increased ductility levels. The solutions were satisfied for only one of the intersections with given spectra in most of the cases. However, none of the computed ductility of the intersecting points matched the associated ductility of intersecting demand spectrum for some cases (e.g. 2-story frame for 0.90Düzce, 8-story frame for 1.13Parkfield and 1.26Düzce). Also, non-convergence occurred for 12-story frame for 1.77 and 1.92Düzce earthquakes because demand spectra could only intersect capacity curve for high ductility levels but the computed ductility of intersecting point is much lower that the computed ductility of intersecting point could never match the ductility of intersecting demand spectrum.

2.1 SUMMARY AND DISCUSSION OF RESULTS

The procedures evaluated in this study are approximate that seismic displacement demand of MDOF structure is estimated from the displacement demand of an equivalent SDOF system with basic properties derived from the capacity curve of MDOF structure. This approximation is based on certain assumptions inherent in the procedures that capacity curve of the structure is usually obtained from a pushover analysis with an invariant lateral force distribution. Also, only the effect of elastic first mode is considered to determine force-displacement relationship of equivalent SDOF system and to convert the capacity curve into a capacity diagram. The effects of inelasticity of lateral load pattern and higher modes on target displacement are neglected. Thus, the accuracy of the predictions depend on the approximations involved in the theory of the procedures, structural properties and ground motion characteristics.

The approximate procedures were evaluated based on the 'exact' results obtained from nonlinear time history analyses of actual frames instead of equivalent SDOF systems. Capacity Spectrum Method (ATC-40 Procedure A) [3], Displacement Coefficient Method (FEMA-356) [20] and Constant Ductility Procedure [8] are mostly employed for design evaluation purposes that seismic demands are generally estimated under smooth design spectra rather than individual ground motion records. These procedures were shown to produce both conservative and non-conservative estimations of the actual displacement demand. Capacity Spectrum Method (ATC-40 Procedure A) [3] generally underestimates the demand for all frames with errors approaching to 40% and

Displacement Coefficient Method (FEMA-356) [20] generally yields overestimations approaching to 100 %. However, Constant Ductility Procedure [8] yields more improved results consistent with the inelastic demand spectrum that the procedure is more appropriate to be used for design evaluation purposes. On the other hand, Nonlinear Dynamic Analysis of Equivalent SDOF System estimates the demand with a higher degree of accuracy for the cases considered so the procedure should be preferred to estimate seismic displacement demand in case the ground motion record is available.

Nonlinear Dynamic Analysis of Equivalent SDOF System and Displacement Coefficient Method (FEMA-356) [20] directly give an estimation of target displacement. However, Capacity Spectrum Method (ATC-40 Procedure A) [3] and Constant Ductility Procedure [8] are iterative that convergence problems can occur and multiple intersection of demand spectrum with capacity diagram make the procedures more complicated.

The predictions of Capacity Spectrum Method (ATC-40 Procedure A) [3] depend on damping-ductility relations. The effect of different relationships to produce inelastic spectra and the accuracy of these relationships to represent the inelastic demand should be considered since these procedures are sensitive to the shape of demand spectra. Also, the accuracy involved in the construction of demand spectra for high levels of damping should be investigated when Capacity Spectrum Method (ATC-40 Procedure A) [3] is employed for design evaluation purpose because most existing rules for constructing elastic design spectra are limited to ξ= 0 to 20%.

The target of all these procedures is to predict the roof displacement of the MDOF system. The comparisons presented in Chapter 4 revealed that although the pushover analysis provides reasonably accurate results for the roof displacement, the height-wise distribution of the deformations can significantly be mispredicted. Therefore, for global response estimations, the SDOF approximations might be reasonable provided that local behavior could not be accurately predicted.

CHAPTER 6

CONCLUSIONS AND FUTURE STUDY RECOMMENDATIONS

6.1 SUMMARY

The basic steps required to predict the seismic behavior of a structure using pushover analysis consist of modeling nonlinear member behavior of structure, performing a pushover analysis on the structure with an appropriate lateral load pattern using a software, predicting the maximum displacement demand of the structure by an approximate procedure and estimating important response parameters at predicted maximum displacement demand reasonably close to those predicted by nonlinear time history analyses.

In this study, these basic steps were studied in detail on low, mid and high-rise reinforced concrete and steel moment resisting frames covering a broad range of fundamental periods. Firstly, computational scheme and underlying principles in modeling nonlinear member behavior of DRAIN-2DX [44] and SAP2000 [14] which are commonly utilised softwares to perform pushover analysis were identified. Then, pushover analyses were performed on case study frames using 'Uniform', 'Elastic First Mode', 'Code', 'FEMA-273' and 'Multi-Modal (or SRSS)' invariant lateral load patterns and certain seismic demands were predicted at six deformation levels representing elastic and various levels of nonlinear behavior for four randomly selected individual ground motion records. Also, seismic demands were estimated by an improved pushover procedure named Modal Pushover Analysis (MPA) [9]. The accuracy of invariant lateral load patterns and MPA in predicting seismic demands was evaluated by comparing the pushover predictions with the 'exact' results obtained from nonlinear time history analyses and the applicability of pushover analyses in predicting seismic demands was investigated for low, mid and high-

rise frame structures. Although seismic demand prediction of pushover analysis was performed at 'exact' peak roof displacements for invariant lateral load patterns in this study, maximum inelastic displacement demands of R/C case study frames were also predicted by Nonlinear Dynamic Analysis of Equivalent SDOF System, Capacity Spectrum Method (ATC-40 Procedure A) [3], Displacement Coefficient Method (FEMA-356) [20] and Constant Ductility Procedure (Chopra&Goel) [8] at all deformation levels for all ground motions. The assumptions involved in the theory of these approximate procedures and the accuracy of the predictions were identified.

6.2 CONCLUSIONS

The study on the implementation of pushover analysis and on modeling nonlinear member behavior by DRAIN-2DX [44] and SAP2000 [14] yielded the general conclusion that the results obtained from pushover analysis may depend on the software used due to its limitations and element library. However, similar results in terms of the pushover curves and hinge patterns can be obtained from the two different softwares employed here provided that the same approach is used in modeling the nonlinear properties of members as well as their structural features. The following specific conclusions can be drawn:

- The computational approach of DRAIN-2DX and SAP2000 to peform pushover analysis are similar that both softwares use an event-to-event solution strategy and utilise some parameters that control the pushover analysis although there are some variations in these parameters.
- Geometric nonlinearity can be considered through P-delta effects for both softwares. However, DRAIN-2DX can not account for true large displacement effects.
- Analysis terminates if plastic hinges occur during "Gravity" pushover analysis in DRAIN-2DX. However, SAP2000 allows plastic hinging during "Gravity" pushover analysis.
- Nonlinear member behavior is modeled by concentrated plastic hinges but plastic hinges can only be defined at member ends in DRAIN-2DX while plastic hinges can be defined at any point along the span of member as well as member ends in SAP2000.
- SAP2000 utilises "Unload Entire Structure", "Apply Local Redistribution" and "Restart Loading Using Secant Stiffness" member unloading methods while

DRAIN-2DX probably performs pushover analysis by "Unload Entire Structure" option although no information is presented in the user guide.

- Both default and user-defined nonlinear member behavior can be utilised in SAP2000 while DRAIN-2DX uses only user-defined nonlinear member behavior.
- Default and user-defined steel moment and PMM hinges of SAP2000 have same characteristics except plastic rotation capacities and strain hardening ratios while default and user-defined concrete moment and PMM hinges of SAP2000 could have totally different characteristics.
- The results of pushover analysis performed by SAP2000 using default concrete hinge properties should be interpreted with caution since default concrete hinges could not simulate the exact nonlinear behavior of the structure.
- Pushover analyses performed by SAP2000 using default and user-defined hinge properties yielded differences in capacity curves, sequence of plastic hinging and hinge pattern.
- In DRAIN-2DX, plastic hinges are assumed to yield only in bending and nonlinear behavior of columns are simulated by idealized interaction diagrams which neglect inelastic axial deformations that actual column behavior could not be defined.
- DRAIN-2DX could only model bilinear moment-curvature relationships of members to represent nonlinear behavior and the program could not set a limit for maximum deformation capacities of the members so pushover curves obtained from DRAIN-2DX yield unlimited lateral deformation capacities for structures. On the other hand, SAP2000 could model initial failure (strength degradation) and maximum deformation capacities of members under lateral loading that the structures have a definite maximum lateral displacement capacity.
- Both softwares produced almost same pushover curves for both steel and R/C frames except for frames having plastic hinging at columns at initial stages of yielding. Idealized interaction diagrams utilised in DRAIN-2DX could not effectively represent exact inelastic column behavior that DRAIN-2DX yields lower base shear capacity in case plastic hinges at columns are widely observed. Also, the approach utilised by DRAIN-2DX to model strain hardening in bendig yielded a lower base shear capacity for steel frames. However, the differences in capacity curves observed due to the limitations of DRAIN-2DX to model interaction diagrams and strain hardening are negligibly small that either

SAP2000 or DRAIN-2DX can be used to perform pushover analysis in practice for frame structures.

- Both softwares yielded almost same sequence of plastic hinging and plastic hinge pattern.

The primary observations from the study on the accuracy of seismic demand prediction of invariant lateral load patterns utilised in traditional pushover procedure and of Modal Pushover Analysis (MPA) in predicting seismic demands showed that the accuracy of the pushover results depends strongly on the load path, properties of the structure and the characteristics of the ground motion. The examination of the results revealed the following specific conclusions:

- The variation in the height-wise distribution of triangular lateral load patterns ('Elastic First Mode', 'Code', 'FEMA-273' and 'Multi-Modal (SRSS)') is negligible for low to mid-rise frames (fundamental period less than about 1.0 s) while the variation in the height-wise distribution of triangular lateral load patterns is observed to be significant for long-period frames.
- None of the invariant lateral load patterns and MPA could capture the 'exact' seismic demand obtained from nonlinear time history analysis at any deformation level.
- The error involved in seismic demand prediction of any invariant lateral load pattern and MPA was observed to become larger as the frame height (i.e. as the fundamental period of the frame) increases.
- The error involved in story displacement and inter-story drift ratio prediction of any invariant lateral load pattern and MPA was observed to be larger in nonlinear deformation levels. However, the change in error with nonlinearity was mostly insignificant for invariant lateral load patterns while no clear trend was observed for MPA at nonlinear deformation levels.
- 'Uniform' lateral load pattern mostly emphasized demands in lower stories over demands in upper stories as observed in story displacement, inter-story drift ratio, story shear and plastic hinge location predictions while triangular lateral load patterns predicted the response more homogenously over the frame height. Also, the error involved in 'Uniform' loading predictions of story displacement and inter-story drift ratio demands were observed to reach unacceptably large values

compared to the predictions of triangular lateral load patterns. Therefore, seismic demand predictions of triangular lateral load patterns were better than 'Uniform' loading predictions for all frames at all deformation levels.

- The triangular load patterns yielded almost same predictions of global capacity curve, story displacement, inter-story drift ratio, story shear and plastic hinge location for low to mid-rise frames since the variation in height-wise distribution of triangular lateral load patterns is negligible for low to mid-rise frames. Therefore, any triangular lateral load pattern could be used to predict seismic demands of low to mid-rise frames.
- Appreciable differences were observed in the seismic demand prediction of triangular lateral load patterns for long-period frames since the variation in the height-wise distribution of triangular lateral load patterns is significant for high-rise frames.
- The story displacement and inter-story drift ratio prediction of triangular lateral load patterns mostly lay between the predictions of 'Multi-Modal (SRSS)' and 'Elastic First Mode' lateral load patterns for long-period frames. Therefore, it would be better to estimate the story displacement and inter-story drift ratio demand of long-period structures by considering the average of the 'Multi-Modal (SRSS)' and 'Elastic First Mode' predictions or 'Code' load pattern which corresponds to that average in most cases.
- 'FEMA-273' and 'Multi-Modal (or SRSS)' lateral load patterns yielded the lower and upper bounds of base shear capacities obtained from triangular lateral load patterns for long-period frames, respectively and it was observed that capacity curves obtained from 'Elastic First Mode' or 'Code' lateral load pattern represent an average of global capacity curves determined by triangular lateral load patterns for long period frames.
- None of the invariant lateral load patterns could capture the approximate dynamic behavior globally and at story levels. The 'Uniform' and triangular lateral load patterns seem to be the upper and lower bounds of approximate dynamic global behavior while all invariant lateral load patterns underestimated the dynamic behavior at almost all story levels as illustrated in story pushover curves.
- The plastic hinge patterns of the frames that result from the seismic excitations applied showed variations among the ground motions even at the same roof displacements due to characteristics of the ground motions and the frames.

- None of the pushover analyses procedures employed here were able to reasonably capture neither the exact sequence of hinging nor their locations. Plastic hinge location predictions of triangular lateral load patterns were observed to be better than those of 'Uniform' loading for 5, 8 and 12-story R/C frames. The predictions of all lateral load patterns and MPA were poorer in the high-rise frames. Although MPA yielded improved predictions of plastic hinge locations, plastic hinge location prediction of invariant lateral load patterns and MPA was inadequate and non-conservative for all frames. Since no obvious superiority of one load pattern over the others was observed the use of the simplest pattern, the first mode based, is recommended.
- Although 'FEMA-273' and 'Multi-Modal (SRSS)' lateral load patterns consider higher mode effects (at least elastic higher modes), these load patterns yielded no improved predictions of seismic demand for long-period frames.
- No clear trend was observed in the predictions of MPA due to the approximations inherent in the procedure. MPA mostly estimated the story displacement and inter-story drift ratio demands with a similar degree of accuracy as triangular lateral load patterns for low to mid-rise frames although some exceptions were observed. However, MPA mostly predicted the inter-story drift demands at lower stories similar to triangular lateral load patterns while improved predictions were observed at upper stories for long-period frames as MPA considers higher mode effects.

In summary, the ability of pushover procedures to simulate the height-wise deformation profiles were observed to be better in the elastic response range of the frames, but significant discrepancies were observed at inelastic deformation levels. Although the pushover analyses procedures provided reasonable predictions for low- to mid-rise frames, the degree of accuracy decreased significantly for high-rise frames no matter what load pattern is employed. In view of the results presented here, the use of the simplest load pattern, 'Elastic First Mode' or 'Code' is recommended for the pushover analyses of low- to mid-rise frame structures. However, the effects of higher modes that are dominant in high-rise frames lead to unrealistic deformation profiles obtained from pushover analysis and the results could not get improved significantly with the complicated Modal Pushover Analysis procedure. Therefore, for accurate predictions to obtain reasonable inelastic deformations at all floor levels the nonlinear time history analysis should be employed.

Also, the use of 'Uniform' load pattern is not recommended for all frames as it does not resemble a realistic distribution of inertia forces along the height as evidenced from the large discrepancies in the relevant results.

The choice of the pushover procedure depends on the level of accuracy desired for the case in hand. This study showed that the accuracy gained through complicated pushover procedures is not significant even for high-rise frames and thus does not justify their costs. Simple load patterns can be used provided that their ability to capture local behavior is limited for high-rise buildings.

Following conclusions can be derived from the study on maximum displacement demand prediction of approximate procedures for R/C frames:

- All the procedures utilised to predict maximum displacement demand are approximate in the sense that seismic displacement demand of MDOF structure is estimated from the displacement demand of an equivalent SDOF system with basic properties derived from the capacity curve of MDOF structure.
- The accuracy of the predictions depends on ground motion characteristics and structural properties as well as the approximations inherent in the procedures.
- All procedures yielded almost same displacement demand prediction with about 10% accuracy in elastic range but discrepancies were observed at nonlinear deformation levels.
- The error involved in maximum displacement demand prediction of each procedure was observed to be larger in nonlinear deformation levels. However, no clear trend was observed in the change of error with nonlinearity
- The error involved in the estimations of approximate procedures was observed to be independent of number of stories.
- Capacity Spectrum Method (ATC-40 Procedure A) [3] mostly underestimated the displacement demand (as much as 40% at nonlinear deformation levels).
- Displacement Coefficient Method (FEMA-356) [20] mostly overestimated the displacement demand as much as 100% at nonlinear deformation levels.
- The Nonlinear Dynamic Analysis of Equivalent SDOF System and Constant Ductility Procedure [8] followed a similar trend which lies between Displacement Coefficient Method (FEMA-356) [20] and Capacity Spectrum Method (ATC-40 Procedure A) [3] predictions.

- The Nonlinear Dynamic Analysis of Equivalent SDOF System and Constant Ductility Procedure [8] predictions were mostly reasonably conservative while the predictions of Nonlinear Dynamic Analysis of Equivalent SDOF System were more accurate.
- Nonconvergence could be observed in Capacity Spectrum Method (ATC-40 Procedure A) [3] and Constant Ductility Procedure [8] as the procedures involve an iterative solution. Also, multiple intersections of response (demand) spectra with capacity curve were observed in both procedures due to the jagged shape of demand spectra. In such cases, the iterative solution needs to be performed more carefully to determine the right demand point consistent with the demand spectra.
- The Nonlinear Dynamic Analysis of Equivalent SDOF System should be preferred to estimate maximum displacement demand in case ground motion record is available and Constant Ductility Procedure [8] would be more appropriate in case a design or response spectrum is available.

The degree of accuracy of these procedures are assessed based on their ability to predict the roof displacement of MDOF which is not simply a successful estimation of the story response quantities.

6.3 RECOMMENDATIONS FOR FUTURE STUDY

This study employed a few number of reinforced concrete and steel moment resisting frames and a limited number of ground motion excitations. An extensive study containing a larger number of frames covering a broad range of fundamental periods and a set of representative ground motion records would enhance the results obtained in the accuracy seismic demand prediction of pushover procedures and in the accuracy of maximum displacement demand prediction of approximate procedures. Also, adaptive lateral load patterns could be included in the extended study.

The accuracy of lateral load patterns in predicting seismic demands should also be investigated at target displacements estimated by an approximate procedure rather than at 'exact' displacement demand.

The accuracy of approximate procedures in estimating the maximum displacement demand could be studied on ground motions whose effects on structures can be represented reasonably by smoothened response spectra. Finally, all the issues mentioned could be extended into three dimensional structures.

REFERENCES

[1] Allahabadi R., 1987, *Drain 2DX – Seismic Response and Damage Assessment for 2D Structures*, Ph.D. Thesis, University of California at Berkeley, California.

[2] ANSYS Inc., *ANSYS Structural,* 275 Technology Drive Canonsburg, PA.

[3] Applied Technology Council, ATC-40, 1996, *Seismic Evaluation and Retrofit of Concrete Buildings*, Volume 1-2, Redwood City, California.

[4] Bentz E.C., 2000, *Sectional Analysis of Reinforced Concrete*, Ph.D. Thesis, Department of Civil Engineering, University of Toronto.

[5] Bracci J.M., Kunnath S.K. and Reinhorn A.M., 1997, *Seismic Performance and Retrofit Evaluation of Reinforced Concrete Structures*, Journal of Structural Engineering, ASCE, Vol. 123, 3-10.

[6] Chintanapakdee C. and Chopra A.K., 2003, *Evaluation of Modal Pushover Analysis Using Generic Frames*, Earthquake Engineering and Structural Dynamics, Vol. 32, 417-442.

[7] Chopra A.K., 1995, *Dynamics of Structures-Theory and Application to Earthquake Engineering*, Prentice Hall, New Jersey.

[8] Chopra A.K. and Goel R.K., *Capacity – Demand Diagram Methods for Estimating Seismic Deformation of Inelastic Structures: SDOF Systems* , PEER Report 1999/02, Pacific Earthquake Engineering Research Center, University of California, Berkeley.

[9] Chopra A.K. and Goel R.K., *A Modal Pushover Analysis Procedure to Estimating Seismic Demands for Buildings: Theory and Preliminary Evaluation*, PERR Report 2001/03, Pacific Earthquake Engineering Research Center, University of California, Berkeley.

[10] City of Los Angeles (COLA), 1995, *Earthquake Hazard Reduction in Existing Reinforced Concrete Buildings and Concrete Frame Buildings with Masonry Infills,* January 31, 1995.

[11] Clough R.W., Johsnton S.B., 1996, *Effect of Stiffness Degradation on Earthquake Ductility Requirements*, Proceedings of Japan Earthquake Engineering Symposium, Tokyo, Japan, 227-231.

[12] Computers and Structures Inc. (CSI), 1992, *SAP90: A Series of Computer Programs for the Finite Analysis of Structures*, Berkeley, California.

[13] Computers and Structures Inc. (CSI), 1995, *ETABS: Three Dimensional Analysis of Building Systems*, Berkeley, California.

[14] Computers and Structures Inc. (CSI), 1998, *SAP2000 Three Dimensional Static and Dynamic Finite Element Analysis and Design of Structures V7.40N*, Berkeley, California.

[15] Eberhard M.O. and Sözen M.A., 1993, *Behavior-Based Method to Determine Design Shear in Earthquake Resistant Walls*, Journal of the Structural Division, American Society of Civil Engineers, New York, Vol. 119, No.2, 619-640.

[16] Fajfar P. and Fischinger M., 1987, *Nonlinear Seismic Analysis of R/C Buildings: Implications of a Case Study*, European Earthquake Engineering, 31-43.

[17] Fajfar P. and Gaspersic P., 1996, *The N2 Method for the Seismic Damage Analysis of R/C Buildings*, Earthquake Engineering and Structural Dynamics,Vol. 25, 31-46.

[18] Federal Emergency Management Agency (FEMA), 1997, *NEHRP Guidelines for the Seismic Rehabilitation of Buildings*, FEMA-273.

[19] Federal Emergency Management Agency (FEMA), 2000, *State of the Art Report on Systems Performance of Steel Moment Frames Subject to Earthquake Ground Shaking*, Prepared by the SAC Joint Venture for the Federal Emergency Management Agency, Washington, DC.

[20] Federal Emergency Management Agency (FEMA), 2000, *Prestandard and Commentary for the Rehabilitation of Buildings*, FEMA-356.

[21] Freeman S.A., 1998, *Development and Use of Capacity Spectrum Method*, Proceedings of the Sixth U.S. National Conference on Earthquake Engineering, Seattle, Washington.

[22] Gupta B., 1999, *Enhanced Pushover Procedure and Inelastic Demand Estimation for Performance-Based Seismic Evaluation of Buildings*, Ph.D. Dissertation, University of Central Florida, Orlando, FL.

[23] Gülkan P. and Sözen M.A., 1974, *Inelastic Response of Reinforced Concrete Structures to Earthquake Ground Motions*, Journal of the American Concrete Institute, Vol. 71, 601-609.

[24] International Conference on Building Officials (ICBO), 1982, *Uniform Building Code*, Whittier, CA.

[25] Iwan W.D., 1980, *Estimating Inelastic Response Spectra from Elastic Spectra*, Earthquake Engineering and Structural Dynamics, Vol. 8, 375-388.

[26] İnel M., Tjhin T. and Aschheim A.M., 2003, *The Significance of Lateral Load Pattern in Pushover Analysis*, İstanbul Fifth National Conference on Earthquake Engineering, Paper No: AE-009, İstanbul, Turkey.

[27] Jan T.S., Liu M.W. and Kao Y.C., 2004, *An Upper-Bound Pushover Analysis Procedure for Estimating the Seismic Demands of High-Rise Buildings*, Engineering Structures, Vol. 26, 117-128.

[28] Kappos A.J. and Manafpour A., 2000, *Seismic Design of R/C Buildings with the Aid of Advanced Analytical Techniques*, Engineering Structures, Vol. 23, 319-332.

[29] Kowalsky M.J., 1994, *Displacement-Based Design Methodology for Seismic Design Applied to R/C Bridge Columns*, Master's Thesis, University of California at San Diego, La Jolla, California.

[30] Krawinkler H. and Seneviratna G.D.P.K., 1998, *Pros and Cons of a Pushover Analysis of Seismic Performance Evaluation*, Engineering Structures, Vol.20, 452-464.

[31] Lawson R.S., Reinhorn A.M. and Lobo R.F., 1994, *Nonlinear Static Pushover Analysis - Why, When and How?*, Proceedings of the 5th US National Conference on Earthquake Engineering, Chicago, Vol. 1, 283-292.

[32] Mahaney J.A., Paret T.F., Kehoe B.E. and Freeman S.A., 1993, *The Capacity Spectrum Method for Evaluating Structural Response During the Loma Prieta Earthquake*, Proc., 1993 Nat. Earthquake Conf., Central U.S. Earthquake Consortium, Memphis, Tenn., 2, 501-510.

[33] Miranda E., 2000, *Inelastic Displacement Ratios for Structures on Firm Sites*, Journal of Structural Engineering, Vol. 126, 1150-1159.

[34] Miranda E. and Ruiz-García J., 2002, *Evaluation of Approximate Methods to Estimate Maximum Inelastic Displacement Demands*, Earthquake Engineering and Structural Dynamics, Vol. 31, 539-560.

[35] Moghadam A.S., *A Pushover Procedure for Tall Buildings*, 12th European Conference on Earthquake Engineering, Paper Reference 395.

[36] Munshi J.A. and Ghosh S.A., 1998, *Analyses of Seismic Performance of a Code Designed* R*einforced Concrete Building*, Engineering Structures, Vol. 20, 608-616.

[37] Mwafy A.M. and Elnashai A.S., 2001, *Static Pushover versus Dynamic Analysis of R/C Buildings,* Engineering Structures, Vol. 23, 407-424.

[38] Nassar A.A. and Krawinkler H., 1991, *Seismic Demands for SDOF and MDOF Systems,* Report No.95, John A. Blume Earthquake Engineering Center, Stanford University.

[39] Newmark N.M. and Hall W.J., 1982, *Earthquake Spectra and Design*, Earthquake Engineering Research Institute, Berkeley, CA.

[40] *Nonlınear Dynamic Time History Analysis of Single Degree of Freedom Systems (NONLIN)*, developed by Dr. Finley A. Charney, Advanced Structural Concepts, Golden, Colorado and Schnabel Engineering, Denver, Colorado.

[41] Park R. and Paulay T., 1975, *Reinforced Concrete Structures*, John Wiley and Sons, Inc., 769.

[42] Parme A.L., Nieves J.M. and Gouwens A., 1966, *Capacity of Reinforced Rectangular Columns Subject to Biaxial Bending*, Journal of the American Concrete Institute, Vol. 63, 911-923.

[43] Powell G.H., 1993, *Drain-2DX Element Description and User Guide for Elements*, Structural Engineering Mechanics and Materials Report No.93/18, University of California, California.

[44] Prakash V., Powell G.H. and Campbell S., 1993, *Drain-2DX Base Program Description and User Guide*, Structural Engineering Mechanics and Materials Report No.93/17, University of California, California.

[45] RISA Technologies (RISA), 1993, *RISA-2D : Rapid Interactive Structural Analysis- 2 Dimensional*, Lake Forest, California.

[46] Rosenblueth E. and Herrera I., 1964, *On a Kind of Hysteretic Damping*, Journal of Engineering Mechanics Division, ASCE, Vol. 90, 37-48.

[47] SAC, 1997, *Draft Report on Ground Motions*, Earthquake Engineering Research Institute, Berkeley, CA.

[48] Saiidi M. and Sözen M.A., 1981, *Simple Nonlinear Seismic Response of R/C Structures*, Journal of Structural Division, ASCE, Vol. 107, 937-952.

[49] Sasaki F., Freeman S. and Paret T., 1998, *Multi-Mode Pushover Procedure (MMP)-A Method to Identify the Effect of Higher Modes in a Pushover Analysis*, Proc. 6th U.S. National Conference on Earthquake Engineering, Seattle, CD-ROM, EERI, Oakland.

[50] *SeismoSignal*, 2002, developed by Stelios Antoniou and Rui Pinho, SeismoSoft Company.

[51] Shibata A. and Sözen M.A., 1976, *Substitute Structure Method for Seismic Design in R/C*, Journal of Structural Division, ASCE, Vol. 102, 1-17.

[52] Takeda T., Sözen M.A. and Nielson N.N., 1970, *Reinforced Concrete Response to Simulated Earthquakes*, Journal of Structural Division, ASCE, Vol. 96, 2557-2573.

[53] *Turkish Earthquake Code: Specifications for the Buildings to be Constructed in Disaster Areas*, 1998, Ministry of Public Works and Settlement, Ankara, Turkey.

[54] *Utility Software for Earthquake Engineering (USEE)*, 2001, developed by the Mid-America Earthquake Center as part of Project ST-18, supported primarily by the Earthquake Engineering Research Centers Program of the National Science Foundation under Award Number EEC-9701785.

[55] Vidic, T., Fajfar, P. and Fischinger, M., 1994, *Consistent Inelastic Design Spectra: Strength and Displacemen*, Earthquake Engineering and Structural Dynamics, 23(5) 507-521.

APPENDIX A

FRAME DATA AND RESULTS OF PUSHOVER ANALYSIS

A.1 DESCRIPTION OF CASE STUDY FRAMES

A.1.1 REINFORCED CONCRETE FRAMES

- **2-Story Reinforced Concrete Frame**

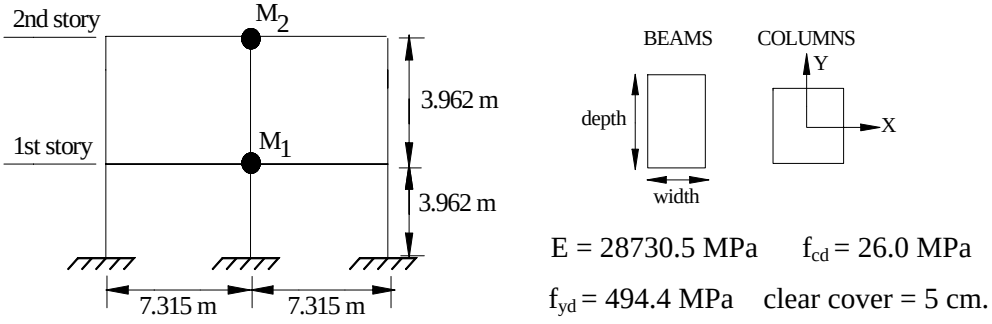

E = 28730.5 MPa f_{cd} = 26.0 MPa

f_{yd} = 494.4 MPa clear cover = 5 cm.

Figure A.1 : The Configuration of 2-Story Reinforced Concrete Frame

Table A.1 : Section and Loading Properties of 2-Story Reinforced Concrete Frame

Story	Beams				Mass (t)	DL (kN/m)	LL (kN/m)
	Dimension (cm)		Reinforcement (mm^2)				
	Depth	Width	Top	Bottom			
1	55.88	30.48	1342	3148.4	177.70	24.71	1.05
2	50.8	30.48	1342	2503.2	97.55	19.23	0.98

Story	Column	Dimension (cm)		Number of Bars		Bar Area (mm^2)
		x-dir	y-dir	x-dir	y-dir	
1-2	Exterior	60.96	60.96	5	5	645.16
	Interior	60.96	60.96	5	5	645.16

Table A.2 : Dynamic Properties of 2-Story Reinforced Concrete Frame

Modal Properties	Mode	
	1	2
Period (sec)	0.488	0.148
Modal Participation Factor	1.336	0.336
Modal Mass Factor	0.834	0.166

- **5-Story Reinforced Concrete Frame**

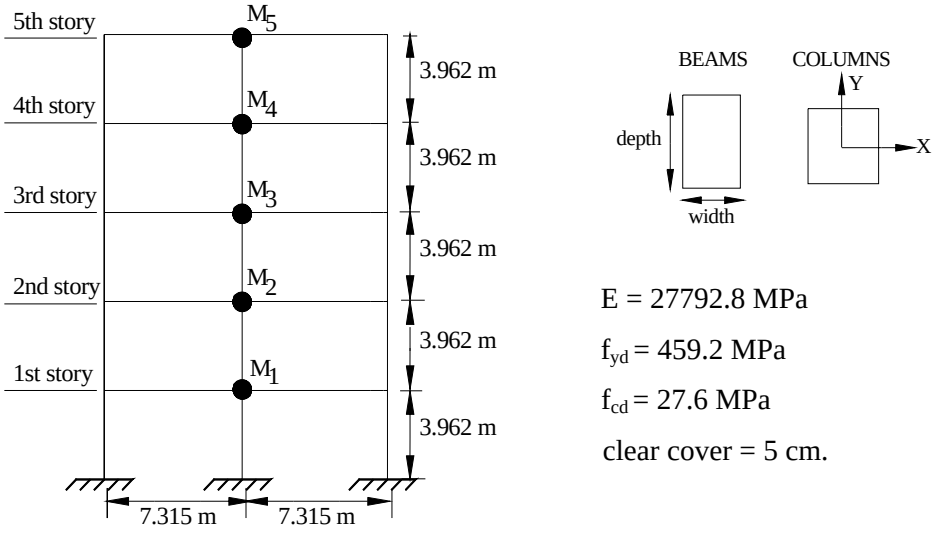

Figure A.2 : The Configuration of 5-Story Reinforced Concrete Frame (x)

Table A.3 : Section and Loading Properties of 5-Story Reinforced Concrete Frame (x)

Story	Beams				Mass (t)	DL (kN/m)	LL (kN/m)
	Dimension (cm)		Reinforcement (mm^2)				
	Depth	Width	Top	Bottom			
1-4	66.04	40.64	5083.86	3148.38	104.025	20.49	1.31
5	50.8	30.48	3793.54	2503.22	77.056	15.64	0.53

Story	Column	Dimension (cm)		Number of Bars		Bar Area (mm^2)
		x-dir	y-dir	x-dir	y-dir	
1-5	Exterior	71.12	71.12	6	6	885.8
	Interior	71.12	71.12	6	6	885.8

Table A.4 : Dynamic Properties of 5-Story Reinforced Concrete Frame (x)

Modal Properties	Mode		
	1	2	3
Period (sec)	0.857	0.272	0.141
Modal Participation Factor	1.348	0.528	0.258
Modal Mass Factor	0.794	0.116	0.054

- **8-Story Reinforced Concrete Frame**

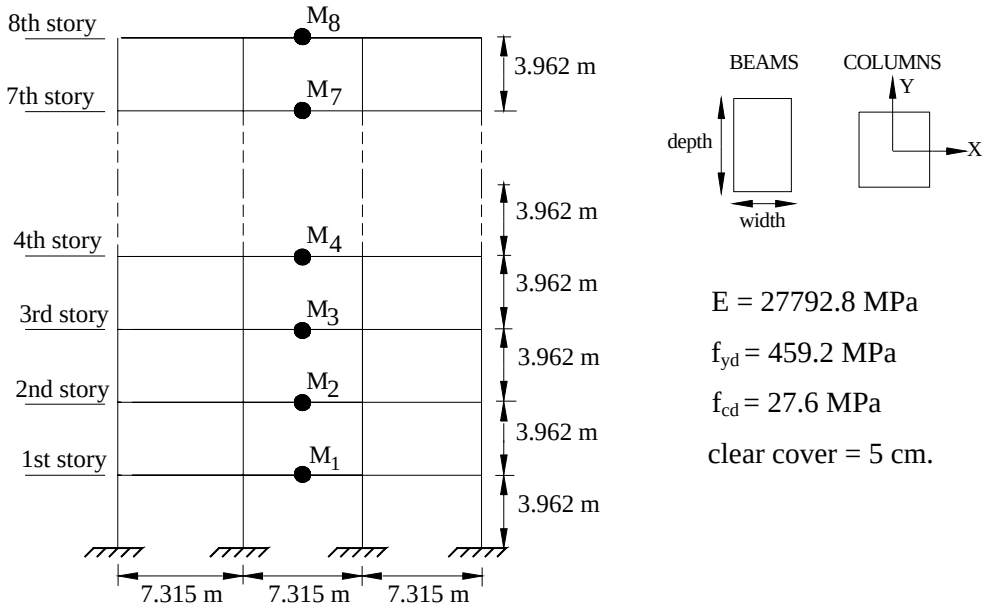

Figure A.3 : The Configuration of 8-Story Reinforced Concrete Frame

Table A.5 : Section and Loading Properties of 8-Story Reinforced Concrete Frame

Story	Beams				Mass (t)	DL (kN/m)	LL (kN/m)
	Dimension (cm)		Reinforcement (mm^2)				
	Depth	Width	Top	Bottom			
1-4	90	50	5400	4850	230.450	18.64	1.21
5-7	75	40	4500	3600	230.450	18.64	1.21
8	60	30	1800	1125	202.920	14.55	0.49

Story	Columns	Dimension (cm)		Number of Bars		Bar Area (mm^2)
		x-dir	y-dir	x-dir	y-dir	
1-3	Exterior	110	110	10	10	510
	Interior	110	110	10	10	510
4-6	Exterior	100	100	8	8	510
	Interior	100	100	8	8	510
7-8	Exterior	92	92	6	6	510
	Interior	92	92	6	6	510

Table A.6 : Dynamic Properties of 8-Story Reinforced Concrete Frame

Modal Properties	Mode		
	1	2	3
Period (sec)	1.064	0.374	0.192
Modal Participation Factor	1.409	0.613	0.319
Modal Mass Factor	0.727	0.144	0.050

- **12-Story Reinforced Concrete Frame**

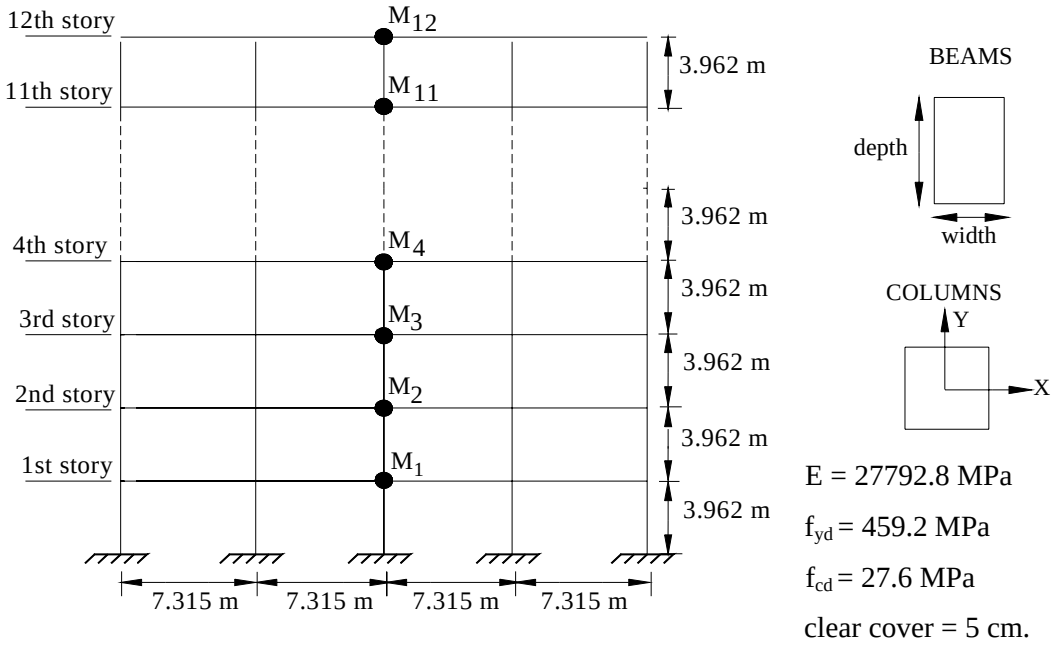

Figure A.4 : The Configuration of 12-Story Reinforced Concrete Frame

Table A.7 : Section and Loading Properties of 12-Story Reinforced Concrete Frame

Story	Beams				Mass (t)	DL (kN/m)	LL (kN/m)
	Dimension (cm)		Reinforcement (mm^2)				
	Depth	Width	Top	Bottom			
1-3	101.6	50.8	6625.79	6116.12	346.860	16.78	1.1
4-7	91.44	50.8	6625.79	6116.12	346.860	16.78	1.1
8-11	76.2	45.72	5096.76	4077.41	346.860	16.78	1.1
12	60.96	45.72	2038.71	1019.35	294.330	13.45	0.44

Story	Columns	Dimension (cm)		Number of Bars		Bar Area (mm^2)
		x-dir	y-dir	x-dir	y-dir	
1-3	Exterior	121.92	121.92	12	12	509.7
	Interior	152.4	60.96	7	7	509.7
4-8	Exterior	111.76	111.76	8	8	509.7
	Interior	144.78	60.96	6	6	509.7
9-12	Exterior	101.6	101.6	7	7	509.7
	Interior	127	60.96	5	5	509.7

Table A.8 : Dynamic Properties of 12-Story Reinforced Concrete Frame

Modal Properties	Mode		
	1	2	3
Period (sec)	1.610	0.574	0.310
Modal Participation Factor	1.398	0.615	0.372
Modal Mass Factor	0.730	0.130	0.052

A.1.2 STEEL FRAMES

- **2-Story Steel Frame**

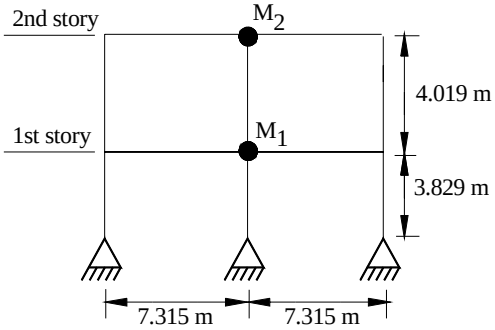

E = 458900 MPa

F_y = 291.37 MPa

Figure A.5 : The Configuration of 2-Story Steel Frame

Table A.9 : Section and Loading Properties of 2-Story Steel Frame

Story	Columns		Beams	Mass (t)	DL (kN/m)	LL (kN/m)
	Exterior	Interior				
1	W14x90	W14x90	W24x62	92.26	12.50	1.04
2	W14x90	W14x90	W12x26	27.90	5.53	0.98

Table A.10 : Dynamic Properties of 2-Story Steel Frame

Modal Properties	Mode	
	1	2
Period (sec)	0.535	0.155
Modal Participation Factor	1.272	0.272
Modal Mass Factor	0.972	0.028

- **5-Story Steel Frame**

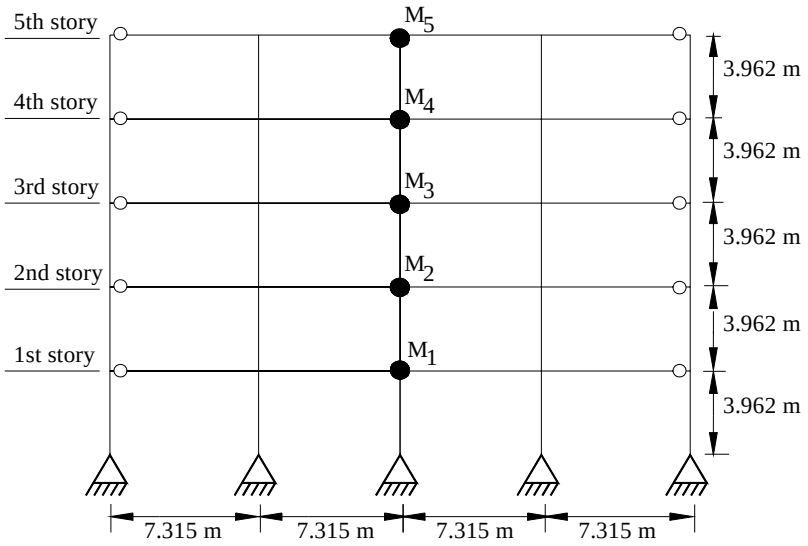

E = 262000 MPa

F_y = 268.89 MPa

Figure A.6 : The Configuration of 5-Story Steel Frame

Table A.11 : Section and Loading Properties of 5-Story Steel Frame

Story	Columns		Beams	Mass (t)	DL (kN/m)	LL (kN/m)
	Exterior	Interior				
1	W14x311	W14x283	W33x118	109.86	14.64	1.82
2	W14x176	W14x176	W30x90	109.86	14.64	1.82
3	W14x176	W14x176	W24x62	109.86	14.64	1.82
4	W14x120	W14x120	W21x50	109.86	14.64	1.82
5	W14x120	W14x120	W18x35	46.81	6.62	0.74

Table A.12 : Dynamic Properties of 5-Story Steel Frame

Modal Properties	Mode		
	1	2	3
Period (sec)	1.039	0.379	0.196
Modal Participation Factor	1.412	0.594	0.266
Modal Mass Factor	0.862	0.104	0.022

- **13-Story Steel Frame**

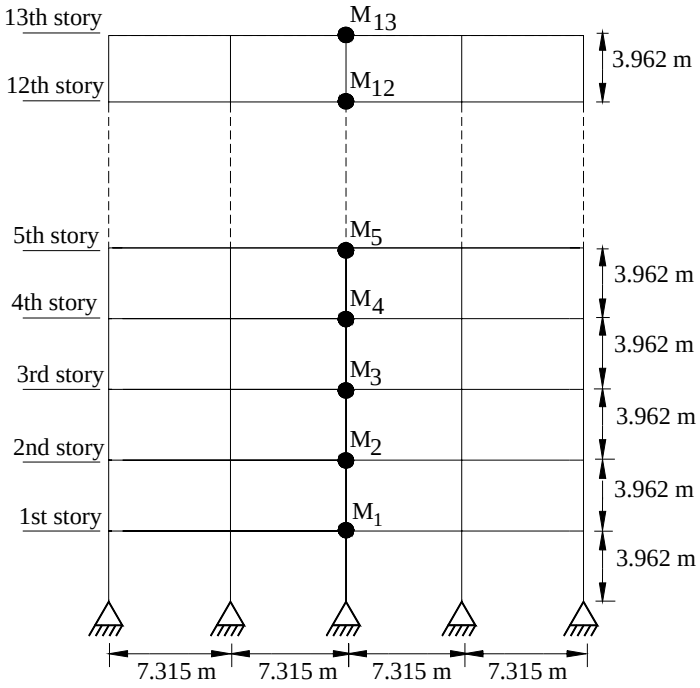

E = 199948 MPa

F_y = 268.89 MPa

Figure A.7 : The Configuration of 13-Story Steel Frame

Table A.13 : Section and Loading Properties of 13-Story Steel Frame

Story	Interior Columns	Beams	Mass (t)	DL (kN/m)	LL (kN/m)
1-2	W27x539	W24x450	237.31	9.12	0.74
3-5	W27x448	W24x207	237.31	9.12	0.74
6-7	W24x450	W24x207	237.31	9.12	0.74
8	W24x450	W24x162	237.31	9.12	0.74
9-11	W24x250	W24x162	237.31	9.12	0.74
12	W24x146	W24x162	237.31	9.12	0.74
13	W24x146	W24x84	184.48	6.39	0.30

Story	Exterior Columns		
	A (cm^2)	I_x (cm^4)	I_y (cm^4)
1-2	2038.71	1149215	1149215
3-5	1269.67	538187.2	538187.2
6-8	1058.06	433838	433838
9-11	667.74	256356.9	256356.9
12-13	289.03	90863.32	90863.32

Table A.14 : Dynamic Properties of 13-Story Steel Frame

Modal Properties	Mode		
	1	2	3
Period (sec)	1.922	0.692	0.403
Modal Participation Factor	1.364	0.571	0.358
Modal Mass Factor	0.781	0.125	0.048

A.2 STORY PUSHOVER CURVES FOR STEEL FRAMES

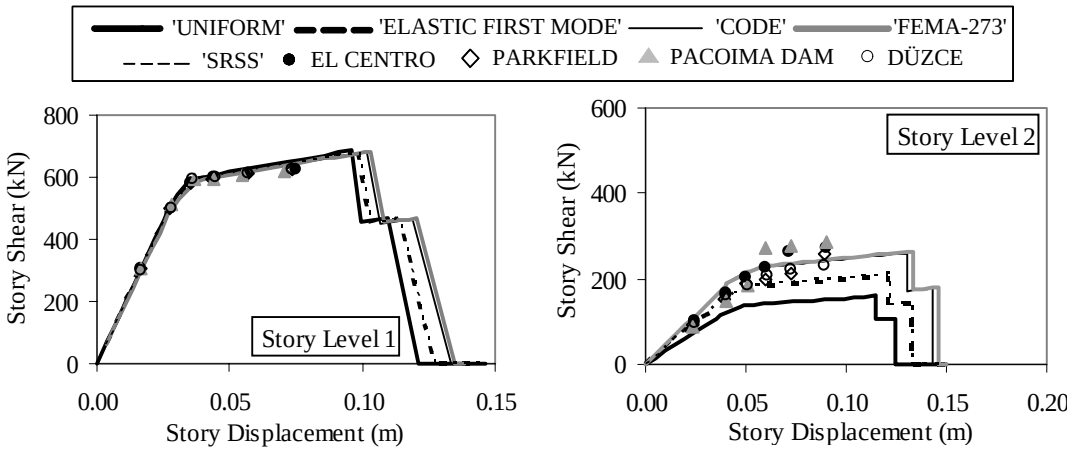

Figure A.8 : Story Pushover Curves for 2-Story Steel Frame (Story Levels 1-2)

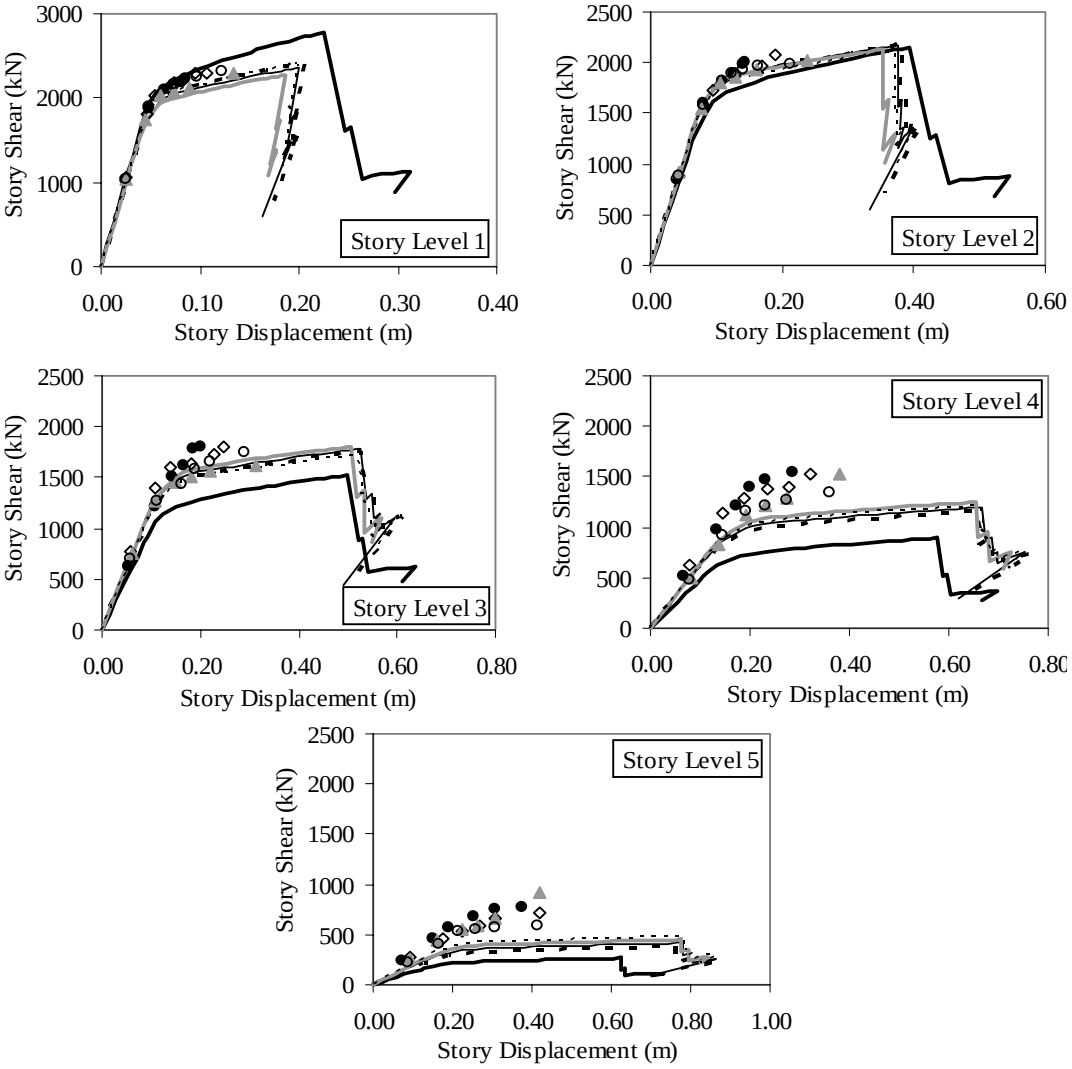

Figure A.9 : Story Pushover Curves for 5-Story Steel Frame (Story Levels 1-5)

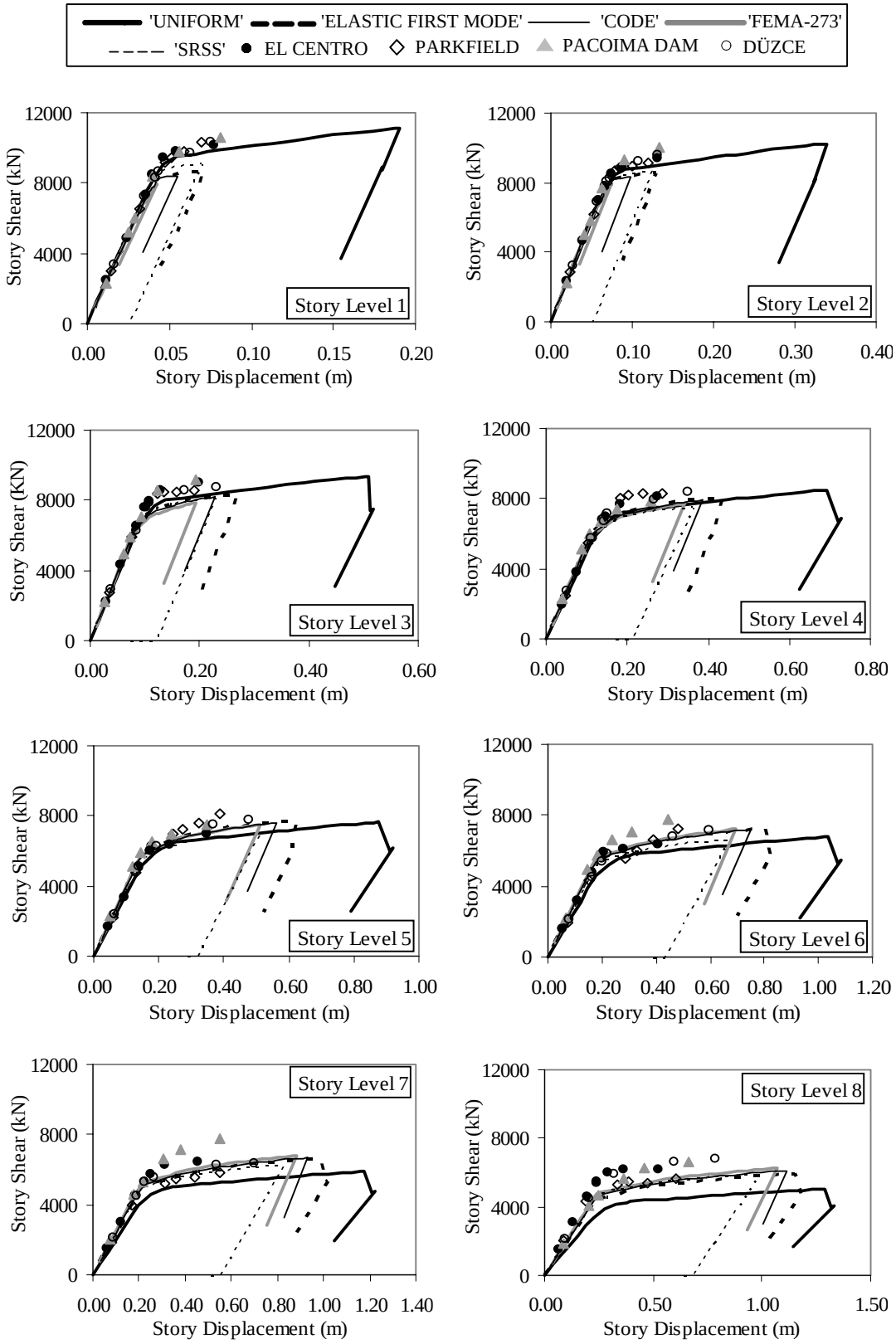

Figure A.10 : Story Pushover Curves for 13-Story Steel Frame (Story Levels 1-8)

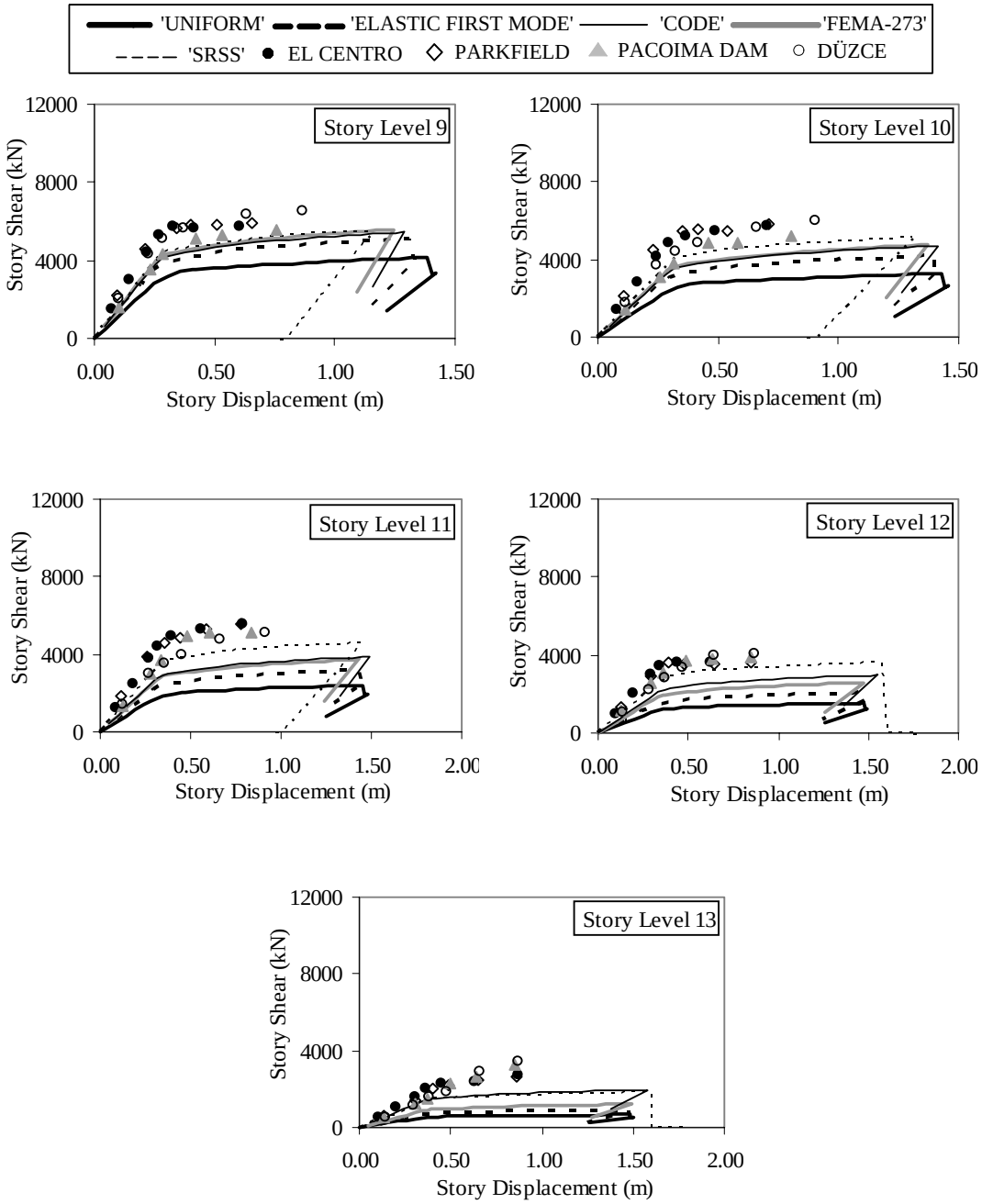

Figure A.11 : Story Pushover Curves for 13-Story Steel Frame (Story Levels 9-13)

A.3 PLASTIC HINGE LOCATIONS

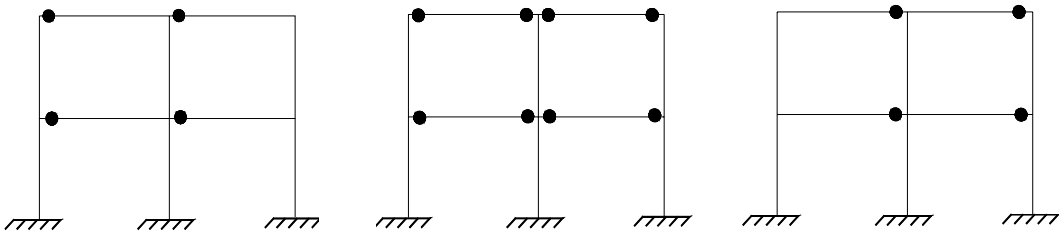

a) El Centro

b) Parkfield, Pacoima Dam, Düzce

c) 'Uniform', 'Code', 'Elastic First Mode' 'Multi-Modal (SRSS)'

Figure A.12 : Plastic Hinges for 2-Story R/C Frame (Deformation Level II)

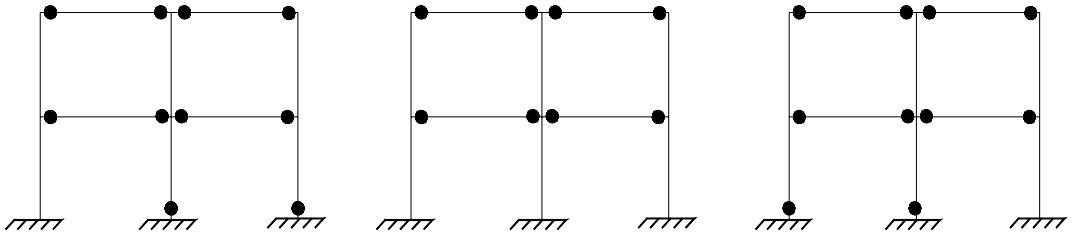

a) El Centro

b) Parkfield, Pacoima Dam

c) Düzce

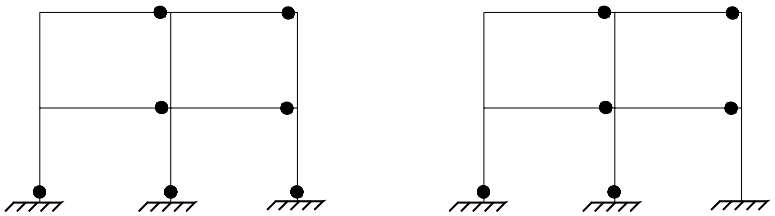

e) 'Uniform'

f) 'Elastic First Mode', 'Code' 'Multi-Modal (SRSS)'

Figure A.13 : Plastic Hinges for 2-Story R/C Frame (Deformation Level III)

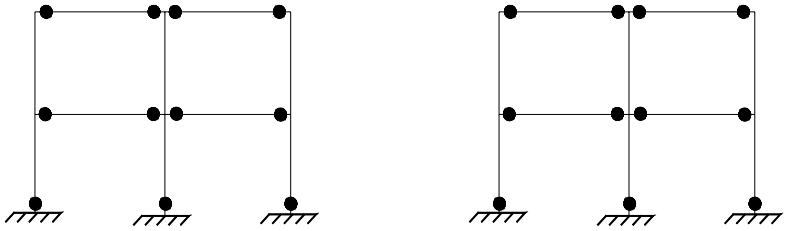

a) El Centro, Parkfield, Pacoima Dam, Düzce

b) 'Uniform', 'Elastic First Mode' 'Code', 'Multi-Modal (SRSS)'

Figure A.14 : Plastic Hinges for 2-Story R/C Frame (Deformation Level VI)

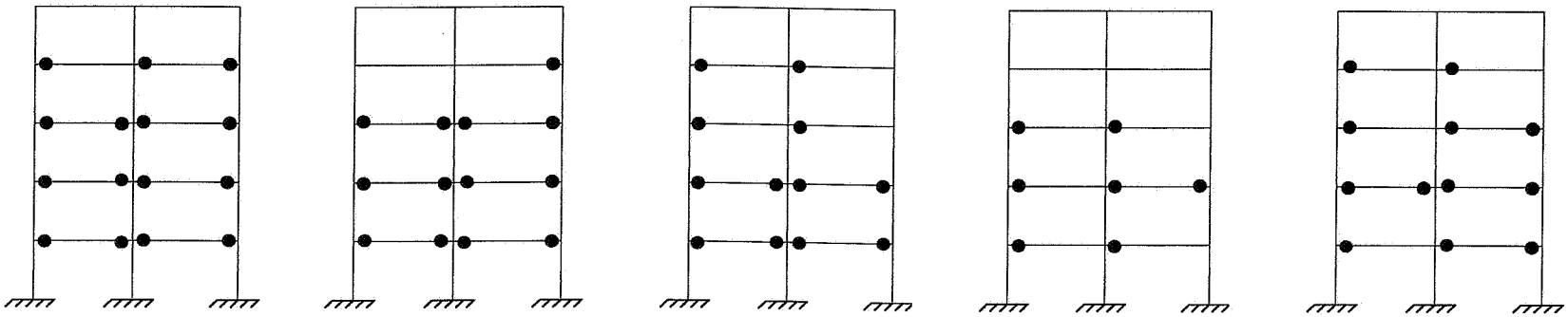

a) El Centro b) Parkfield c) Pacoima Dam d) Düzce e) MPA (El Centro)

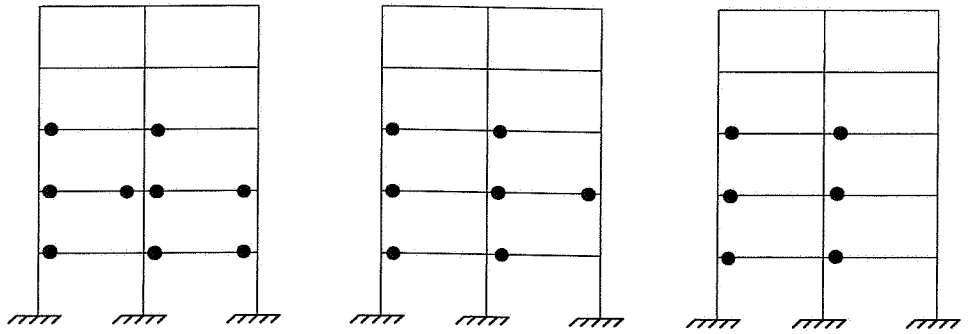

f) 'Uniform' g) 'Elastic First Mode', 'Code', 'FEMA-273' h) 'Multi-Modal (SRSS)'

Figure A.15 : Plastic Hinges for 5-Story R/C Frame (Deformation Level II)

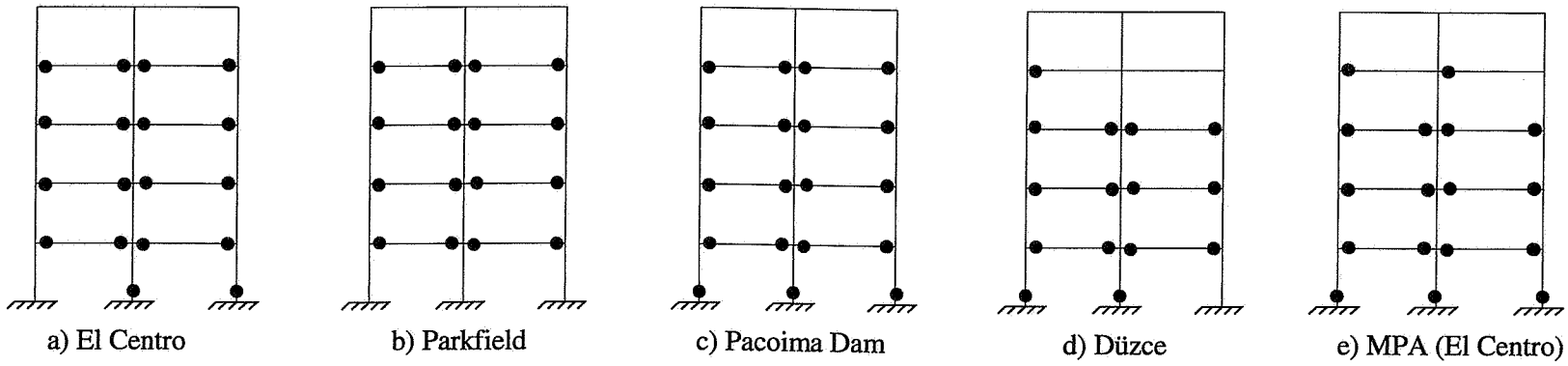

Figure A.16 : Plastic Hinges for 5-Story R/C Frame (Deformation Level III)

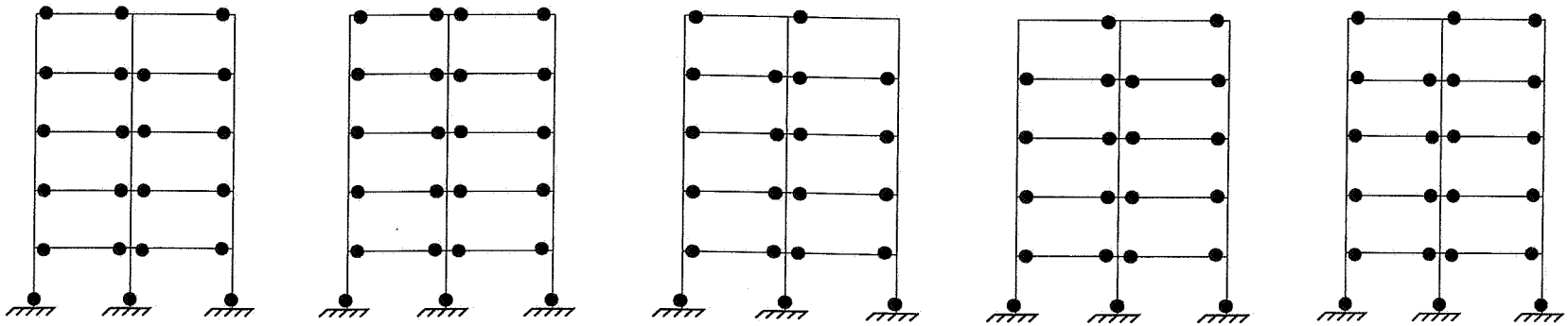

a) El Centro b) Parkfield c) Pacoima Dam d) Düzce e) MPA (El Centro)

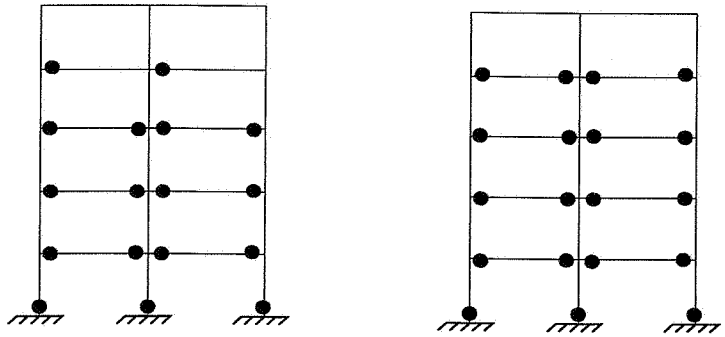

f) 'Uniform' g) 'Elastic First Mode', 'Code' 'FEMA-273', 'Multi-Modal (SRSS)'

Figure A.17 : Plastic Hinges for 5-Story R/C Frame (Deformation Level VI)

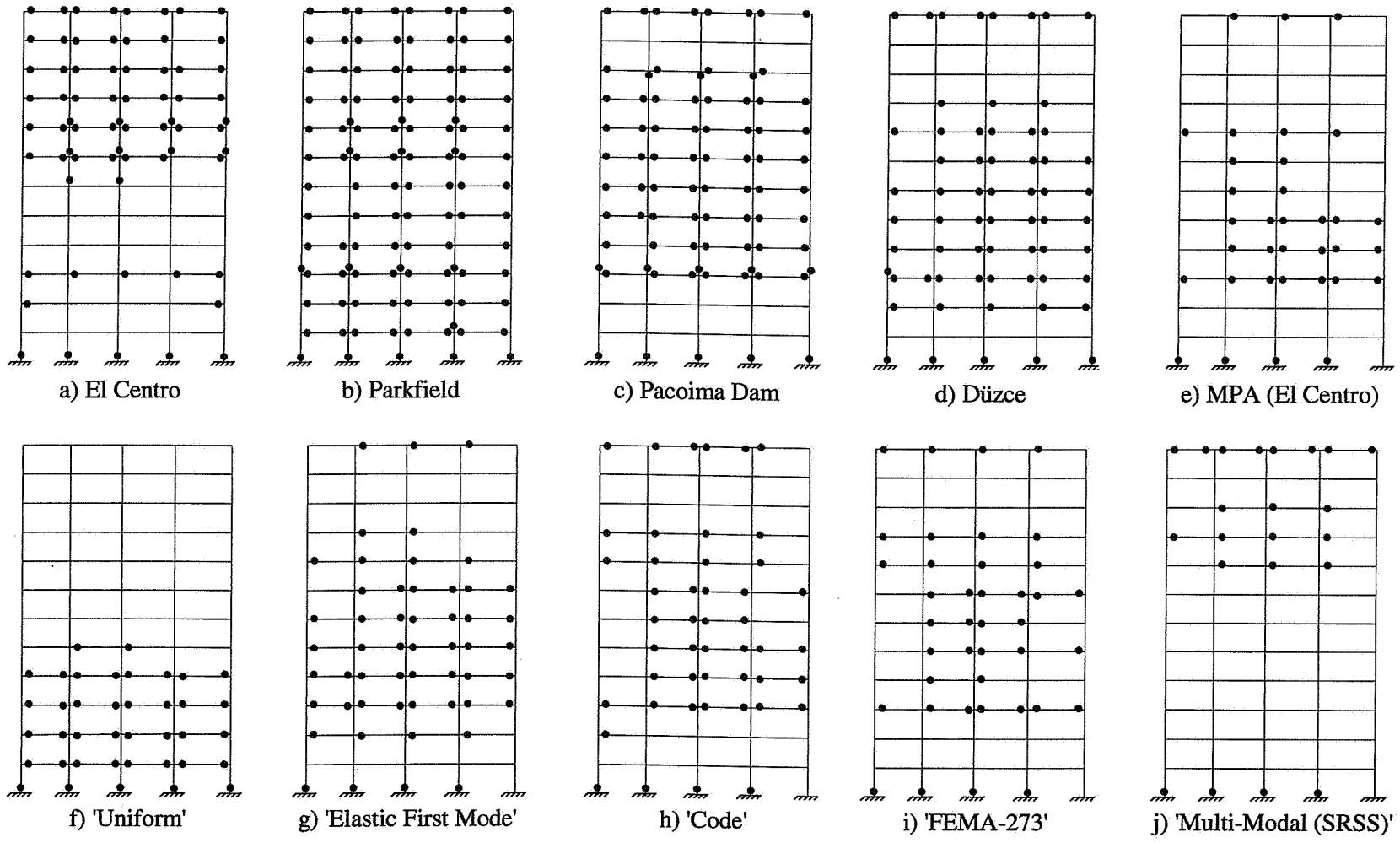

Figure A.18 : Plastic Hinges for 12-Story R/C Frame (Deformation Level II)

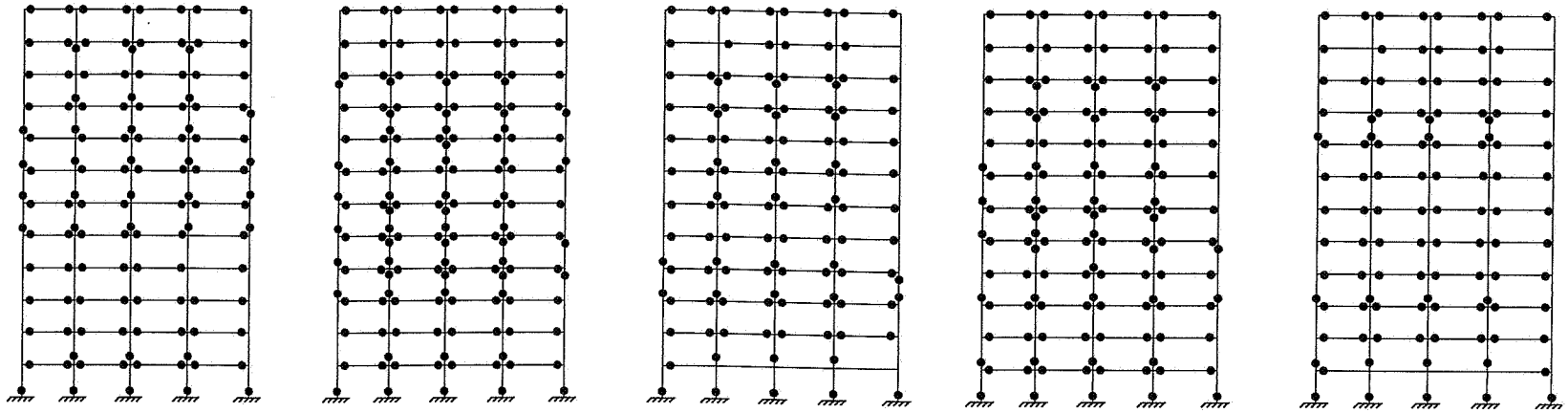

a) El Centro b) Parkfield c) Pacoima Dam d) Düzce e) MPA (El Centro)

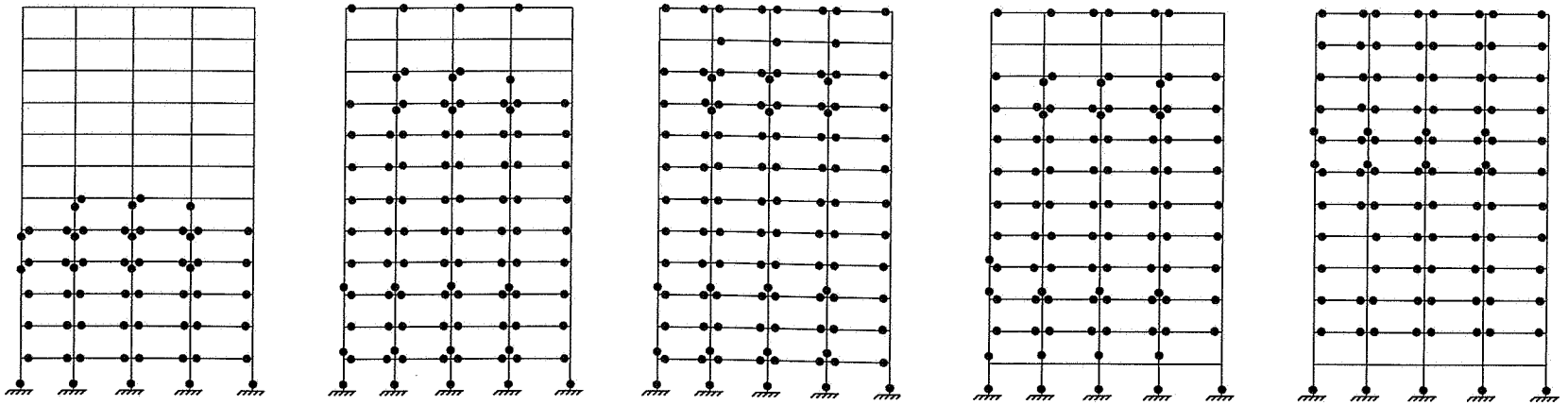

f) 'Uniform' g) 'Elastic First Mode' h) 'Code' i) 'FEMA-273' i) 'Multi-Modal (SRSS)'

Figure A.19 : Plastic Hinges for 12-Story R/C Frame (Deformation Level III)

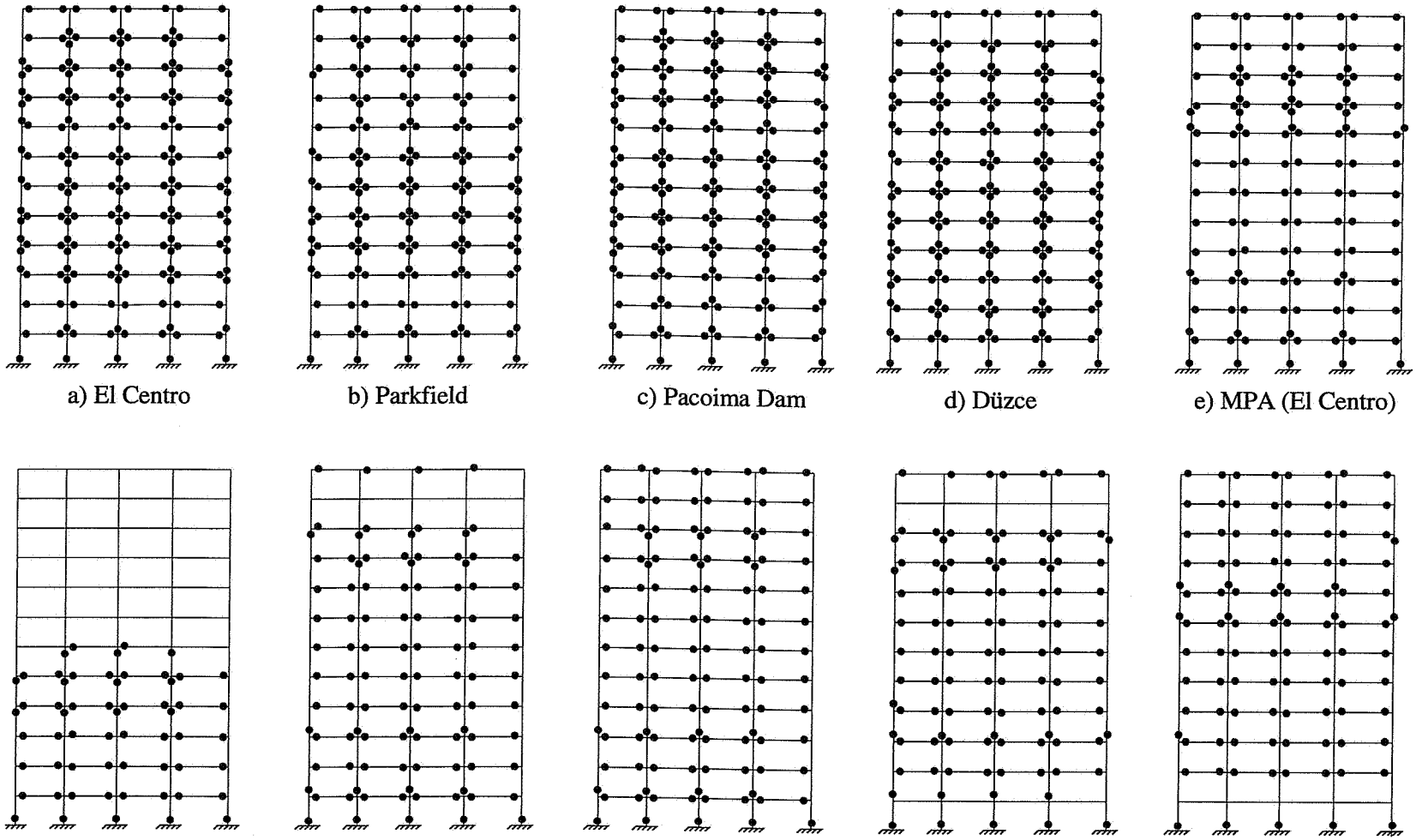

Figure A.20 : Plastic Hinges for 12-Story R/C Frame (Deformation Level VI)